

**COMBINATION OF SUBTRACTIVE & ADDITIVE MANUFACTURING
TECHNIQUES IN A MULTI-PURPOSE CNC MACHINE**

A Final Year Project Report

Presented to

SCHOOL OF MECHANICAL & MANUFACTURING ENGINEERING

Department of Mechanical Engineering

NUST

ISLAMABAD, PAKISTAN

In Partial Fulfillment
of the Requirements for the Degree of
Bachelor of Mechanical Engineering

by

ARSLAN ALI
FAHAD KHAN
UMER FAROOQ
USMAN TAHIR



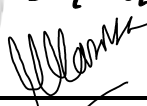
May 2020

EXAMINATION COMMITTEE

We hereby recommend that the final year project report prepared under our supervision by:

ARSLAN ALI	175503.
FAHAD KHAN	174833.
UMER FAROOQ	199297.
USMAN TAHIR	186176.

Titled: “**COMBINATION OF SUBTRACTIVE & ADDITIVE MANUFACTURING TECHNIQUES IN A MULTI-PURPOSE CNC MACHINE**” be accepted in partial fulfillment of the requirements for the award of MECHANICAL ENGINEERING degree with grade ____

Supervisor: Dr. Mushtaq Khan, HOD-DDME	 Dated: _____
Committee Member: Amir Mubashir	 Dated: <u>20/08/2020</u>
Committee Member: Hamza Asif Nizami	 Dated: _____

(Head of Department)

(Date)

COUNTERSIGNED

Dated: _____

(Dean / Principal)

ABSTRACT

Anything designed on paper or in CAD software, remains there unless fabricated up to the mark. Rapid Prototyping includes various manufacturing techniques that let us transform digital designs into physical objects, which can either be used to improve the product through design iterations or can be displayed as a product right after production. Any manufacturing technique can be classified as either subtractive, additive or formative. Rapid prototyping applies these production technologies to produce scale models or complete products using CAD data, with little or no human intervention. This project focuses at the combination of additive and subtractive manufacturing techniques like 3D printing, CNC milling and laser engraving. Such a machine can be helpful for the industry as well as the education department as it enables the users to make use of, both most commonly used rapid manufacturing techniques in a hybrid CNC environment.

ACKNOWLEDGMENTS

The efforts of the project participants who discretized the project, researched each aspect of the project extensively, formulated practical design parameters and procured equipment based on those design parameters is to be acknowledged. The project supervisor, Dr. Mushtaq Khan is to be especially thanked for the supervision and advisory regarding the project that governed and helped with several the design parameters. We also give credit to the whole sellers who gave us a description of the local marketplace in terms of components available and their prices. NUST administration and staff members who facilitated our usage of workshops and laboratories in SMME for testing and set-up of our equipment are credited as well as the lab workers and supervisors who helped manufacture certain parts of the machine.

ORIGINALITY REPORT

FYP

ORIGINALITY REPORT

9%	7%	1%	6%
SIMILARITY INDEX	INTERNET SOURCES	PUBLICATIONS	STUDENT PAPERS

PRIMARY SOURCES

1	www.nbcorporation.com Internet Source	1%
2	www.legacycncwoodworking.com Internet Source	1%
3	www.pololu.com Internet Source	<1%
4	www.3erp.com Internet Source	<1%
5	Submitted to Engineers Australia Student Paper	<1%
6	en.m.wikipedia.org Internet Source	<1%
7	www.coursehero.com Internet Source	<1%
8	www.britannica.com Internet Source	<1%
9	en.wikipedia.org Internet Source	<1%

TABLE OF CONTENTS

ABSTRACT	ii
ACKNOWLEDGMENTS	iii
ORIGINALITY REPORT	iv
LIST OF TABLES	viii
LIST OF FIGURES	ix
NOMENCLATURE	xii
CHAPTER 1: INTRODUCTION	1
Problem Statement	3
Objectives	3
CHAPTER 2: LITERATURE REVIEW	4
CNC Structural Configuration	4
Stepper Motor vs. Servo Motor	5
Linear Actuation Mechanisms	7
Mechanical Actuators	7
Electronics	13
CHAPTER 3: METHODOLOGY	16

Cutting Force Calculation	17
Maximum Force Calculation	18
Linear Bearing Selection	19
Clamp Design	20
X-Axis Plate Design.....	21
Z-Axis Plate Design.....	23
Spindle Selection	24
Stepper Motor Torque Calculation.....	27
Electronics	28
CHAPTER 4: RESULTS AND DISCUSSIONS.....	49
Manufacturing.....	49
Computer Aided Design and 3D Modeling.....	52
Finite Element Analysis.....	54
Topology Optimization.....	57
Milling Simulations.....	61
Deform Simulation Analysis	64
CHAPTER 5: CONCLUSION AND RECOMMENDATIONS	67
Recommendations:.....	67

Automatic Bed Levelling	67
PID Spindle Speed Control	73
1.5 KW Spindle Attachment	79
Conclusion	81
REFERENCES	84
APPENDIX I: ELECTRONICS	87
APPENDIX II: BOM.....	88

LIST OF TABLES

Table 1: Different Hybrid Machine Comparison.....	2
Table 2: Stepper Motor vs. Servo Motor	5
Table 3: LM Guideways vs. Round Shaft Guideways.....	9
Table 4: Different Actuators	13
Table 5: Different Boards Comparison.....	15
Table 6: Results of Clamp.....	21
Table 7: Results of X-Axis Plate	23
Table 8: Results of Z-Axis Plate.....	24
Table 9: Feed Per Tooth For Different Tool Diameter & Workpiece	25
Table 10: Different Milling Factors and their operation.....	26
Table 11: Chinese Spindle	26
Table 12: Stepper Specification	27
Table 13: Selection for controller	33
Table 14: Selection for firmware	35
Table 15: Effect of increasing gain independently	77

LIST OF FIGURES

Figure 1: Ball Screw	11
Figure 2: Lead Screw	11
Figure 3: Timing Belt.....	12
Figure 4: Rack & Pinion	12
Figure 5: Ramps 1.4.....	31
Figure 6: GRBLCNC Shield.....	32
Figure 7: MACH3 CNC Breakout Boards.....	32
Figure 8: External Stepper Motor Driver Wiring	38
Figure 9: Laser Module & TTL Modulation Driver Wiring.....	39
Figure 10: CNC Spindle & DC Speed Governor Wring.....	41
Figure 11: Heat Bed Wiring.....	42
Figure 12: Hotend Wiring.....	43
Figure 13: Fans Wiring	45
Figure 14: Mechanical End Stop Wiring	47
Figure 15: Rendered Design 1	52
Figure 16: Rendered Design 2	52
Figure 17: Rendered Design 5	53

Figure 18: Rendered Design 4	53
Figure 19: Rendered Design 3	53
Figure 20: FEM of Bolts	55
Figure 21: FEM of Spindle Clamp.....	55
Figure 22: FEM of Z-Axis Bracket.....	56
Figure 23: FEM of X-Axis Bracket	56
Figure 24: FEM of Clamp.....	57
Figure 25: Tool Head Clamp 2	58
Figure 26: Tool Head Clamp	58
Figure 27: Mounting Bracket for X-Axis	59
Figure 28: Mounting Bracket for X-Axis 2	59
Figure 29: Mounting Bracket for Y-Axis 2	60
Figure 30: Mounting Bracket for Y-Axis	60
Figure 31: Top View of End Mill Simulation.....	62
Figure 32: Orthogonal Cutting.....	63
Figure 33: Orthogonal Cutting 2.....	63
Figure 34: Deformed 3D Simulation	66
Figure 35: BLTouch Probe	68

Figure 36: Inductive Probe.....	68
Figure 37: Microswitch.....	69
Figure 38: Pinda Probe.....	69
Figure 39: Ezabl Pro	69
Figure 40: Piezo Probe.....	70
Figure 41: PID speed control flowchart.....	76
Figure 42: PID control circuit connection	78
Figure 43: VFD & AC Spindle Integration.....	80
Figure 44:Complete Wiring System	87

ABBREVIATIONS

CNC	Computer Numeric Control
FDM	Fuse Deposition Modeling
DLP	Digital Light Processing
FEM	Finite Element Method
DOC	Depth of Cut
WOC	Width of Cut
MRR	Material Removal Rate
3D	3 Dimensional
PWM	Pulse Width Modulus
PID	Proportional Integral Derivative
IDE	Integrated Development Environment
PCB	Printed Circuit Board
TTL	Transistor Transistor Logic
RPM	Revolution Per Minute

NOMENCLATURE

F_T	Bolt Tensile Force
n	Load Factor for bolts
N	No of Bolts
z	Feed per tooth
d	Tool diameter
f	Feed rate
E	Machine tool efficiency factor
V_c	Cutting Velocity
A_t	Tensile Stress Area
F_w	Worst-case Scenario Force
C_f	Total Cutting Force
hp	Spindle Power
C	Feed Factor
K_p	Power Constant

CHAPTER 1: INTRODUCTION

Prototyping is an essential element of the design and engineering process. Traditionally, though, it has created challenges as design teams strive to create makeshift models that provide a valid basis for a concept. This has, in the past, required nearly the same processes, costs, tooling and setup as the final product, making prototypes a prohibitive venture for many businesses. Rapid prototyping, in contrast, offers many advantages and applications that set it apart from traditional prototyping. Rapid prototyping is the fast fabrication of parts using digital design data. Major additive and subtractive manufacturing techniques that are 3D printing and CNC milling are usually employed in rapid prototyping. In Pakistan industries and research institutes are struggling with rapid prototyping because 3D printers and CNC machines are quite expensive and even the import of 3D printers is subjected to NOC from ministry of interior. Pakistan has banned the import of 3D printers citing security reasons

Our objective is to combine both additive and subtractive manufacturing techniques in a single hybrid CNC machine keeping in mind the constraints posed by the nature of work done on each individual machine. 3D printing, CNC milling and laser engraving if combined in a single unit, can be a better solution for rapid prototyping and small-scale production facilities. CNC machining along with 3D printing and laser engraving can be liable solution to the problems faced by designers, researchers and students. Such a machine can give lives to the imaginations of designers, researchers, engineers and students.

Hybrid CNC machines have been the interest of researchers from the past few decades. Some manufacturers have developed hybrid 3D printers that are also capable of milling and laser engraving. These all-in-one CNC machines are quite expensive due to the diversity of operations that they promise. Our focus is to minimize the costs and to

design an open source hybrid CNC machine that could perform up to the mark. Some hybrid CNC machines are listed below along with their specifications and costs:

Table 1: Different Hybrid Machine Comparison

Hybrid CNC machine	Manufacturing Methods	Working Space	Target Audience	Cost
5AXIS MAKER	3D Printing, CNC Milling, Touch Probe Scanning	400 x 400 x 400	Professional, Research	\$6,300
Z Morph VX	3D printing, dual extrusion 3D printing, CNC milling & engraving, laser cutting & engraving	250 x 235 x 165	Professional, Small Business	\$4,399
Snapmaker	3D printing, CNC milling, laser engraving	125 x 125 x 125	Maker	\$799
Our Hybrid CNC Machine	3D printing, CNC milling, laser engraving	350 x 350 x 350	Maker, Small Business, Research	\$930

Problem Statement

Combination of additive and subtractive manufacturing techniques in a single hybrid CNC machine to propose a better rapid prototyping solution for the industry and research departments. 3D printers, CNCs and laser engravers have specific design requisites which need to be addressed to keep the performance of all machines at an optimum. This issue due to the diversity in design of all machines should be confronted by a robust and modular design, along with a proper control and feedback system.

Objectives

The objectives of our project are,

- To propose a better and cheaper rapid prototyping solution to the industry by combining three major rapid prototyping manufacturing techniques in a single hybrid CNC machine.
- To design and fabricate the hybrid CNC machine keeping in mind the constraints posed by the nature of work done on each machine. That is to maximize the structural rigidity of the machine for better milling operations without affecting the robustness of 3D printing.
- To effectively combine 3D printing, CNC milling and laser engraving in a single unit to help the students and researchers refine their designs through experimental analysis on the prototypes and practical design iterations.
- To integrate the Hybrid CNC machine with sensors to make use of auto bed leveling feature of the marlin firmware.

CHAPTER 2: LITERATURE REVIEW

CNC Structural Configuration

There are two types of CNC structure configurations categorized based upon gantry motion. One type is when the gantry is moving, and the other type is when bed is moving. Sliding gantries are generally less stable due to the weight of these large moving gantries. Moreover, unsupported shafts are not a good idea most of the times since it is difficult to restrict deformations and flex which compromises the tolerance of the CNC. However, when the work pieces are bulky, this is where sliding gantries come into play. A sliding gantry is a better choice in this case since sliding beds cannot bear the stresses induced by moving a bulky work piece.

Sliding beds on the other hand, are more stable due to minimalistic motion of the critical gantry structure. Moreover, longer space between the bushing centers in a moving table design would mean less leverage to flex the shafts. On the moving gantry the distance between cutter center line and x axis bearings is a constant which is some advantage. In theory this could also be accomplished on a moving table with stationary bearings and moving rails which is hard to do well, however. Also, a moving gantry allows a well-supported worktable.

In our case, we are building hobbyists CNC so bulky work pieces will not be our domain. Also, we believe stability and endurance are an imperative. Consequently, we will opt for the fixed gantry design because for our case the pros of a fixed gantry outweigh the cons.

Stepper Motor vs. Servo Motor

The types of motors available for CNC machines are basically of two types: Servo motors and stepper motors. The debate on which one to use has been going on for the past decade.

Table 2: Stepper Motor vs. Servo Motor

Characteristic	Stepper Motor	Servo Motor
Cost	Stepper motors are less expensive than servo motors with the same power rating.	Servo motors are more expensive than stepper motors with the same power rating.
Efficiency	Stepper motors consume more power and produce more heat and operate at about 70% efficiency.	Servo motors are more efficient yielding between 80% and 90% under light loads.
Braking Capabilities	Stepper motors brake extremely well.	Servo motors do not brake as well as stepper motors.
Torque at High Speed	Stepper motors rapidly lose torque at 90% of their maximum rpm.	Servo motors maintain their rated torque up to about 90% of their no-load rpm.
Motor Life	Stepper motors only have one wearing part resulting in longer motor life.	Servo motor brushes should be replaced every 2,000 hours or operation. Servo motors also have encoders that may need to be replaced periodically.
Reliability	Stepper motors are extremely reliable in a wide range of environments.	Servo motors are less reliable than stepper motors because of the encoder. The overall reliability or servo motors is also dependent upon the environment and how well the motor is protected.

The most critical part of CNC design is the calculation of cutting forces that the gantry and bed bears. This is because these are the largest forces which the machine needs to overcome to perform the necessary milling operations. These cutting forces are a

function of the work piece material, the chip thickness, the cutting configuration, the milling tool and many other factors. Our CNC gantry and bed must bear these cutting forces to work properly. Therefore, the computation of these forces is so vital.

The first approach that can be used to compute the cutting forces is by experimentally finding force coefficients on a test setup described below:

$$F_x = -\frac{N_t a}{4} \times K_{rc} \times c - \frac{N_t a}{\pi} \times K_{rc}$$

$$F_y = \frac{N_t a}{4} \times K_{tc} \times c - \frac{N_t a}{\pi} \times K_{tc}$$

$$F_z = \frac{N_t a}{4} \times K_{ac} \times c - \frac{N_t a}{\pi} \times K_{ac}$$

These are the cutting forces that are encountered during a milling operation. However, we don't know the above cutting force coefficients. To compute these below describe experiment needs to be setup:

- Select material to be milled.
- Set up a tube of that material on a lathe.
- Orient the turning tool with 0 inclination angle, flat rake face and no chip breaker.
- Select speeds most often used in your application.
- Measure cutting forces using dynamometer
- Repeat test for a range of feed rates.
- Run the cutting coefficient identification algorithm.

Once these coefficients have been found we can find the cutting forces that will be established on our custom-made CNC. The force coefficients will obviously remain the same and all other variables in the above equation are available.

The second procedure of computing these coefficients is by first computing the spindle power. This spindle power computation is done by using the following formula which has been found and proven by vigorous experimentation. The power required to cut a material depends upon the rate at which the material is being cut and upon an experimentally determined power constant, K_p , which is also called the unit horsepower, unit power, or specific power consumption. The power constant is equal to the horsepower required to cut a material at a rate of one cubic inch per minute. The formula to compute the power is as follows:

$$P_c = K_p C Q W$$

K_p is the power constant, Q is the material removal rate, C is the feed factor for power constant & W is the wear factor.

Once, this power has been calculated, find the cutting torque using the RPMs used. Use this torque and the geometry of the milling tool to compute the tangential force on the tool which is in fact the cutting force on the tool.

Linear Actuation Mechanisms

To ensure that our tool heads transverse in 3D space, we need linear actuation mechanisms. Actuation mechanisms help the tool heads to move in predetermined tracks with desired motion characteristics like velocity and acceleration. Linear actuation mechanisms can be of various types like mechanical actuators, hydraulic actuators and pneumatic actuators. For CNC milling and 3D applications usually mechanical actuators are used due their design versatility and easy numeric control.

Mechanical Actuators

Mechanical actuators convert the rotational motion of motors to linear motion of axis of the CNC machine. They make use of various components like ball screws, lead

screws or timing belts to convert rotational motion to translational motion. Along with these motion transformation mechanisms, guide ways are used to help the entire structure transverse in predetermined locations with minimal friction along the path of motion. Different types of guideways are used in CNC machines. Some major options that are available are:

Linear Motion Guideways

LM guideways, also known as linear motion bearings, are mechanical components that bear the machining loads and help the translation in axis, minimizing the frictional hindrances and hence maximizing the accuracy and precision of the CNC machine. Linear motion guideways make use of the basic physical phenomenon that rolling friction is way less than the sliding friction. Compared to the sliding counterparts its coefficient of friction is 1/50.

Round Shaft Guideways

Round shaft guideways also make use of lower kinetic friction, but they are way much cheaper than linear motion guideways. The bearings are the most important part of the round shaft technology-based machine drive system which helps to transmit the motion in linear direction by minimizing the friction. Debris is not a concern for round shaft guideways, but they are usually not as much accurate and compact as LM guideways.

LM guideways are preferred over round shaft guide ways. Following table lists the pros and cons of both available options:

Table 3: LM Guideways vs. Round Shaft Guideways

Parameter	LM Guideways	Round Shaft Guideways
Friction	Friction coefficient is 0.004 for ball type and 0.003 for roller type LM guideway. Both Friction coefficient is almost same. Circulating balls in the linear carriage help to reduce the friction coefficient.	Friction coefficient is low but higher than the friction coefficients of LM guideways.
Positional Accuracy	A key advantage of LM guide rails is high positioning accuracy, especially useful in milling and grinding machine tools. They hold from 0.0002 to 0.001 in. over a length of 10 ft, with typical 3 to 10- μ m/m parallelism between the bearing guide and rail.	Round rails can hold a travel straightness of 0.01-in. for 10 ft. To attain this accuracy, they need to mount only at the ends, although many are supported at several points or along their full length.
Structural Rigidity	LM guideways have minimal play because of preload and hence they have high static rigidity. LM guideways have equal loading capacity in all directions. Hence higher load capacity, stiffness and accuracy.	Round shaft guideways are prone to mechanical play and hence they don't have that much static rigidity. Round shaft guideways have lower load capacity and stiffness.

<p>Assembly allowances</p>	<p>Square-rail designs are especially sensitive to flatness errors that can cause binding and high drag that can cut life in half. Surfaces must be carefully prepared, or the parts shimmed and adjusted during installation, adding to costs.</p>	<p>Advantage of round-rail bearings is the ability to run smoothly when mounted to less-than-perfect surfaces, often defined as a flatness error greater than 150 $\mu\text{m}/\text{m}$. Shaft guideways are more forgiving of misalignment and poor parallelism.</p>
<p>Speed</p>	<p>Since, linear guideways have little friction resistance, only small driving force is needed to move a load. So, high speed motion is possible with a low driving force.</p>	<p>Not suitable for very rapid acceleration applications. At high working speeds they can be noisy and shaky, thus reducing the accuracy and precision.</p>
<p>Maintenance</p>	<p>Maintenance is quite easy because grease can be easily supplied through the grease nipple on the linear guideway block.</p>	<p>In round shaft guideways it can be quite difficult to supply enough lubrication to the contact surfaces because finding an appropriate lubrication point is not easy.</p>
<p>Reliability</p>	<p>LM guideways can be more reliable and accurate if installed on flat surfaces, following the recommended installation procedure.</p>	<p>Shaft guideways, no doubt are forgiving to misalignments and poor parallelism but they are not much reliable because of lower structural rigidity and stiffness.</p>

Ball Screw

A ball screw is an actuator that translates rotational motion to linear motion with little friction. A ball screw consists of a threaded shaft and a nut, and either one can act as the traversing component. Ball screws work in a similar fashion to ball bearings, where hardened steel balls move along an inclined-hardened inner and outer race. A threaded shaft provides a helical raceway for ball bearings which act as a precision screw. Also, able to apply or withstand high thrust loads, they can do so with minimum internal friction. They are made to close tolerances, so they are suitable for use in situations in which high precision is needed. To maintain their inherent accuracy and ensure long life, great care is needed to avoid contamination with dirt and abrasive particles.



Figure 1: Ball Screw

Trapezoidal

A leadscrew is a screw used as a linkage in a machine, to translate turning motion into linear motion. Because of the large area of sliding contact between their male and female members, screw threads have larger frictional energy losses compared to other linkages. They are not typically used to carry high power, but more for intermittent use in low power actuator and positioner mechanisms. Lead screws are used in a



Figure 2: Lead Screw

very broad range of applications, sold as individual products or incorporated into screw jacks and electro-mechanical actuators. As with screw jacks, Industrial automation, medical, defense and transport applications are particularly popular lead screws. Leadscrews are a key component in electric linear actuators.

Timing Belt

A timing belt is a flexible belt with teeth molded onto its inner surface. It is designed to run over matching toothed pulleys or sprockets. It is used in a wide array of in mechanical devices, e.g., high-power transmission is desired. This has no slippage and is often used to transfer motion for indexing or timing purposes. As it has no slippage so that the pulley and the belt always move together. They are made of rubber or

other flexible polymer, reinforced with very tough tensile fibers, usually glass, running lengthwise. The tensile fibers are what give timing belts their resistance to stretching.



Figure 3: Timing Belt

Rack & Pinion

Rack and pinion are mechanical device consisting of a bar of rectangular cross section. Rack and pinion having teeth on one side that meshes with teeth on a small gear. The pinion may have straight teeth, as in the figure, or helical teeth that mesh with teeth on the rack

that are inclined to the pinion-shaft axis. If the pinion rotates about a fixed axis, the rack



Figure 4: Rack & Pinion

will translate; i.e., move on a straight path. Some automobiles have rack-and-pinion drives on their steering mechanisms that operate in this way. A rack and pinion with two racks and one pinion is used in actuators. For example, in a rack railway, the rotation of a pinion mounted on a locomotive or a railroad car engages a rack placed between the rails and helps to move the train up a steep gradient.

Table 4: Different Actuators

Parameters/Actuators	Ball Screw	Trapezoidal	Timing Belt	Rack & Pinion
Cost	*	***	****	*
Structural Rigidity	****	***	**	****
Replaceability	**	**	****	*
Reliability	****	**	*	****
Backlash	****	**	*	****
No Slipping	****	***	*	****
Accuracy & Precision	****	***	**	****

Very Good (****) Good (***) Satisfactory (**)

Adequate (*)

Electronics

We discussed in detail the mechanical components of the hybrid CNC machine. This portion of the project report will discuss the major electronic components and circuitry that would be responsible for the working of the machine. Linear actuation mechanisms are driven by electric motors. Stepper motors and servo motors can be used for this purpose. Focus of electrical systems is to control the stepper motors to transverse the tool head in 3D space with motion parameters as demanded by the operation. 3D printers, laser engravers and CNC machines have different range of operating parameters

like velocities and accelerations. We need to select the motors that can fulfill our requirements according to each mode of the hybrid CNC machine. Apart from the stepper motors, these machines have secondary accessories along with the main tool head that needs to be controlled by the controller. Various controllers are available for each type of machine like:

- Ramps 1.4 (Typically used for 3D printers)
- GRBL CNC shield (Typically used for 2D plotter machines and CNC milling machines)
- Eleks Maker Driver Board (Typically used for laser engravers)
- Breakout Boards (Typically used for 3-axis and 5-axis CNC machines)

CNC machines, 3D printers and laser engravers have one thing in common that is the axis traversing mechanism. So, we can use any controller board that can control 4 stepper motors at a time. Along with the stepper motors we also need to control various primary and secondary accessories, like the RPM of spindle for proper milling operations, temperature of heating bed and hot end for better 3D printing, limit switches for homing our hybrid CNC machine, 3D printer extruder stepper motor to push the filament through the hot end, power of the laser module according to the operation, turning on and off the laser module and spindle. We need a controller that enables us to control all these accessories of our hybrid CNC machine.

Table 5: Different Boards Comparison

Parameters/Boards	RAMPS 1.4	CNC Shield	Eleks-Maker Driver Broad	5-Axis Breakout Board
No. of stepper motor	5	4	3	5
Micro stepping	Up to 1/128 (Recommended 1/32)	Up to 1/32	Up to 1/32	Up to 1/128
No. of end stops	6	6	0	3
3-D printing accessories (Thermistor + Fans + Hotend)	Supported	Not Supported	Not Supported	Not Supported
Spindle speed control	Not Supported	Supported	Not Supported	Supported
Laser power control	Not Supported	Supported	Supported	Not Supported

Stepper Motor Driver

Stepper motor drivers are specifically designed to drive stepper motors, which are capable of continuous rotation with precise position control, even without a feedback system. Stepper motor drivers offer adjustable current control and multiple step resolutions, and they feature built-in translators that allow a stepper motor to be controlled with simple step and direction inputs. The modules are generally basic carrier boards for a variety of stepper motor driver ICs that offer low-level interfaces like inputs for directly initiating each step.

An external microcontroller is typically required for generating these low-level signals. Stepper drives work by sending current through various phases in pulses to the stepper motor. There are four types of drives which include wave drives, two-phase on,

one-two phase-on drives and micro stepping drives. Microcontroller based steppers drivers can achieve very high rotation speeds in stepper motors. Using a microcontroller, it is possible to have extreme control over exactly how each individual coil is energized inside the motor. This is necessary to obtain high speeds because as speed increases, timing of the coils firing must be perfectly in sync.

After some of the background study we came to know some of the most used stepper motor driver in the market. So, we compare all those drivers in the shown below table.

Table 6: Different Boards Comparison

Specification/Drivers	TB6600	A4988	DRV8825	TB6560	Units
Rated Voltage	9~42	8~35	8.2~45	7~32	V
Logic Input Voltage	3~5.5	3~5.5	-0.3~5	0.5~5.5	V
Output Current	0.5~4.0	±2	1.5	0.6~3	A
Micro Step	1, 1/2, 1/4, 1/8, 1/16, 1/ 32	1/2, 1/4, 1/8, 1/16	1, 1/2, 1/4, 1/8, 1/16, 1/ 32	1, 1/8, 1/16	-
Temperature	-10~45	-20~85	-40~150	0~50	°C

CHAPTER 3: METHODOLOGY

After the process of literature review, our next task is to implement the knowledge we gained to design our CNC hybrid machine which can 3D-print, laser engrave and mill at the same time while not compromising performance. Milling is the process which pushes the physical limits of the structure of a CNC. Hence, if our CNC can properly perform milling operations without deformations beyond our set tolerances then it will also be able to laser engrave and 3D-print.

There are many ways to perform structural analysis of our gantry and moving bed. Stress analysis is imperative, and modal analysis also ensures a foolproof design of the machine.

The first step in the design of any CNC machine is the computation of cutting forces. Two methods were discussed in the literature review. When it comes to our case, the first problem we face is that in our university we cannot setup the cutting force experimental setup described in literature review. Unavailability of the dynamometer and a custom lathe tool manufacture for orthogonal cutting forces us to abandon that approach of design. Moreover, the second approach is a well scrutinized approach which has been vigorously tested and perfected. It also provides an accurate result for the purposes of hobbyists CNC, and the procedure is also easy to use.

Cutting Force Calculation

$$P_c = K_p C Q W$$

To calculate the spindle power, we formed an excel file in which we computed the spindle power for various depths and widths of cut for wood. Here, the recommended values of cutting velocity and chip load were used and various coefficients were obtained from numerous sources. Once our code gave us a spindle power, we input this spindle

power against RPMs to get the torque. Finally, the torque was divided by the radius of the cutting tool to get the cutting force. The various calculations have been linked in the appendices.

Maximum Force Calculation

Our hybrid CNC machine is structurally loaded by only one of the modes of the machine that is CNC milling. 3D printing and laser engraving have no tool head and workpiece interactions, so no loads on the CNC structure. On the other hand, milling is the process where tool shears through the workpiece to produce chips of desired thickness. Due to this workpiece and tool interaction the tool experiences some cutting forces which are explained in the literature review section. This force is calculated for a milling operation using the power required for that operation that is computed using material removal rate and other milling parameters for that process. This force comes to be 200N. This force is the tangential component, which is about 80 percent of the total cutting force. The radial component of force is 0.8 times the tangential component, and it is computed to be 160N. The resultant cutting force comes out to be about 255N. We will be using a cutting force of 400N in our future calculations to cater for tool tramming and run out issues.

As far as the spindle power is enough to enable the tool shear through the workpiece the only force acting on the entire CNC frame is the cutting force that is computed to be 400N. If the spindle is stuck while rotating and is unable to cut through the material and the stepper motor continues to push the tool through the workpiece, tool will experience some bigger forces. We need to compute this force to ensure the structural integrity of our CNC machine. This force is equal to the axial thrust produced by the stepper motor under this scenario. This force is dependent on the maximum torque that can be applied by the stepper motor i.e. 3.1Nm in our case. So, when a 3Nm stepper

motor pushes the stuck tool through the workpiece the force experienced by the tool is computed to be 3800N.

Linear Bearing Selection

There are two rules which govern the geometric constraints of rails and linear bearings.

- The 2:1 rule states that for every inch between the bearings, the payload's center of gravity (COG) should not go any further than two inches from this rail.
- The 5:1 rule states that for every inch between the rails, you need to make sure that your COG is within five inches.

When we apply these rules, the distance between rails of x-axis is easily found.

- X-axis geometric locations of linear bearings and linear rails is:
 - The distance between rails is 110mm
 - The distance between linear bearings on the same rail is 86.3mm
- Y-axis geometric locations of linear bearings and linear rails is:
 - The distance between rails is 175mm
 - The distance between linear bearings on the same rail is 86.3mm

This means that we now know the locations of linear bearings and linear guide rails on the CNC on x- axis.

Now we will calculate the static load on the linear bearings. We assumed the worst-case scenario on our CNC and used the maximum force computed above in the methodology section to compute the static load. This static load was computed by using the linear bearing force distribution formulas provided in appendix 1.

The bearing with the maximum static load is selected and this load is multiplied by the static load safety factor. Now we have the static load rating computed. This static

load rating is compared with the linear bearing tables and a bearing with higher static load is selected.

The life of the bearing can also be computed. Since we have selected the bearing, we know its dynamic load rating. This dynamic load rating is used with the loads calculated previously to find the life of the bearing.

- The life of x- axis bearings is 330km
- The life of y-axis bearings is 174km

Clamp Design

To design the clamp, we first need to know where and how the clamp will be used in our CNC. We know that the clamp will face the maximum force (previously discussed in literature review) during the worst-case scenario. Also, our clamp must be strong enough to provide a rigid support for the spindle to which it is attached. we will perform the stress analysis on the clamp using the above force as an input.

Our flow work process is first performing manual calculations (requirement of FYP) and then transferring them on MathCAD, then executing FEM analysis and finally writing a corresponding MATLAB code.

Flow work process

- We formed a database of all the necessary analysis calculations on MathCAD. Calculations are in the Appendix I.
 - Forces were translated from the spindle onto the clamp.
 - Tensile and shear load calculation in clamp bolts.
 - Bolt design and bold load factor calculation.
 - Bearing stress calculation due shear force of bolt holes.
 - Bending stress calculation in clamp.

- We proof-checked our clamp design against the MathCAD calculations by performing FEM analysis on SolidWorks.
 - First a proper CAD model was made on SolidWorks.
 - To perform FEM analysis loads and material was defined.
 - Fixtures and contact sets were defined.
 - Direct sparse solver and FFEPlus solver were run, eventually completing the analysis.
- We finally formed a code on MATLAB of our design calculations.

Our focus was on calculating stresses the clamp would bear and the bolt stresses induced.

The stresses and load factors produced were as follows:

Table 6: Results of Clamp

Clamp		
Stress	Value	Units
Bearing stress	226	MPa
Shear Stress	5.93	MPa
Bending Stress	99.7	MPa
Bolt Shear Stress	339.2	MPa
Load Factor	3	--

X-Axis Plate Design

To design the plate, we first need to know its exact purpose and need of incorporation. We need the plate to attach the spindle to the linear rail bearings on the x-axis. Hence, this implies a geometric constraint on the x-axis plate (due to the 5:1 and 2:1

rules of linear bearings). Moreover, the bolts on the plate should be far apart from corners and edges such that no end to end distance is more than 1.5 diameters of a bolt.

Now, once again we will analyse the plate for stresses and shears. Bolt design will also be analyzed. The x-axis plate must be strong enough to bear the maximum force because of the worst-case scenario and provide a rigid support for the clamp and spindle assembly. Hence, this force will be used as an input in our design analysis.

Our flow work process is first performing manual calculations (requirement of FYP) and then transferring them on MathCAD, then executing FEM analysis and finally writing a corresponding MATLAB code.

Flow work process

- We formed a database of all the necessary analysis calculations on MathCAD. Calculations in Appendix.
 - Forces were translated from the spindle onto the x-axis plate.
 - Tensile and shear load calculation in x-axis plate bolts.
 - Bolt design and bolt load factor calculation.
 - Bearing stress calculation due shear force of bolt holes.
- We proof-checked our clamp design against the MathCAD calculations by performing FEM analysis on SolidWorks.
 - First a proper CAD model was made on SolidWorks.
 - To perform FEM analysis loads and material was defined.
 - Fixtures and contact sets were defined.
 - Direct sparse solver and FFEPlus solver were run, eventually completing the analysis.
- We finally formed a code on MATLAB of our design calculations.

The results produced were as follows:

Table 7: Results of X-Axis Plate

X-Axis Plate		
Stress	Value	Units
Bearing Stress	31.5	MPa
Normal Stress	2.7	MPa
Bolt Shear Stress	130.7	MPa
Load Factor	1.61	--

Z-Axis Plate Design

To design the plate, we first need to know its exact purpose and need of incorporation. We need the plate to attach the x-axis gantry components on the linear bearings of z-axis. Hence, this implies a geometric constraint on the z-axis plate (due to the 5:1 and 2:1 rules of linear bearings). Moreover, the bolts on the plate should be far apart from corners and edges such that no end to end distance is more than 1.5 diameters of a bolt.

Now, once again we will analyze the plate for stresses and shears. Bolt design will also be analyzed. The z-axis plate must be strong enough to bear the maximum force because of the worst-case scenario and provide a rigid support for the clamp and spindle assembly. Hence, this force will be used as an input in our design analysis.

Our work-flow process was as followed:

- We formed a database of all the necessary analysis calculations on MathCAD. Calculations in Appendix.
 - Tensile load calculation in z-axis plate bolts.
 - Bolt design and load factor calculation

- Bearing stress calculation due to bolt tensile load and shear force.
- Shear load and stress calculation.

The results produced were as followed:

Table 8: Results of Z-Axis Plate

Z-Axis Plate		
Stress	Value	Units
Load Factor	3.89	--
Normal Stress	2.84	MPa
Bearing Stress	28.3	MPa
Bolt Shear Stress	32.8	MPa

Spindle Selection

CNC milling is a crucial manufacturing process employed for the production of parts that cannot be produced by 3D printing or laser cutting. Like the products where structural strength and stiffness are needed to be analyzed in the prototype. Currently, we are aiming to mill wood on our CNC machine. There are variety of CNC spindles and routers available for milling. CNC spindles are generally characterized as DC and AC spindles. AC spindles are generally more expensive than the DC spindle because they have a wide range of rpm and they promise higher torque. AC spindles also require VFD for rpm regulation on the other hand DC spindles can be controlled easily by some microcontroller like Arduino Mega 2560 and secondary electronics like speed regulator circuits. We decided to choose DC spindle for our hybrid CNC machine because of the budget constraints and the compatibility of these spindles with our controller.

DC spindles are available in variety of rpm ranges and output powers. We need to select an appropriate spindle for our application. Following are the milling parameters for wood milling operations:

Table 9: Feed Per Tooth for Different Tool Diameter & Workpiece

Tool Diameter	Hard Woods	Softwood/ Plywood	MDF/Particle Board	Soft Plastics	Hard Plastics
3mm	0.08-0.13	0.1-0.15	0.1-0.18	0.1-0.15	0.15-0.2
6mm	0.23-0.28	0.28-0.33	0.33-0.41	0.2-0.3	0.25-0.3
10mm	0.38-0.46	0.43-0.51	0.51-0.58	0.2-0.3	0.25-0.3

The cutting velocity for milling wood is recommended to be within 183 to 305 MPM. Using this cutting velocity and the recommended chip loads we calculate the rpm required to mill a specific type of wood. We select the spindle based on various rpm values that we obtain after the analysis of milling parameters.

As far as the power of the spindle is concerned, it can be computed for different milling operations using the width of cut, depth of cut, RPM and some other coefficients like machine tool efficiency factor, tool wear factor, feed factor and power constant.

Table 10: Different Milling Factors and their operation.

Factors	Operation Type	Value
Tool Wear Factor for Milling	Light and medium face milling operation	1.10-1.25
Power Constant	For wood	0.25
Machine tool efficiency factor	Ball screw drive	0.8-0.9

We computed spindle power required for some light milling operations on wood, using excel. We changed the DOC, WOC and tool geometry and studied how it affects the power required for that milling operation. 500W Chinese spindle was selected because it has a wide range of RPM (3,000 to 12,000) and adequate power for milling wood and plastics.

Table 11: Chinese Spindle

Spindle	Power (W)	RPM	Torque (Nm)	AC/DC	RPM Controller	Weight (kg)
Chinese Spindle	500	3000-12000	0.59	DC	PWM spindle speed controller	2

Stepper Motor Torque Calculation

Linear actuators are major components of CNC machines. Linear actuators are driven by the stepper motors. Stepper motor torque calculations are the crucial part of our design analysis. The torque required to traverse the axis in each direction is equal to the sum of load or running torque and acceleration torque. The stepper motor calculations are shown in the Appendix I. We selected 3Nm torque model 57SHD4934 -34B for our application.

Table 12: Stepper Specification

Hybrid Stepping Motor 57SHD4934-34B		
Parameter	Value	Unit
Step angle	1.8	°
No.of phase	2	
Insulation resistance (min)	1E+11	Ω
Rotor inertia	650	g.cm ³
Mass	1.3	kg
Rated voltage	8.4	V
Rated current	3	A
Resistance per phase	2.8 ± 10%	Ω
Inductance per phase	11 ± 20%	mH
Holding torque	3000	mNm
Detent torque	100	mNm

Electronics

Electronics is an essential part in any machinery for proper working and operation of the machine. CNC machines have the ‘Brain’ to do the processing and ‘muscle’ to do the working. But it’s the controller that connects them. As we are combining three different types of machine in a single unit, for that to happen to perform we can’t just use different electronics for each of it. It would work but that wouldn’t be a good design, so we had faced some challenges to go through the variety of available options for CNC controllers and firmware, to come up with a unique solution to control our machine affectively and to properly cater all our requirements from 3 different modes of our Hybrid CNC machine. To attain maximum functionality from our CNC machine, we needed to control the following using a single controller:

4 NEMA 23 stepper motors

We need precise and controlled motion in 3 axis. To power the linear actuation mechanisms accordingly we need two stepper motors one for each X-Axis and Y-Axis and two more stepper motors for Z-axis because we have dual ball screw arrangement for the Z-axis to increase the workspace for our Hybrid CNC machine. In number of controllers, we had the option for controlling 4 stepper motors even some controllers allow the control of 5 stepper motors. We need to select a controller which allows us to control 4 stepper motors. Moreover, we must avoid selecting the controllers with built in stepper motor drivers. As we aim to use NEMA 23 57SHD4934-B, we must use better driver to handle large currents. It’s one of the requirements for our CNC so we had to explore the options depending upon other factors and need to choose the best controller for our machine.

3D printer extruder stepper motor

3D printers use stepper motor to feed the filament to the hot end. The rate at which the filament is fed may vary according to the filament being used, nozzle dimension and printing speed. The 3D printer extruder has a stepper motor which is responsible for controlled feeding and retraction of the filament to optimize the 3D print results. For precise and controlled feeding of the filament, the extruder stepper motor needs to be controlled. So, the controller must have the 5th slot to monitor and guide the motion of extruder stepper motor.

Heating bed PID temperature control for 3D printer

To optimize and improve the 3D print results, heated beds are used to provide optimum temperatures to the first print layers to adhere properly to the bed, providing solid base for the print to begin. Heat beds provide more controlled cooling of the prints preventing defects like warping and poor adhesion. Mostly 12V PCB heat beds are used, as they pose an affective and cheap solution. So, the controller we select must have the ability to power such heat bed and to monitor its temperature for more improved printing results.

CNC spindle rpm control

CNC milling is a numeric controlled process. The end results and finish of the milling procedure depends on the structural rigidity of the CNC machine and on how close our spindle RPM are to the theoretically calculated value. A CNC machine must have the ability to adjust the spindle RPM according to the G-Code commands, maintaining that RPM is another milestone which must be achieved for much better milling performance and surface finish. The spindle RPM control needs auxiliary circuitry and electronics to work properly. The main CNC controller must be capable of

sending 0-5V PWM signal to the DC spindle speed controller, to adjust the spindle RPM according to the G-Code commands.

PWM/TTL modulation signal for laser

Laser modules are effective for engraving and cutting purposes. For much better cutting performance and gradient laser engravings the laser power needs to be monitored via G-Code. A proper combination of laser power, speed and focus, gives fabulous cutting and engraving results. Laser power can be adjusted using PWM/TTL modulation. The laser that was selected for this Hybrid CNC machine, came with a TTL modulation board, which needs a 0-5V PWM signal to control the laser power. The main CNC controller must be capable of sending 0-5V PWM signal to the TTL modulation driver of the laser module to adjust the laser power according to the G-Code commands.

Hotend temperature control for 3D printer extruder

3D printers use hot ends to melt the fed filament properly and to deposit the filament layer by layer to complete a print. Hotend needs to be heated up to the desired temperatures throughout the print according to the filament being used. So, the controller we select must have the ability to power such hot end and to monitor its temperature throughout the print for smooth functioning of the 3D printer and to avoid nozzle clogging and filament overheating.

Fans for 3D printer

Fans are crucial part of 3D printers and CNC machines. They help to keep the electronics and power supplies cool. The fans on the hot end sink help to dissipate the unnecessary heat. Fans close to the nozzle help to cool the freshly extruded filament. They require variable voltages ranging from 0V-12V, such a controller which have this ability will be chosen.

Controllers

Various controllers are available in the market to control CNC machines. But most of them are dedicated for one machine mode. To meet all our requirements, we may need auxiliary circuitry. We need to select the controller such that we must use minimum auxiliary circuitry and electronics.

Ramps 1.4 with Arduino Mega 2560

Ramps 1.4 is the controller dedicated for 3D printers. Ramps serves as the interface between the Arduino Mega 2560, the brain of the machine and the electronics responsible for physical operation of the machine. The main computer controlling the CNC machine translates the G-Code commands to the digital signals. Unfortunately, Arduino Mega doesn't have enough capability to control the CNC machine hardware solely. This is where Ramps 1.4 comes, it takes the information from the Arduino Mega, amplifies it and direct it down to the proper hardware like stepper motor drivers, thermistors and heaters. Ramps 1.4 is probably the most commonly used electronic hardware for the control of CNC machines. It has sockets to provide signals to five stepper motor drivers. Three of them are dedicated for axis stepper motors, while the other two are for 3D printer extruders. These terminals can be used to power the fan and to control its speed. Three thermistors are also integrated in the Ramps board to interface with the devices connected to the heater terminals to intelligently monitor and control the temperatures. Ramps board have additional pin outs that allow for the easy connections for auxiliary electronics like servo motors, LEDs, LCD, fans, Bluetooth module, CNC spindle control driver and laser module driver.



Figure 5: Ramps 1.4

GRBL CNC shield with Arduino UNO

GRBL CNC shield is a drive expansion board that was designed by Protoneer.co.nz. It is designed to be compatible with GRBL firmware. It is dedicated for CNC milling machine control, but it can be used for other types of machines like 3D printers and laser engravers. However, the functionality might be limited due to the small number of pinouts available for dedicated tasks. For complete control we might need auxiliary circuitry. A CNC shield allows the precise motion control of four stepper motors, via removable pololu drivers. It allows for six end stops to detect the extremes of all axis. It has 14 digital input/output pins which can be used to control the CNC machine accessories. Out of these 14 pins, 6 can be used as PWM outputs. CNC shield has pins to control the spindle direction and spindle speed. Same pins can be used to provide PWM signals to the TTL modulation board to control the laser power.

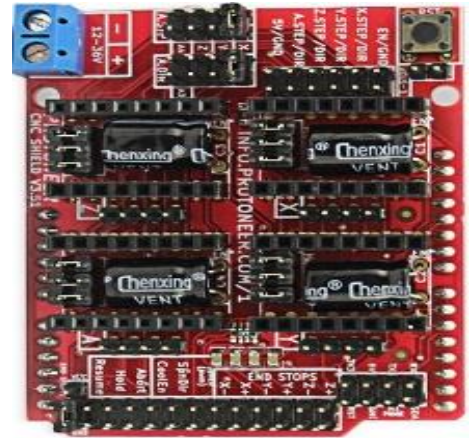


Figure 6: GRBLCNC Shield

MACH3 CNC Breakout Boards

CNC breakout boards as the name suggests are usually designed to control milling machines. They overpower the use of the Arduino and communicate directly with the PC via parallel port. They have multiple relays to interface with the CNC hardware. Mostly they are compatible with MACH, Linux CNC (EMC2) etc. A 5 axis CNC breakout board can guide five stepper motors.



Figure 7: MACH3 CNC Breakout Boards

They have limited pinouts to interface with the limit switches and other sensors for tool length compensation and auto leveling. As they are dedicated for CNC milling machines, they provide 0-10V analogue voltage for the Variable Frequency Drive to control the spindle direction and speed.

Table 13: Selection for controller

Qualities/Controllers	Ramps 1.4	GRBL CNC Shield	MACH3 CNC Breakout Board
No. of Stepper Motors	5	4	5
End Stops	6	6	6
Micro-Stepping	1/32	1/32	1/32
Heating Bed PID Control	Yes	No	No
Hotend PID Control	Yes	No	No
Spindle RPM Control	Yes	Yes	Yes
Laser Power Control	Yes	Yes	Yes
Fans	Yes	Yes	Yes
LCD	Yes	No	No

Firmware

Now let's consider some options available for the firmware. Various open source firmwares are available for dedicated machines, but we must choose the one with flexible and versatile operation capabilities. Some of the firmware options that we considered for our Hybrid CNC machine were:

Marlin

Marlin is an open source firmware dedicated for 3D printers. Apart from running on the 3D printers, Marlin can also drive CNC milling machines and laser engravers.

Marlin is compatible with a range of hardware and electronics. Some of the key distinguishing features of Marlin are full featured G-Codes, smart motion system, closed loop PID temperature control for heat bed and hot ends, auto bed leveling, multiple extruder and support for filament runout sensors. Marlin is configurable for a wide variety of machines. Ramps 1.4 board is compatible with marlin firmware.

GRBL

Grbl is an open source firmware dedicated for the control of numeric control machines. Grbl supports only 3 axis. No rotary axis can be configured. Grbl includes complete acceleration management with look ahead feature. This means that the controller can look up to 18 motions into the future and plan its motion strategy to provide smooth motion and acceleration. Grbl has a laser mode, which governs the laser power depending on the motion involved. It has constant laser power mode and dynamic laser power mode. On the other hand, dynamic laser power mode automatically adjusts the laser power according to the machine motion. This helps in proper and adequate energy transfer to the workpiece. This helps in clean and precise engraving and cutting.

MACH3

MACH3 is an industrial scale firmware, that eradicate the use of low-end electronics hardware like Arduino and converts the PC into a CNC machine controller. It's typically designed to control CNC machines. It has variety of features like both stepper motor and servo motor motion control, spindle speed control, multiple relay control and complete panel customization. MACH3 can be used to control CNC mills and laser engravers but cannot monitor 3D printer accessories.

Table 14: Selection for firmware

Firmware/Qualities	CNC Machine Control	3D Printer Accessories Control	Autobed Levelling	Controller
Marlin	Yes	Yes	Yes	Ramps 1.4 + Arduino Mega 2560
GRBL	Yes	No	No	CNC Shield + Arduino UNO
Repetier	Yes	Yes	Yes	Ramps 1.4 + Arduino Mega
MACH3	Yes	No	Yes	CNC Breakout Boards

Controller and firmware selection decision:

Based on the comparison study made we can figure out which controller would be the best for our hybrid CNC machine setup. As discussed earlier we have plenty of requirements to be fulfilled by the controller due to the diversity of electronic hardware required in all modes of the multi-purpose CNC machine. Each controller was studied in complete detail along with the complete study of auxiliary circuitry required for each controller. As far as the control of CNC machine mode is concerned CNC breakout boards are quite ready to use for AC spindle setups. For DC spindle speed control, we need auxiliary circuit to convert the 0-10V analogue signal to 0-5V signal for the spindle speed controller. CNC machine control via Ramps 1.4 along with Arduino Mega 2560 and CNC shield along with Arduino UNO require same auxiliary circuitry to monitor the spindle RPM. Both controllers are supposed to provide 0-5V PWM signal to the DC spindle speed governor. 0V corresponds to 0 RPM and 5V corresponds to maximum RPM which in our case are 12,000. For laser engraver mode, breakout boards can be configured to give 0-5V PWM signal, which when fed to the TTL modulation board adjusts the laser power accordingly. Laser engraving machine control via Ramps 1.4 along with Arduino Mega 2560 and CNC shield along with Arduino UNO require same

auxiliary circuitry to monitor the laser power. Both controllers are supposed to provide 0-5V PWM signal to the TTL modulation board. For CNC shield this PWM output of 0-5V can be taken from the Z limit switch pin which is connected to Arduino digital pin 11. For Ramps 1.4 board, this 0-5V PWM signal can be taken from the pin 44.

For the 3D printer mode of our hybrid CNC machine, we needed a controller that effectively controls the basic electronic hardware of a normal 3D printer. Grbl CNC shield cannot control extruder stepper motor with the four-stepper motor setup for our 3-axis machine. Moreover, CNC shield is not capable of interfacing with the heaters of the heated bed and hot end for PID temperature control. CNC shield also has limited digital input output pins to control other accessories like fan, auto level sensors and LCD for future design improvements. As discussed earlier, CNC breakout boards cannot be used with the 3D printers, if somehow, we are able to connect the basic 3D printer hardware with the CNC breakout board, the firmware for such breakout boards will bottle neck the performance of our hybrid CNC machine.

Ramps 1.4 board along with the Arduino Mega 2560 was chosen as the controller for the hybrid CNC machine, due to the full 3D printer hardware control proposed by the Ramps 1.4, including 4 stepper motors, 3D printer extruders, heat bed, hot end, fans, auto level sensors, limit switches and LCD. Moreover, as discussed earlier Ramps can easily provide the PWM signals required for the spindle speed control and the laser power control. Complete circuitry will be discussed in detail in coming sections of the report.

After successful selection of the controller for the hybrid CNC machine the firmware was yet to be decided. As discussed earlier that each firmware has its pros and cons regarding the machine control. The firmware selection could be made easily by filtering from the available choices based on compatible controllers. Since we have selected Ramps 1.4 as our controller, MACH3 that usually runs on CNC breakout boards is no more a valid option for the hybrid CNC machine. Grbl has its modified versions to

make it compatible with the Ramps 1.4 board, but due to the minimal evidence of its credibility and effectiveness as a machine controller, it was not selected. Marlin is the only firmware left after critically analyzing and filtering the available options. Ramps 1.4 board is compatible with Marlin, moreover Marlin can be used to control all the three modes of our hybrid CNC machine after proper configuration and hardware selection. Marlin has some drawbacks when it comes to the laser control, it does not have dynamic laser power control to adjust the laser power according to the machine motion, which is the distinguishing feature of Grbl. But, due to the other control advantages like PID temperature control for heat bed and hot end, auto bed leveling, filament runout sensor integration and smart motion system with look ahead feature, Marlin was finally chosen as the firmware for our Hybrid CNC machine.

Wiring and Hardware Setup

External Stepper Motor Driver Wiring

Due to the design requirements of each mode of the hybrid machine, the gantry was designed to be quite beefy and sturdy to stand the deflections caused by the forces resulting from the tool and workpiece interaction. To fulfil the robustness criteria for 3D printer mode, despite the bulky gantry, NEMA 23 57SHD4934-B hybrid stepper motors were used due to their ability to provide much better torque at higher RPM than other alternatives. This comes in exchange for higher current rating than other substitutes.

Ramps 1.4 usually use removable Pololu stepper motor drivers which are usually rated for 2 amperes. NEMA 23 57SHD4934-B have rated current of 3 amperes. TB6600 stepper motor driver was selected to be used as external stepper driver for our hybrid CNC machine to deal with the higher current requirements. Ramps 1.4 has power terminal rated for 12V and 5A, to power the stepper motor drivers. This is quite low than our current requirements, so external drivers with external power supply must be used to

get the best out of the stepper motors. Following is the wiring diagram for connecting TB6600 stepper motor driver with the Ramps 1.4 board.

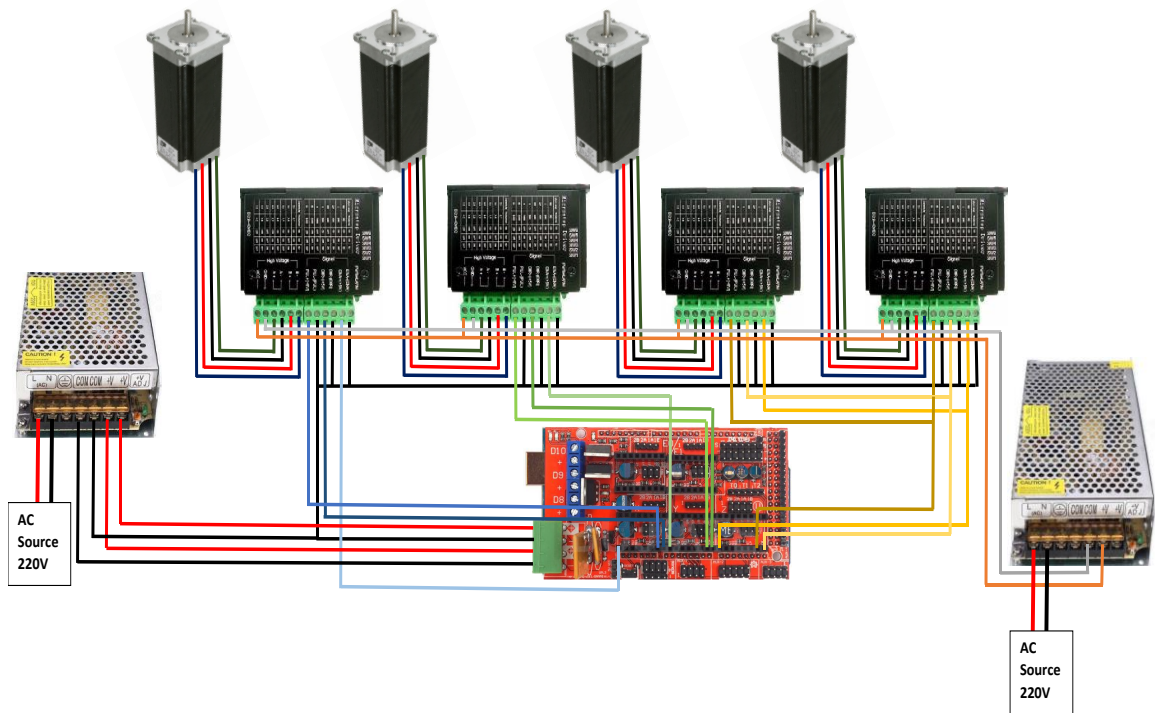


Figure 8: External Stepper Motor Driver Wiring

Laser Module and TTL Modulation Driver Wiring

For basic laser engraver functioning the controller is only entrusted with the responsibility to turn on and off the laser diode according to the G-Code commands. This can be achieved by simply using a relay to turn the laser on and off according to the G-Code interpretation coming from the controller in the form of a digital signal. For more advanced laser engraving machine operation, the laser power must be controlled with the G-Code to optimize the energy being transmitted to the workpiece. Proper combination

of laser power, speed and focus are required for precise and proper laser engraving and cutting.

Laser power can be controlled using TTL modulation laser drivers, which take 0-5V PWM input from the controller and adjust the laser power accordingly. 0V corresponds to laser off or minimum laser power. 5V corresponds to the laser on at 100% power. As Arduino has 16-bit PWM output, the 0-5V signal can be broken down to 256 discrete power levels. Marlin fan control M-Codes (M106 and M107) will be used to control the laser. M106 S0 corresponds to laser off, M106 S255 corresponds to laser on at full power and M106 S127 corresponds to laser on at 50% power.

The wiring of the TTL modulation laser driver depends on the demand of the laser module. Some laser drivers work with 0-12V input from the controller, this input can be directly drawn from the Ramps' fan output pin D9 without any modification of the firmware. Most of the laser TTL modulation boards require 0-5V signal from the controller. To control such laser modules with the fan M-Code commands we need to make few changes to the Marlin firmware to remap the fan output from pin D9 (12V) to pin 44 (5V). These changes are made in the pins_RAMPS_13.h file in the Marlin firmware folder. After the hardware connections the laser module voltage and current should be adjusted for safe and proper laser module functioning. Following is the wiring diagram for connecting TTL modulation laser driver board and laser diode with the Ramps 1.4 board.

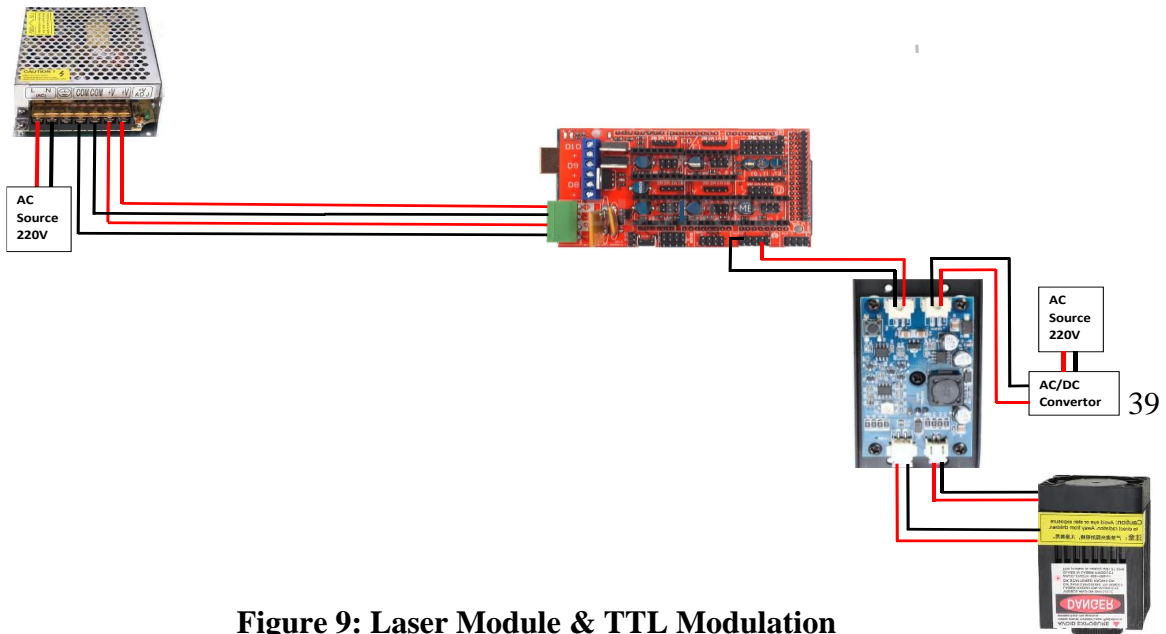


Figure 9: Laser Module & TTL Modulation Driver Wiring

CNC Spindle and DC Speed Governor Wiring

AC spindles are operated by the controller through a Variable Frequency Drive which is responsible for maintaining the said spindle RPM and torque. These VFDs are programmable and only need a 0-10V analogue voltage signal from the controller. DC spindles do not have such dedicated electronics. They are usually shipped with an AC-DC converter with a potentiometer to control and adjust the RPM according to the milling requirements. These are not responsible for maintaining the said RPM and torque under load conditions. To eradicate this manual interruption of setting the RPM via potentiometer and to control the spindle RPM through G-Code commands, we need auxiliary circuitry. DC spindle speed governor is a small controller that eliminates the need of a potentiometer to control spindle RPM. It takes 0-5V PWM signal from the controller and adjust the DC voltage provided to the spindle accordingly to adjust the RPM. This 0-5V PWM signal can be taken from the controller in the same way as it was taken for the laser TTL modulation board. Ramps 1.4 fan pin D9 (12V) can be remapped to PWM pin 44 (5V), by making changes to the pins_RAMPS_13.h file in the Marlin firmware folder.

As Arduino has 16-bit PWM output, the 0-5V signal can be broken down to 256 discrete RPM values. Marlin fan control M-Codes (M106 and M107) will be used to control the spindle RPM. M106 S0 corresponds to spindle off, M106 S255 corresponds to spindle on at maximum RPM that are about 12,000 and M106 S127 corresponds to spindle running at almost half RPM. Following is the wiring diagram for connecting the DC spindle speed governor with the Ramps 1.4 board.

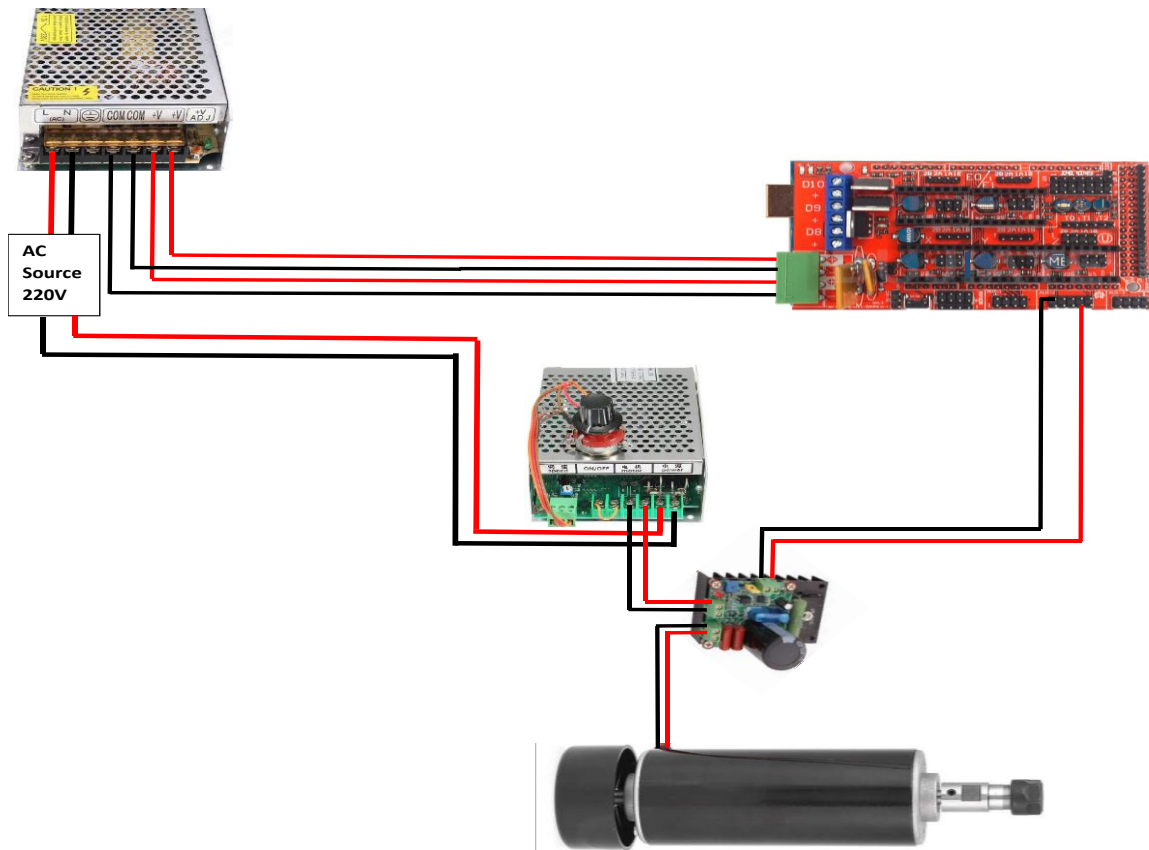


Figure 10: CNC Spindle & DC Speed Governor Wiring

Heat Bed Wiring

Heat beds are usually shipped without soldered electrical connections, due to the multiple input power options available for different controller boards. Some controllers use 24V to run the 3D printer accessories, they require the heat bed wiring connections accordingly. On the other hand, some controllers provide 12V for the 3D printer hardware. Most heat beds come with built in wiring capable to work with both input power options. The user just has to connect the power wire according to the given instructions. Heat beds have 3 pinouts with different connection scheme to handle both

12V and 24V inputs. We decided to use 12V heat bed, as our controller Ramps 1.4 is a 12V controller. One wire is connected to both pin 2 and pin 3 of the heat bed. The other wire is connected to the pin 1 of the heat bed. Proper wire gauge must be used for these connections as they would be dealing with high currents. These heater wires are connected to the D8 pin of Ramps 1.4 board. And the thermistor, attached to the heat bed, is wired to the thermistor hookup pin T1. Polarity is not an issue for this connection. Following is the wiring diagram for connecting the PCB heat bed with the Ramps 1.4 board.

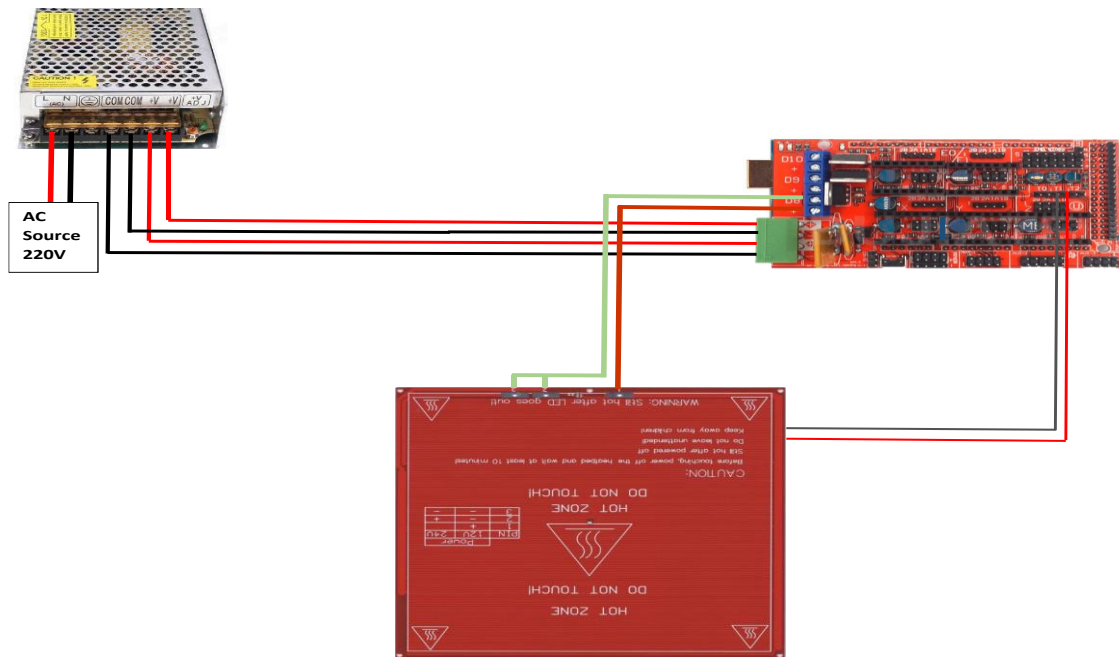


Figure 11: Heat Bed Wiring

Hotend Wiring

Hot end, the most crucial component of a 3D printer that spits molten filament at required temperature, usually comes with a total of six wires. Two from the heating carriage (This is where the heater is located), two from the thermistor in the heating

carriage (This temperature sensor is responsible for communicating with the controller for PID temperature control) and two wires from the heat sink fan (This fan is entrusted with the responsibility to cool down the heat sink and dissipate unnecessary heat). The wiring connections are simple. The heater wires from the heating carriage are connected to the D10 pin of Ramps 1.4 board. Polarity is not an issue for this connection. The thermistor wires are connected to the T0 thermistor hookup pins on the Ramps board. Polarity again is not an issue. Hot end heat sink fan has its dedicated pin slots on the Ramps board, these pins are located between the X axis stepper motor driver slot and fuses or D1 D2 diodes. Following is the wiring diagram for connecting the E3D V6 all metal hot end with the Ramps 1.4 board.

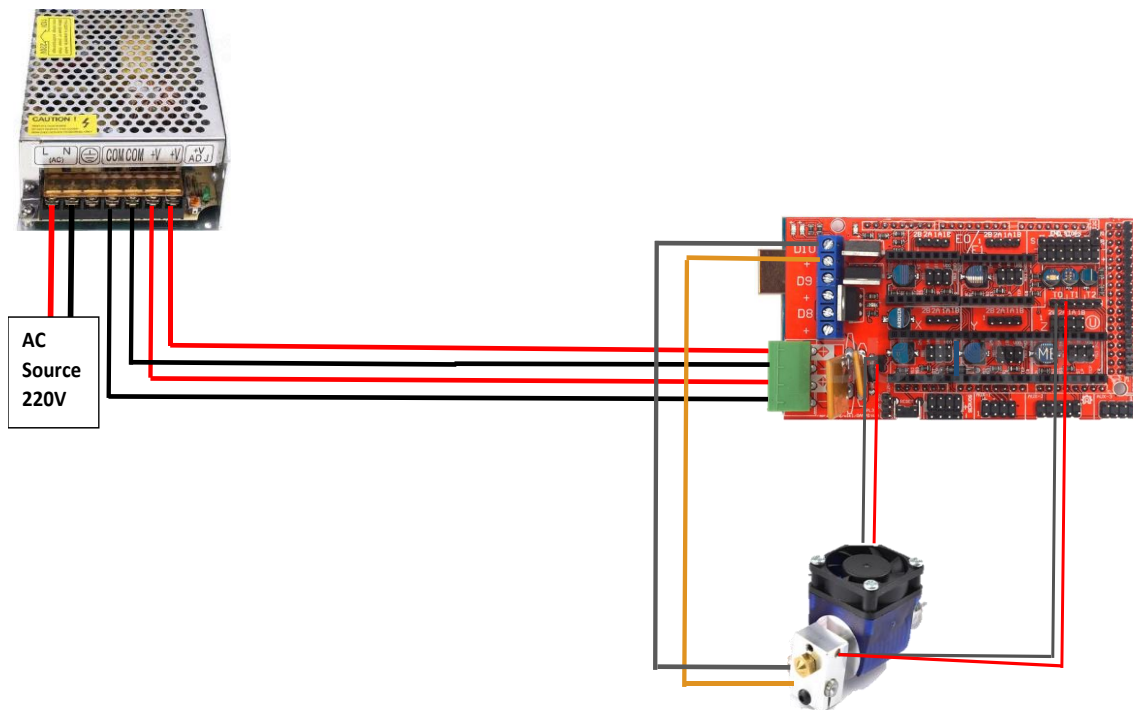
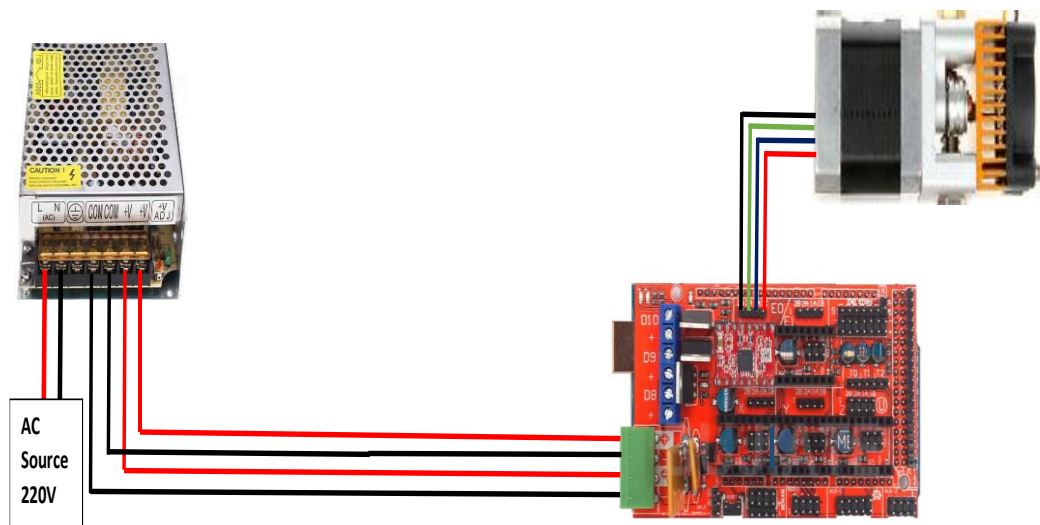


Figure 12: Hotend Wiring

3D Printer Extruder Wiring

3D printer extruder is nothing more than a stepper driver that is either geared or not for better grip over the filament and reduced torque requirements. The only connections required for the 3D printer extruder are of the NEMA 17 extruder stepper motor. NEMA 17 stepper motors are usually rated for currents under 2 amperes, usually 1.7 Amps. So, 3D printer extruder stepper motor can be controlled by the controller using removable Pololu drivers like A4988 and DRV8825. A4988 stepper drivers were used as they were readily available and economical. Following is the wiring diagram for connecting the 3D printer extruder stepper motor with the Ramps 1.4 board.



Fans Wiring

Fans are used to enhance the 3D printer finishing capabilities. One or two fans are placed close to the nozzle to dissipate the heat from the nozzle and to cool down the filament layers for much better finish of 3D prints. Part cooling fan must be monitored intelligently by the controller to get better print results. Part cooling is not required

always. It must be turned on and off according to the G-Code to smartly affect the filament cooling and print results. Some slicers provide proper cooling fan configuration that automatically decides when to turn the cooling fan on and off according to the print requirements. All we must do is to connect the fan to the pin D9 of the Ramps 1.4 board and to configure Marlin for fan control on the pin D9. To configure Marlin accordingly we need to change the power output configuration of our board in the configurations.h file. EFB is the power output configuration that we would need.

However, if we are using fan pin at Ramps PWM pin 44, for laser power control using fan M-Code commands, we must alter the configuration every time we change from laser engraving mode to the 3D printer mode. We can keep two copies of the firmware with proper configurations to reduce the time to shift between the modes of our Hybrid CNC machine and to make it as simple as plug and play. Other fans for electronics hardware cooling can be directly connected to the power source. So, as the system is powered on the fans start working. Following is the wiring diagram for connecting fans with the Ramps 1.4 board.

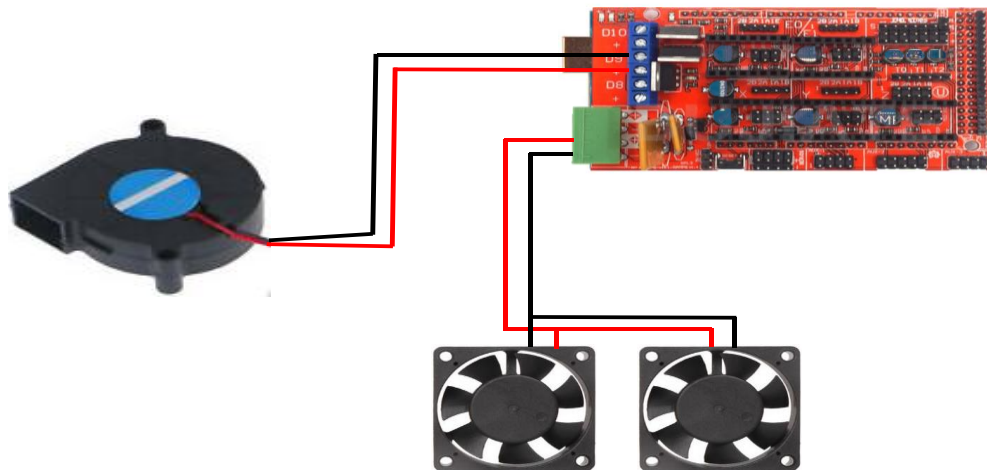


Figure 13: Fans Wiring

Mechanical End Stops Wiring

The machine's mechanical hardware communicates with the controller to operate properly. If accidentally the controller passes an instruction to the stepper driver to move beyond the physical limits of the linear actuation system, in simple words the working length of the ball screw, our CNC might crash or malfunction. Such wrong instructions can lead to accident or complete hardware failure. To avoid such catastrophic situations and to give the machine a homing reference, end stop switches are used. These might be optical or mechanical switches. Ramps 1.4 allows for the connection of 6 end stop switches. To minimize the project cost and due to the reliability of mechanical switching, mechanical end stops were used. It's not necessary to connect all the six end stops. Three end stops can be used to give the machine the idea of home position and axis zero position. For maximum position Marlin can be configured to avoid movement beyond certain distance after the zero position on an axis.

On Ramps 1.4 board end stop connection pins are on the upper right corner when the board is held with power terminal pointing towards left. From left to right we have X-MIN, X-MAX, Y-MIN, Y-MAX, Z-MIN and Z-MAX. The topmost pins are signal pins, bottom most are reference 5V pins and the middle pins are ground pins. While making connections for the 3 pin end stops, care must be taken while connecting the signal and ground wires. Wrong connections might fry the controller or the end stop. Wiring connections are simple, just connect the end stop's signal, ground and VCC wires to the Ramps signal, ground and VCC pins.

Marlin firmware allows to configure the end stop operation according to the requirement of the machine. After wiring the end stops, Pronterface or Repetier Host can be used to check the end stop status that is either it's triggered or not. M119 is the command that returns the end stop's status. End stops can be triggered manually to check whether they are working accordingly or not. If they are not, changes can be made to the

Marlin firmware to invert their trigger response routine. Changes are to be made to the configuration.h file in the Marlin firmware folder. End stop trigger response can be altered by setting their respective const bool variables to true or false.

After the proper end stop configuration, Marlin can be configured to properly home the machine and to set the maximum limits in the software to avoid movements beyond desired limits. Following is the wiring diagram for connecting the mechanical end stop with the Ramps 1.4 board.

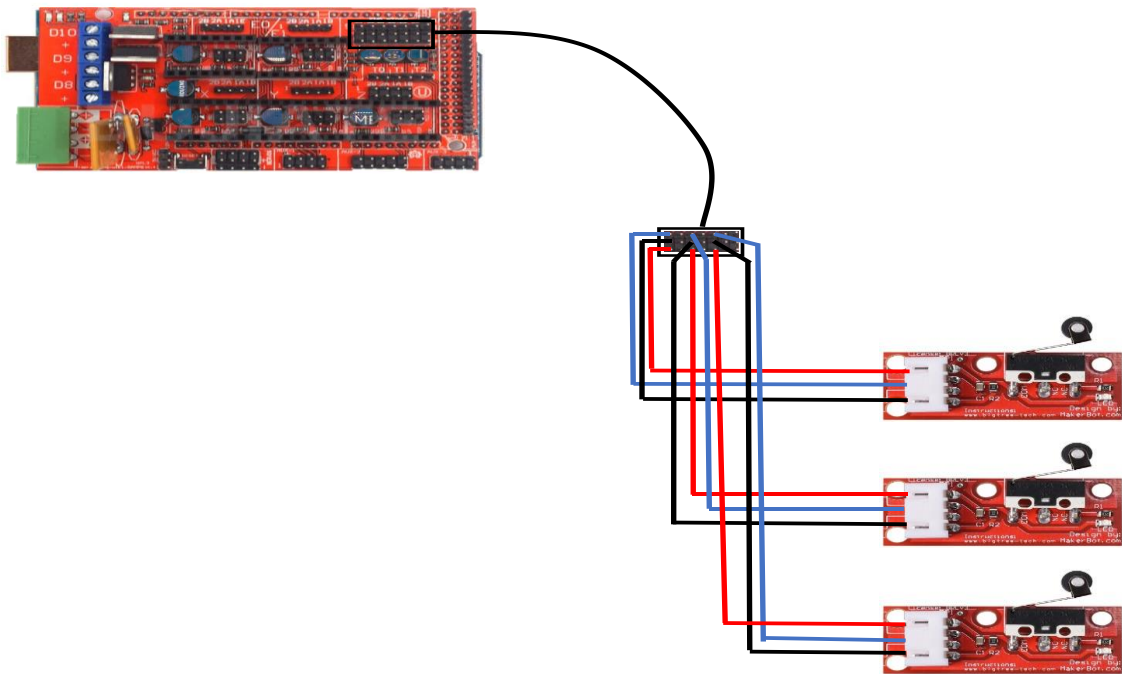


Figure 14: Mechanical End Stop Wiring

Complete Control Box Setup

So far, the complete electronics hardware and circuitry has been explained. CNC spindle and laser circuitry are powered by same output pins on the Ramps 1.4 board. They are shown in the circuit diagram separately and can be connected according to the requirement. One can be unplugged to make use of the other hardware for different machine mode. Its complete wiring diagram is shown in appendix-I.

CHAPTER 4: RESULTS AND DISCUSSIONS

Manufacturing

Once all material and components had been bought, the next phase was to start with the manufacturing of the CNC machine. When manufacturing CNC machines it is recommended to start with the baseplate of the machine and then progress upwards towards the gantry, bed and its component assembly.

Since our goal was to maximize the workspace, we bought a mild steel plate for the baseplate (735*735*12mm). These dimensions were chosen because the linear rails we had were nearly 560mm, and we wished to utilize their full potential. Now the problem with these types of base plates is that it is very intricate to maintain the flatness and parallelism of plates this large and thin. Our baseplate, particularly, had been cut from a large sheet of mild steel using plasma cutting. Now plasma cutting generates thermal stresses and deformations which warp the edges of the plate. Moreover, the baseplate also had prior 'large radius' curvature to start with. These initial bends and warps in the baseplate meant that it was mandatory for us to face mill the plate before using it as a reference plate. A dial caliper was used to measure the offset of the plate along the diagonal. A value of 4mm was obtained. This meant that if both sides were face milled to obtain a flatness of roughly 0.5mm offset, we would be left with a plate of round about 4mm thickness. A 4mm plate thickness with an area of more than 0.5m² is very undesirable due to its increased flexibility. To overcome this issue, we used a hydraulic press to straighten out the plate to some extent. However, even after multiple tries, we could not bring the offset of one surface to less than 2.5mm which was once again too high.

Furthermore, an added issue we faced was that the vertical machining center available to us for face milling had a bed size of 600mm by 1050mm and our plate had a

surface area of 735mm by 735mm. A plausible solution proposed was that we should get our plate face milled in 2 settings. However, this would subject the plate to human error during switching between the first to the next setting. We were already facing an issue with the flatness of the plate and the following issue meant that even after face milling, we wouldn't be able to maintain an offset of 0.5mm. This was uncompromisable and we had to modify our design strategy.

We discussed these issues with our supervisor, and after extensive scrutiny we proposed that we should cut the plates into two long rectangles, bolt these plates in a crossed configuration, and support this structure with height varying aluminum extrusions. This idea was a masterpiece since it overcame both problems. The bed size of our vertical machining center could now accommodate our plate and the initial offset of the plate reduced to 1.5mm which meant we could machine it without losing a lot of material.

The base plate was cut just as stated above, and 4*16mm holes were drilled into both plates. The plates were then face milled. Also, the 4 mm holes for the linear rails, aluminum extrusions and bearing supports were drilled using the VMC to maintain positional accuracy. The next challenge we faced was that these holes had to be tapped manually (due to limitations of equipment). The tapping of 4mm holes is very intricate and requires a lot of expertise. This is because any moment the tap can break while its engraving the threads on the face of the holes, if care is not taken and a force larger than necessary is applied. In case a tap breaks inside the hole this makes the hole useless, which could nevertheless risk us the cost of the plate. Finally, the plates were bolted into cross-configurations using the 16mm bolts to finish with their assembly.

Aluminum extrusions were used to make the feet of the cross-configuration base plate. 8*60mm long aluminum extrusions were cut using a manual cutter. These were tapped using 16mm tap sets. These were bolted with the cross-configuration baseplate

and more bolts were added to the base of the aluminum extrusion blocks. The purpose of these blocks was to adjust the level and parallelism to ground of the cross-configuration baseplate by loosening or tightening the bolts.

After this we moved to the gantry, the y-axis plate was manufactured. Aluminum was chosen as the material and the dimensions were 700mm by 150mm. This was also face milled, drilled and tapped. The y-axis linear bearings would rest on it. The z-axis extrusions were also cut to required lengths, tapped and drilled. Finally, it was time to assemble the linear rails to the gantry and baseplate. This assembly is not an easy task partly since during assembly the parallelism between both rails should be ensured. For this reason, we manufactured dowel pins of very small tolerance that would pin the rails into the right place (ensuring parallelism). Then we would further reduce the discrepancies using a dial caliper that would run on one rail and measure the error on the next one. This effectively gave the difference in distance between the two rails. Finally, all these components and plates were assembled into the structure of the CNC shown in the CAD files.

Hence, if we review our progress, we can see that manufacturing was 85% complete, and the parts left were essentially bed manufacture (x-axis) and clamp design. The bed manufacture wouldn't be a challenge since we had already mastered the intricacies rail parallelism and flatness tolerance. However, the clamp manufacture would be a challenge. This is because our clamp had to be such that could attach a laser engraver, spindle and an extruder head requiring little to no labor. Switching robustly between the 3 should be a necessary feature. Nevertheless, we had an ingenious solution to this challenge, but we couldn't implement it due to the corona virus pandemic breakdown.

We learnt various strategies and processes that makeup the manufacturing industry. From the basics of manual drilling and tapping to the complexities of

parallelization and VMC operation. This journey taught us how different practical manufacturing is from design of a product. Manufacturing in its own self is an art that requires years and years of determination and experience to master.

Computer Aided Design and 3D Modeling

CAD modeling is one of the crucial aspects of mechanical design and manufacturing. Design on paper must be converted to the complete model for further evaluation and refinement of the design along with proper visual representation of what we have in mind, to enable others easily understand our idea and working of the project. CNC machines require proper design and complex design evaluation to analyze the durability and strength of the machining unit. Considering these in mind, a detailed CAD model was prepared using SolidWorks. The model was updated along the entire design course to aid manufacturability and to improve the overall design. We used CAD models for production of parts on the CNC machine to avoid accuracy up to micron level and to ensure the preciseness and accuracy of our machine.

Following are some renders done using our CAD model for better visual presentation and detailing:



Figure 15: Rendered Design 1

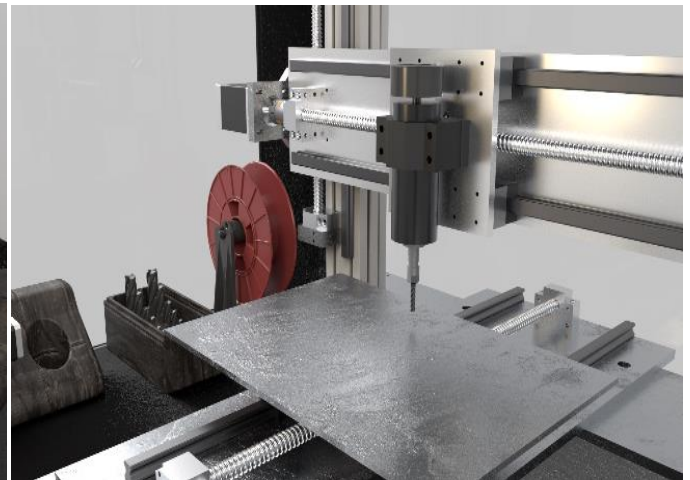


Figure 16: Rendered Design 2



Figure 17: Rendered Design 3



Figure 18: Rendered Design 4

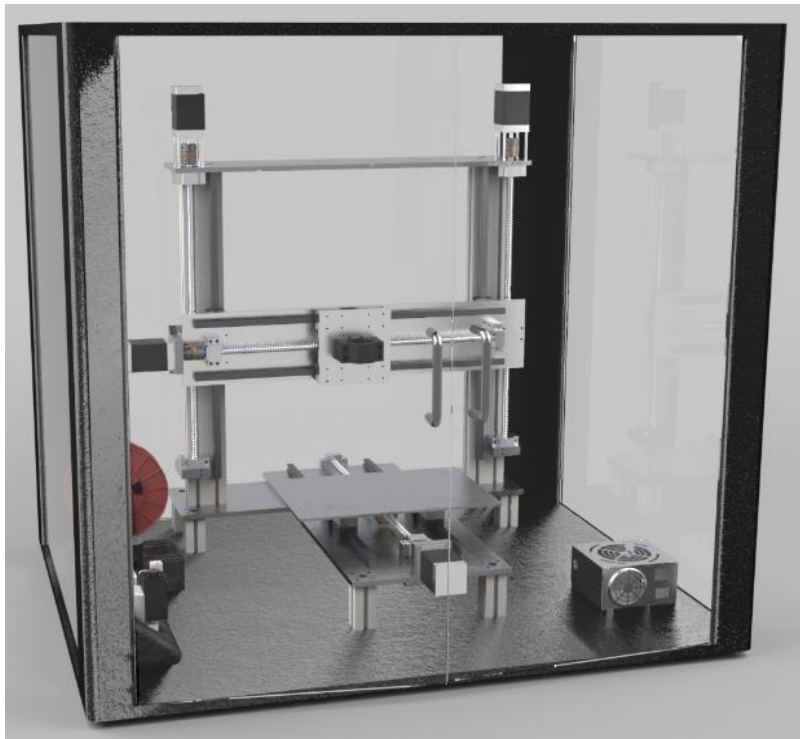


Figure 19: Rendered Design 5

Each model was created using the drawings and information provided by the vendors and information based on our theoretical design. The main target of the project was to design and manufacture the hybrid CNC machine, however due to the scope changes during the COVID-19 outbreak, we shifted our attention from fabricating the hybrid CNC machine to preparing it and refining the design to match the market standards. We added enclosure for our CNC machine and designed the tool head holders to present our hybrid CNC machine as a complete package, ready to compete the market.

Finite Element Analysis

Once we have found the milling cutting forces, we can see what effect these forces have on the whole CNC structure. Once gain it is an important design step to simulate these structural deformations and stresses due to the maximum forces generated during cutting.

The starting point for us in this simulation is that we know the origin point of the cutting force. This is basically the tip of the drill. On the other hand, the software we are using for this structural analysis is SOLIDWORKS. SOLIDWORKS's FEM interface has a very user-friendly interface. To set up Finite element study case we need exact size case model for true prediction of stresses and deflections. To simulate the real-life loading scenarios in SOLIDWORKS we need high computational abilities. However, we can obtain significant results by simplifying the case according to our requirements. In SOLIDWORKS the most important aspects of static design study are fixtures, connections and external loads. Connections refer to the setting how the different components or parts in the design study interact with each other. They are of extreme importance in design study of assemblies. Fixtures refer to the conditions that specify how our parts are constrained. External loads, as the name suggests, are the depiction of loading scenarios; the effects of which we want to evaluate.

We ran these simulations on multiple parts of the CNC machine which we suspected could fail under the immense forces generated due to milling. We computed their deformations, strains and stresses; these were compared with the hand calculations we performed earlier on the whole CNC structure. The parts we were primarily concerned for were the clamps of steppers and the spindle. This is because, these parts were not taken simply off-the-shelf, hence, needed to be examined for failures.

First, we ran the simulation on the clamp spindle assembly and evaluated the forces on the bolts, the stresses on the clamp and the shear strains as well. The case was set up using the procedure highlighted previously. Basically, a remote mass load is set up on the clamp 20cm below the center of the clamp that depicts the milling cutting force. Using, this force as the seed we computed the deflections produced in the clamp, and the forces generated in the bolts. The figure below demonstrates this: we were also able to get the exact same results produced in our hand calculations. The bolt forces generated using FEA were very similar to those produced in Mathcad hand calculations. We can also observe that the stresses produced in the clamp aren't critical and the clamp has no significant deformations.

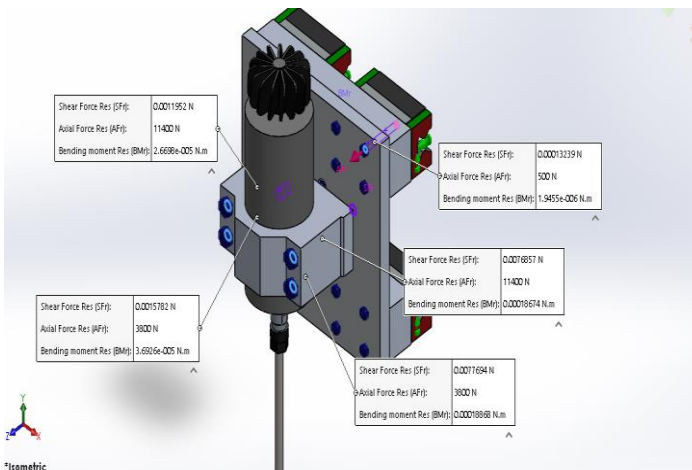


Figure 20: FEM of Bolts

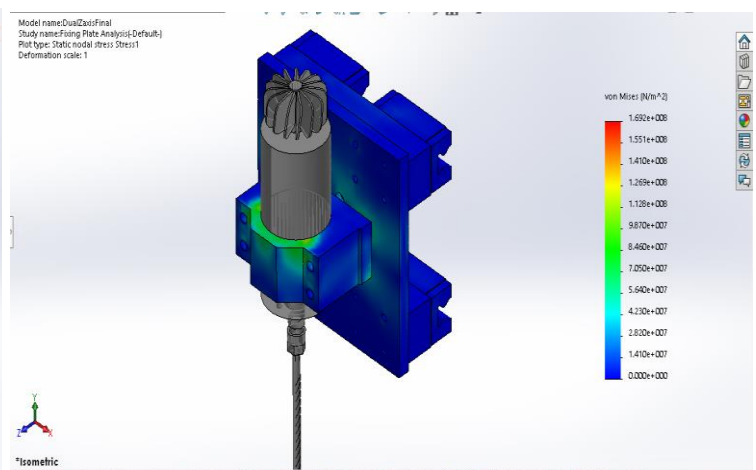


Figure 21: FEM of Spindle Clamp

Secondly, we ran our FEA on the stepper motor clamps. These were critical because these would be the first parts to fail if the forces on the steppers exceeded beyond limits set. Once again, the case was setup using the previously mentioned procedure. Basically, a remote mass load is defined that depicts the weight of the stepper motor and a moment of 3.1Nm is also defined on the slots for stepper bolts. This moment depicts the scenario where due to some reason the ball screw stops, and all the stepper torque is transmitted to the bracket via bolts. The figures below demonstrate this simulation:

In this figure we can see the displacement resolution of the bracket for z-axis. The top corners face the largest displacements, precisely about 0.00125 millimeters. We can also see the control points generated from the moment and the field vectors responsible for it.

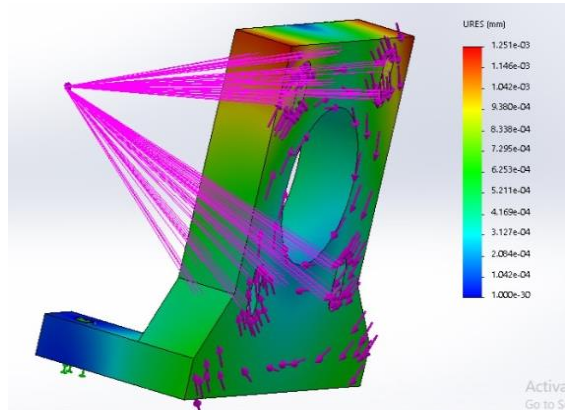


Figure 22: FEM of Z-Axis Bracket

In this figure we can see the strain produced in the other bracket for the x-axis. The moment of 3.1Nm is responsible for the field vectors and the controls points pin, pointing the arrow, are responsible for the remote mass load. We can see the strain concentrations at the bottom of the bracket. These have a magnitude of 0.0011%.

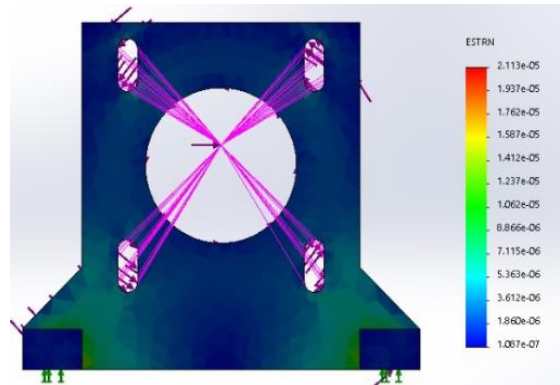


Figure 23: FEM of X-Axis Bracket

Lastly, in this figure we can see the stress concentrations on the spindle clamp. We see that these are high near the holes of the clamp. Precisely, these magnitudes mount to 34.6MPa. This is well below the yield stress of the clamp; hence, we are good to move forward.

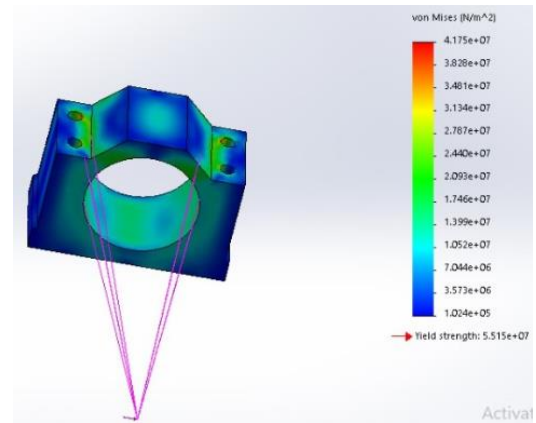


Figure 24: FEM of Clamp

Topology Optimization

Topology optimization is one of the modern additions to the FEM analysis modules. It analyzes the certain loading scenario provided by the user according the provided goals and boundary conditions to optimize the shape and design of the part under consideration. Topology optimization helps to refine the design using various constraint options like best stiffness to mass ratio, minimal mass and maximum displacement. The topology optimization procedure is guided by the data provided by the user like percentage of mass to be removed, manufacturing process and maximum deflection.

Topology optimization module in SolidWorks simulation was used for refining the design of the crucial components like tool head clamp and stepper motor mounting brackets. Mostly, the results of topology optimization are compatible to additive manufacturing only. However, the constraints can be edited to guide the workflow of the algorithm to suit subtractive manufacturing techniques. However, that was quite tedious and complex, so we analyzed our parts without such constraints. The results were satisfying; however, we cannot manufacture them with our manufacturing facilities but it

gives an idea of how much good our design is and what improvements need to be made to maximize the strength to weight ratio of the crucial parts.

Tool Head Clamp

Setting up the topology study is quite easy and is like the basic static design study. We need to provide appropriate boundary conditions, connections if we are analyzing an assembly, loading scenarios to setup the topology study. To guide the optimization algorithm, we need to specify the goals and respective constraints according to which the part would be modified and refined. For spindle clamp the holes for clamping bolts were provided fixed geometry fixture to replicate the real situation. A remote load was added that accounted for the milling force acting on the spindle. Following are the optimized results along with the constraints specified.

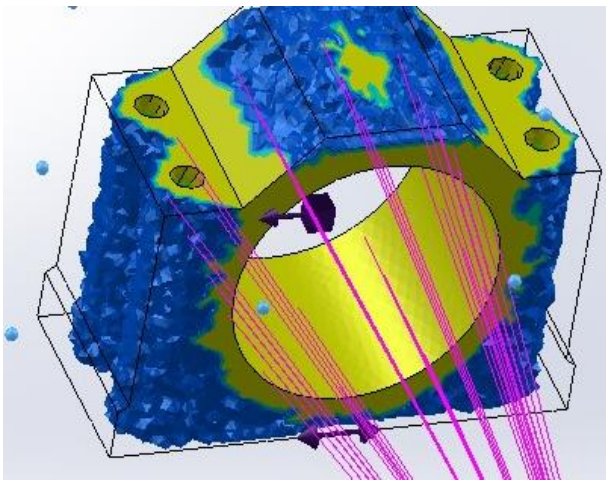


Figure 26: Tool Head Clamp

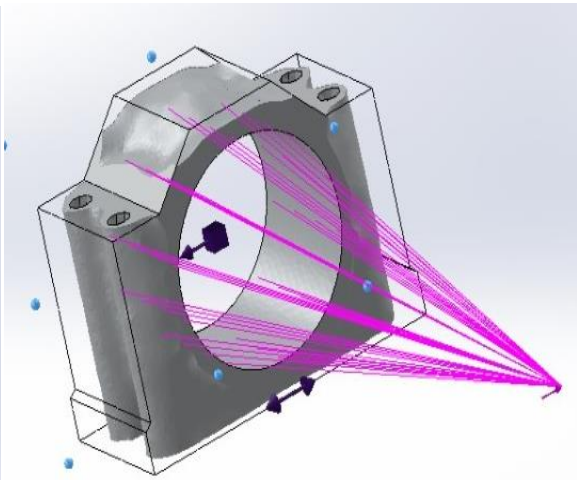


Figure 25: Tool Head Clamp 2

Goal: Best Stiffness to Weight Ratio

Mass Constraint: Reduce Mass by 40 Percent

Mounting Bracket for X-Axis Stepper

The stepper motor mounting is one of the most crucial part, as it has to be stiff enough to bear the stepper motor weight and the jerk that occurs when the stepper suddenly accelerates or decelerates. The bracket must be stiff enough to bear these cyclic loads with minimal deformation to maintain the concentricity of the motor shaft with the ball screw. The bracket was provided fixed geometry fixture to the bolt holes from where it was connected to the axis. A remote load was added to account for the weight of the mounted stepper motor. And a moment of 3.1Nm was added to the slot holes for stepper motor mounting bolts that accounts for a scenario where the ball screw fails to rotate due to some reason and the bolts transmit the stepper torque to the bracket. Following are the optimized results along with the constraints specified.

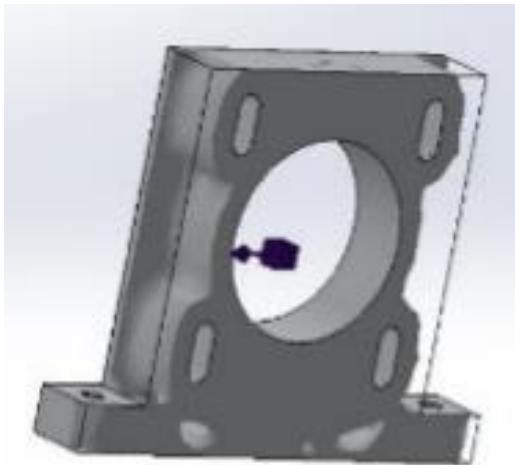


Figure 27: Mounting Bracket for X-Axis

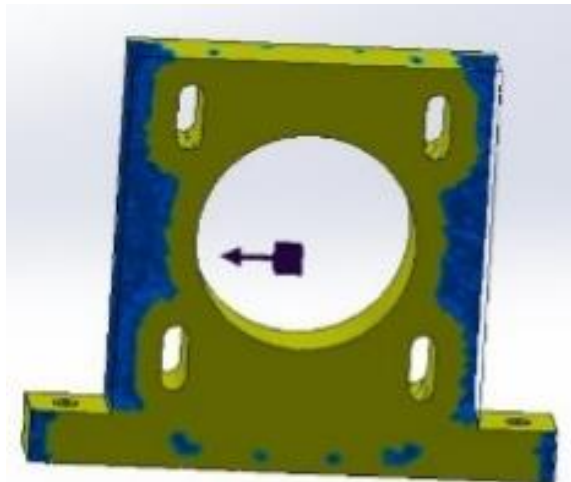


Figure 28: Mounting Bracket for X-Axis 2

Goal: Best Stiffness to Weight Ratio

Mass Constraint: Reduce Mass by 40 Percent

Mounting Bracket for Y-Axis Stepper

The stepper motor mounting is one of the most crucial part, as it has to be stiff enough to bear the stepper motor weight and the jerk that occurs when the stepper suddenly accelerates or decelerates. The bracket must be stiff enough to bear these cyclic loads with minimal deformation to maintain the concentricity of the motor shaft with the ball screw. The bracket was provided fixed geometry fixture to the bolt holes from where it was connected to the axis. A remote load was added to account for the weight of the mounted stepper motor. And a moment of 3.1Nm was added to the slot holes for stepper motor mounting bolts that accounts for a scenario where the ball screw fails to rotate due to some reason and the bolts transmit the stepper torque to the bracket. . Following are the optimized results along with the constraints specified.

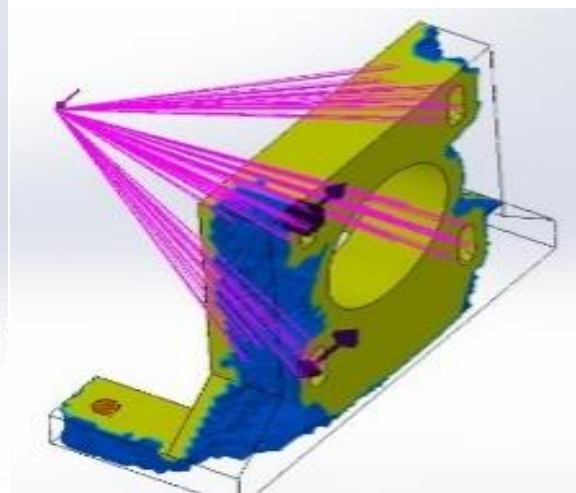
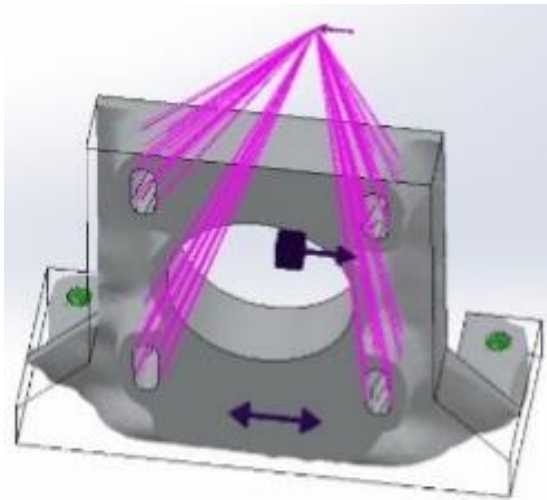


Figure 30: Mounting Bracket for Y-Axis **Figure 29: Mounting Bracket for Y-Axis 2**

Goal: Best Stiffness to Weight Ratio

Mass Constraint: Reduce Mass by 40 Percent

Milling Simulations

An integral part of CNC design is simulating the processes involved during the material removal. This is important because it is highly desirable to know what forces and moments the gantry and structure will be subjected to during its operation. To know what these forces are we need to step back a little and understand where these forces are originally generated from. 3D-printing and laser engraving do not pose high magnitude loads on the gantry but material removal operations such as milling do. These forces are large and need to be computed for an effective design strategy.

Material removal can be of different types like milling, facing, turning, tapping. Our concern is basically on milling since our CNC will be performing milling mainly. The cutting forces generated by milling can be hand calculated but requires solving complex integrals where multiple parameters are needed to be kept in mind. However, we can use computational software to perform these calculations. Finite element method can be used to simulate these cutting forces. The maximum cutting force is then extracted from these simulations and used to simulate structural deformations due to these forces on the gantry and CNC structure.

The milling simulations were performed on Abaqus. The procedure for the Abaqus case development was as follows:

Firstly, an end mill and a workpiece part are imported. Then the material for both parts is defined using the material manager. In our case, the tool used was a carbide 4-flute end-mill and the workpiece was assumed to be aluminum. During the material definitions the damage model used was Johnson-cook damage evolution. Next, an assembly instance was defined where the workpiece was translated to suitable positions relative the tool. The next step is to define the interactions. Here, first the type of contact is defined which in our case was surface to surface. Consequently, the interaction property for this interaction was defined which, once again, in our case was coupled

temperature difference. Next, it is very important to define 2 constraints on the tool. A rigid body constraint and a kinematic coupling. Moving forward, the meshes are generated using element identities. The step time is defined finally, and a suitable solver is used. Our case used the explicit dynamic model. Finally, the field outputs are selected, and the job is run (submitted).

Due to our computational restrictions we couldn't model the exact 3D simulation but what we could do was model the top view of this milling operation as shown below: we can see the maximum generated stress was about 95MPa.

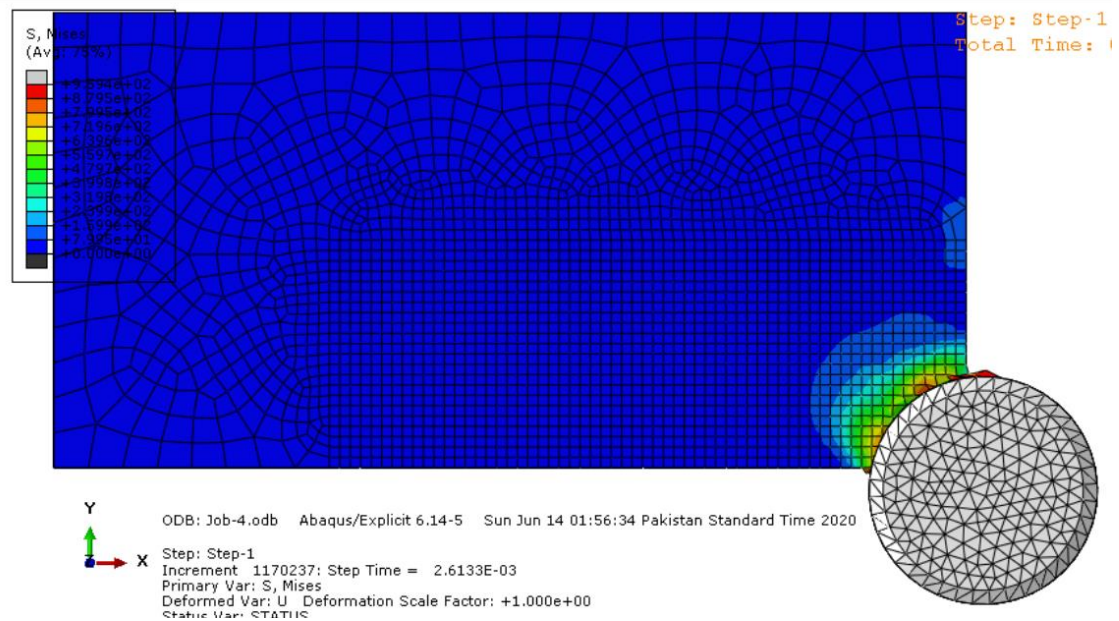


Figure 31: Top View of End Mill Simulation

However, due to these computational restrictions we used another design strategy to compute the cutting forces. There have been considerable efforts in research to understand the basics of orthogonal cutting. What orthogonal cutting proposes is that once you have simulated orthogonal cutting forces, these forces can be extrapolated to milling cutting forces using mechanics models. Models developed for turning and

adapted to milling yield reasonable results, except in some applications. This work develops a method capable of providing cutting data in a fast and reliable way to evaluate the specific cutting force. The orthogonal cutting simulation stated above was performed on Abaqus using essentially the same setup procedure highlighted previously. A snapshot of this simulation can be seen below. This simulation when used to compute the milling cutting forces, a value of 3778N was obtained. The figures below demonstrate the orthogonal cutting simulation analysis:

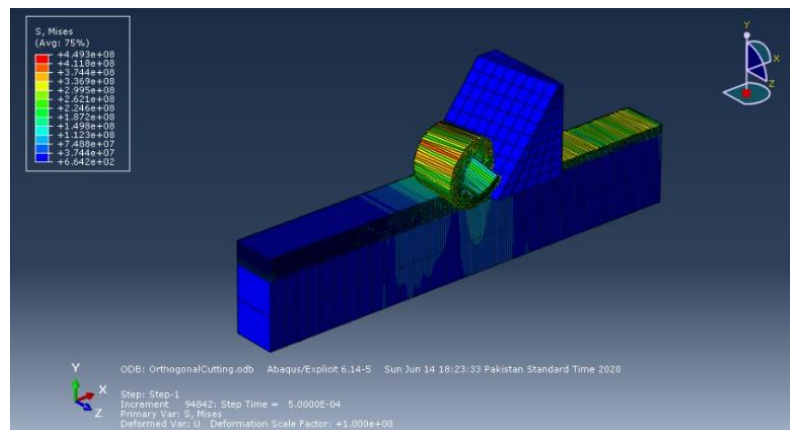


Figure 32: Orthogonal Cutting

In this figure we can see that there is chip breakage and the region where the chips are being separated the stresses are mounting to about 405MPa. This is well above the elastic region of aluminum due to which we see the plastic behavior that is chip formation.

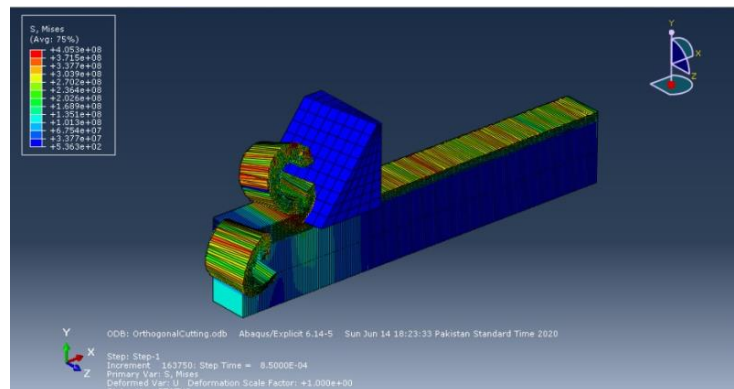


Figure 33: Orthogonal Cutting 2

Deform Simulation Analysis

Deform is a well-known simulation software used for analyzing the workshop processes in a competitive environment before practically performing them in the workshop. Deform 3D is one of the computational environments designed specifically to analyze and optimize the performance of highly nonlinear machining processes. Some of the workshop processes that can be analyzed on Deform 3D include, milling, drilling, turning, forming, extrusion and forging.

Advantages:

Following are the benefits of using deform 3D software for simulation purposes

- Easy to use and user-friendly interface.
- All the workshops processes can be simulated and analyzed free of any licensing costs.
- More accurate results
- Specifically, designed algorithms for robust simulations.

Disadvantages:

There is only one disadvantage of deform is that simulation on it is a time-consuming process. The requirement of computational power for nonlinear simulations is usually quite high. This must not be considered as a disadvantage but for us, it poses a limitation not allowing us to study such processes in complete detail.

Specifications:

Our machine is a hybrid CNC machine. The only thing that poses a danger to our structural strength are the burdensome tool workpiece interactions. We analyzed those interactions using simplified mathematical models, theoretically. To validate the authenticity of our theoretical calculations we did a milling simulation in Deform 3D. In

our case we are doing a milling simulation to see if our mill tool cutter can withstand the wear and tear it faces during cutting the material and to analyze the force acting on the cutter to further use the results to approximate the stresses and deformations in the gantry.

Tool Specification:

Material: Carbide (15% Cobalt)

Tool Diameter: 6.25 mm

Material Specifications:

Material used: AISI 1045 Steel

Results:

After several tries and case modifications we were able to extract useful results from the milling simulation. We performed the simulation for the above-mentioned specifications and the results were quite satisfying. The maximum cutting force predicted by the Deform package that is almost 3.6kN is quite comparable to the theoretically computed cutting force results i.e. 3.7 kN. This is the maximum force that our tool withstands according to our theoretical calculations and deform simulations. This proves that the theoretical calculations we performed earlier using simplified mathematical models was quite accurate. This force is used to design the machine structure and for selection of crucial machine components like linear bearing, CNC spindle and ball screws. Following is the snap from the Deform 3D environment depicting the variation of cutting load on the tool as it pierces through the material.

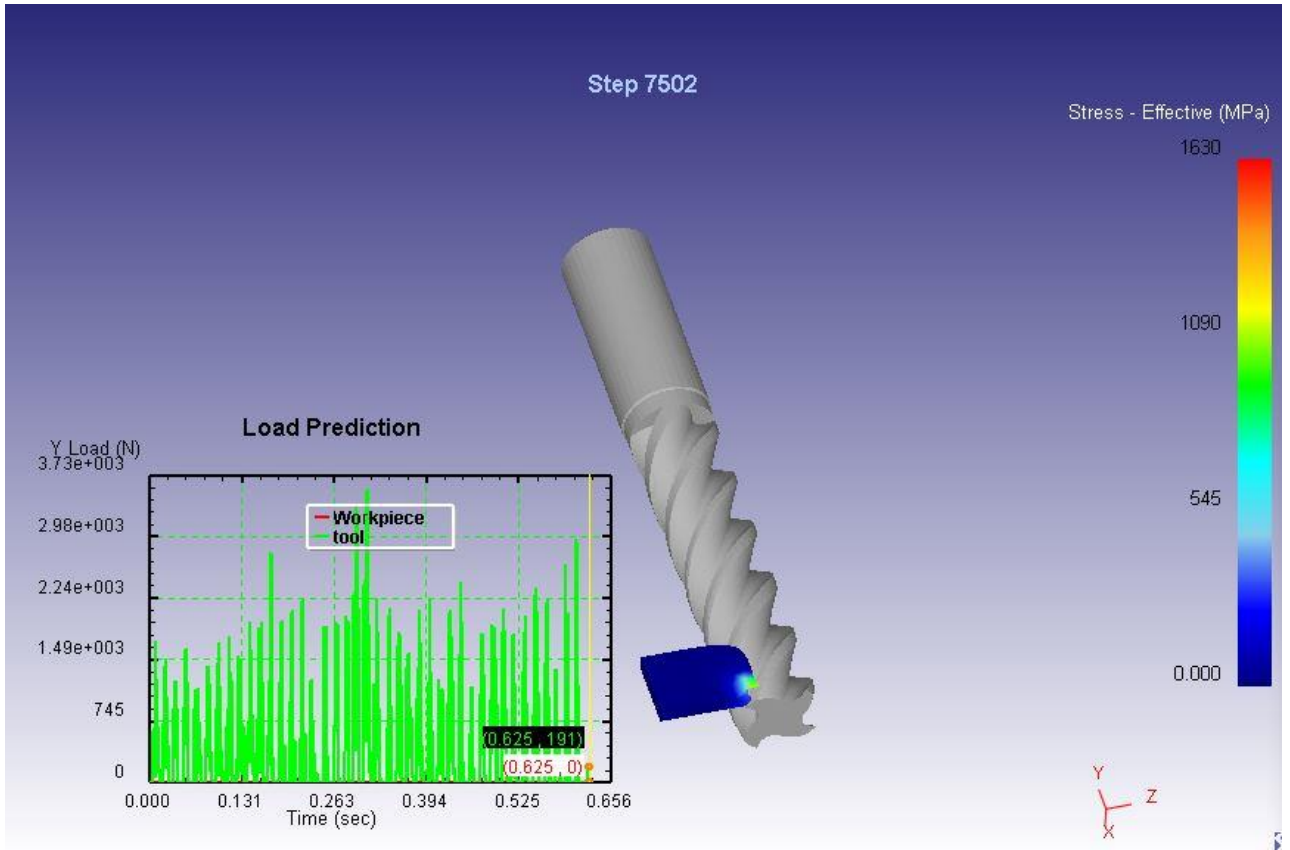


Figure 34: Deformed 3D Simulation

CHAPTER 5: CONCLUSION AND RECOMMENDATIONS

Recommendations:

So far, we have discussed the complete design process and methodology. In this section of the report we present some proposals for improvement of our hybrid CNC machine. We recommend the integration of some valuable features to the current design with complete design instructions and necessary information, to enhance the value of the machine and to bring it to the market as a full-fledged product ready to compete the market.

Some of the recommendation are as follows:

Automatic Bed Levelling

Before discussing about auto bed levelling, we first discuss about levelling in a CNC, such a process in which the z axis (either it has a spindle or a 3D printer extruder) and the bed has a constant distance throughout the bed surface when it is moved across it. This improves the quality of process which is being done. There are two types of levelling which are as:

Manual Bed Levelling

Manual Bed Leveling (MBL) is viewed as dreary and tedious. To make an already difficult situation even worse, the manual procedure should be rehashed after a few prints because there is consistently a chance of the bed skewing following a few hours of utilization.

There are additionally cases where you can't simply get your bed leveled regardless, and this is as a rule because of distorting. Aluminum and PCB beds get twisted and keeping in mind that you can put a glass bed on your PCB, distorted aluminum may require substitution.

Automatic Bed Levelling

Automatic Bed Levelling (ABL) improves the nature of printing and bed grip by taking a few estimations of the bed surface and afterward altering all development to follow the tilt or shapes of the bed. Most beds show up a very level and even, however in any event, when the bed is level, there might be inconsistencies because of tape or other issues on a superficial level. Or on the other hand, there might be abnormalities in the bed or spout stature because of mechanical imperfections. ABL can make up for every one of these sorts of height abnormalities.

Before we discuss on how to step up the auto bed levelling lets first discuss on different types of sensors used in the different 3D printers. Some of them are in the following:

➤ BLTouch Sensor

It can quantify the tilt of (sic) bed surface. This sensor works at any bed surface, be it metal, glass, wood, or something different completely. The sensor itself is genuinely perplexingly complex as far bed sensors go. It comprises a microcontroller, a solenoid switch, and a pushpin probe which meets the bed. The BLTouch utilizes a hall sensor for high exactness, and this sensor, related to the physical pushpin, is the thing that permits it to be utilized with many bed types.

➤ Inductive Probe

The inductive probe uses currents induced by magnetic fields to detect metal objects nearby, eliminating the need to physically touch the bed in order to sense it. But therein lies the problem: Inductive sensors only work on metal beds, since



Figure 35: BLTouch Probe



Figure 36: Inductive Probe

they're triggering just when in contact with metal. This might be a deal-breaker if glass is your preferred print bed material.

➤ Microswitch

It is less precise and perhaps less solid in the long term since the detecting relies upon physical parts that can wear after some time. Be that as it may, these physical switches give the other fancier sensors a run for their cash with regards to the expense and simplicity of the arrangement. Since physical switches are the least complex and most punctual type of Z-homing sensors, they're anything but difficult to get and trifling to set up.



Figure 37: Microswitch

➤ Pinda Probe

The Pinda probe is an inductive test with the expansion of a thermistor to represent variations in the bed temperature. The probe is supposed to be profoundly precise for 3D printers. This might be a decent arrangement too, in any event on the off chance that you have a metal bed.



Figure 38: Pinda Probe

➤ Ezabl Pro

The Ezabl Pro is a uniquely made capacitive sensor. It accompanies a connector board that utilizes an optical isolator to forestall any high voltage harm to your mainboard if there should be an occurrence of wiring botches. Concerning exactness, it's had the option to quantify inside a range of a thousandth of a millimeter, which is the thing that 3D printers need. The Ezabl Pro likewise accompanies supportive



Figure 39: Ezabl Pro

highlights like double protecting, which forestalls any obstruction with different signals.

➤ Piezo Sensor

A Piezo sensor utilizes the Piezo-electric impact to catch changes in pressure, force or strain, and convert these progressions into electrical charge. It has been said that these have near 7-micron accuracy, which is very accurate for a 3D printer. The benefit of the Piezo sensor is that the



Figure 40: Piezo Probe

spout itself can be utilized as the detecting gadget, with no extra segments waiting to be mounted. Additionally, the Piezo sensor can be set on the print head or beneath the print bed to detect the pressure.

Inductive Probe is much reliable to all the above as it's wiring system is easy, has reliable output, economical and easily available in the market so propose to utilize this sensor as for auto bed levelling.

To set up your printer for auto-levelling, you will supplant the z-axis probe with an inductive sensor and refreshing your firmware. You should make a mount for your z-axis probe.

We needed some of the things necessary to set up the auto bed levelling which are as:

- An auto-leveling sensor (LI12A3-4-Z/BY Inductive Proximity Sensor)
- A bracket to hold your sensor on the extruder carriage
- The Arduino IDE and the latest version of Marlin
- Oil tape or copper tape

Stage 1

- First, the auto-leveling sensor will supplant the 3D printer's z-axis end stop on the control board.

- Ensure your sensor has an identifying distance of at least 8mm.
- The sensor has a LED that turns on when activated.

Wiring the LJ12A3-4-Z/BY Inductive Proximity Sensor

- Locate and disengage the z-probe from your control board.
- Connect the output voltage wire to the S signal contribution on a similar column of 3 pins your old z-end stop was associated. On RAMPS sheets this pin is closest to the outside of the board of the lines of end stop pins.
- Connect the other 2 wires labeled + and - to a corresponding positive and negative power source on your board. This can be direct to 12 power supply, where 12v associates board or the auxiliary 12v pins on the RAMPS board can likewise be utilized.
- The sensors referenced here are "normally open" switches. To begin with, it must be should have been checked this line in firmware.
- Test the sensor on some metal, aluminum, copper, and so forth. The LED should light.

Structure a sensor mount and pick the level points

- The sensor just has a detecting distance of roughly 8mm. The sensor mount ought to be movable from an area that is lower than the tip of the spout to a couple of millimeters above.
- Mount the sensor and move the hot end carriage around to 4 points and put 4 bits of foil tape under areas closest to the 4 corners of print bed that the sensor can reach.

Stage 2

- Open the Arduino IDE then go to file > open and select the marlin document inside marlin which have a Configuration.h.

- With the Marlin Sketch open, click on the [Configuration.h] tab. This is the place of the settings of the 3D printer including configuring the auto-leveling highlight.
- Scroll to the segment marked: "Bed Auto Leveling". Enable by removing "/" at the beginning of the line.
- Adjust the position directions to coordinate the area of the foil tape on the print bed.
- file > save, at that point update firmware by interfacing board by means of USB and clicking the arrow button.

Stage 3

Auto-leveling is a command that is run after the " G28 ; home all axis " gcode line in start code or run once in a different document each time you boot up your 3D printer. Now, the firmware required a change a couple of times to get the testing areas set effectively. The auto-leveling order is: G29

Pros of auto bed levelling

- It makes it simpler to change the manufacturing surface without having to reconfigure your printer.
- You get high exactness paying little heed to lopsided warming or bowed form plate. Sensors guarantee the print head is continually moving corresponding to the construct plate.
- No sitting around idly tinkering with the bed and Z stature

Cons of auto bed levelling

- The sensors add weight to the print head.
- Gathering an auto-aligning 3D printer unit can be a troublesome assignment.
- The printer firmware may cover mechanical mistakes like backlash or even an imperfect structure that makes it difficult to have a level bed.

PID Spindle Speed Control

CNC machining is one of the most crucial process among all the modes of the hybrid CNC machine. Subtractive manufacturing at its best can yield amazing results and finished products. CNC milling performance is affected by various factors, namely milling parameters, spindle power, coolant, tooling geometry, workpiece's physical and thermal properties, structural rigidity of machine and fixture. So far, the hybrid CNC machine has been designed to provide maximum structural rigidity and strength to the machine to avoid minor deformations caused by the burdensome tool workpiece interactions. After incorporating proper mechanical strength and structural rigidity to the machine, among the remaining factors, the major ones that require proper attention are the milling parameters that are quite specific for each tool workpiece pair. Among the milling parameters, spindle RPM and feed rate are the ones that we can focus in the future for better milling performance and results.

As discussed, earlier spindle RPM is one of the major factors affecting milling performance and results. Mathematical modeling of milling processes has enabled us to calculate the RPM value required for milling operation depending on the cut features like depth and width of cut, tool geometry like number of flutes and tool diameter and factors for workpiece like power constant. Running the milling process at that RPM and feed rate promises best finish, optimized power usage, minimal tool wear and minimal loads on the spindle. AC spindles are controlled by Variable Frequency Drives which promise RPM and torque control according to the digital signals coming from the controller. DC spindles don't come with such fancy electronics. However, for DC spindle PID speed control auxiliary controllers are available in the market which control and maintain the RPM according to the controller instructions. But these controllers like AC spindle and VFDs packages are quite expensive. SuperPID offers such a controller for about 155 dollars. For future improvements to our hybrid CNC machine package, we purpose a

custom designed PID spindle speed control for better stability and maintenance of RPM and improved milling finish at minimum cost.

Our machine is currently equipped with 500W DC Chinese spindle that is controlled by the 12V Ramps 1.4 controller along with Arduino Mega. Usually DC spindles come with manual speed adjustment potentiometer with the AC/DC converter to control the RPM. The manual RPM adjustment is quite time consuming and is not ideal for proper milling operation. The RPM need to be changed according to the desired cutting velocity required for different milling procedures. Sometimes, high RPM are required when feed rate is high to maintain the feed per tooth value close to the recommended values. For better maneuverability and flexible machine control, the DC spindle has been powered via DC spindle speed governor that uses the PWM input from the controller and adjusts the power supplied to the spindle accordingly to change the RPM. For much better and consistent RPM control we purpose an auxiliary circuit that would help us to maintain the desired RPM using closed-loop PID control.

Proposed PID Controller Design

So far, our electronic setup can control the spindle RPM via G-Code commands surpassing the use of the potentiometer, minimizing the human intervention. The controller sets up the spindle at right RPM but when the tool engages with workpiece the spindle is loaded and the RPM are reduced and the feed per tooth values are no more the same as recommended values resulting in improper surface finish and milling marks on the workpiece. To avoid this from happening we need to monitor the spindle RPM compare them to the target RPM and to enable the controller to change the PWM signal to adjust it accordingly.

The basic concept behind the idea is quite simple, DC spindle speed governor is just acting as an electronic voltage divider and is altering the voltage provided to the spindle according to the input PWM signal from the controller for desired RPM value.

When the spindle is under load, same voltage is being provided by the speed governor and hence the spindle loses RPM. We need to develop a closed-loop PID control which would monitor the spindle RPM continuously, compare it with the set target RPM value and would apply PID algorithm using the combined error to maintain the spindle RPM close to the said value and to minimize the error.

As far as electronics for such a PID controller are concerned, it's quite simple and economical. We just need to add some sensor to measure the spindle RPM value and an Arduino UNO running PID algorithm on it, responsible for calculating the actual spindle RPM based on sensor readings and desired RPM value based on the PWM input provided to it from the main CNC controller that is Ramps 1.4 and calculating the error and correction factor depending on proportional, integral and derivative terms and modulating the final PWM signal accordingly. This continuously modifying PWM signal is fed to the DC spindle speed governor which continuously adjusts the spindle RPM accordingly minimizing the error value for the PID algorithm.

The Arduino Uno can be equipped with the LCD shield showing the actual and target RPM values and their difference to analyze the performance of the PID closed loop system and to tune the gain values for optimized PID control. As far as the algorithm running on Arduino UNO is concerned, various open source codes are available for DC motor closed loop speed control. One of the most extensive and detailed code was available on GitHub repository. Such an open source code can be easily used by just tweaking some parts of the code according to the sensor we would be using and making some improvements to calculate the target RPM value from the input 0-5V PWM signal from the Ramps board. Following is the flowchart depicting the pseudo code for closed loop PID spindle speed control.

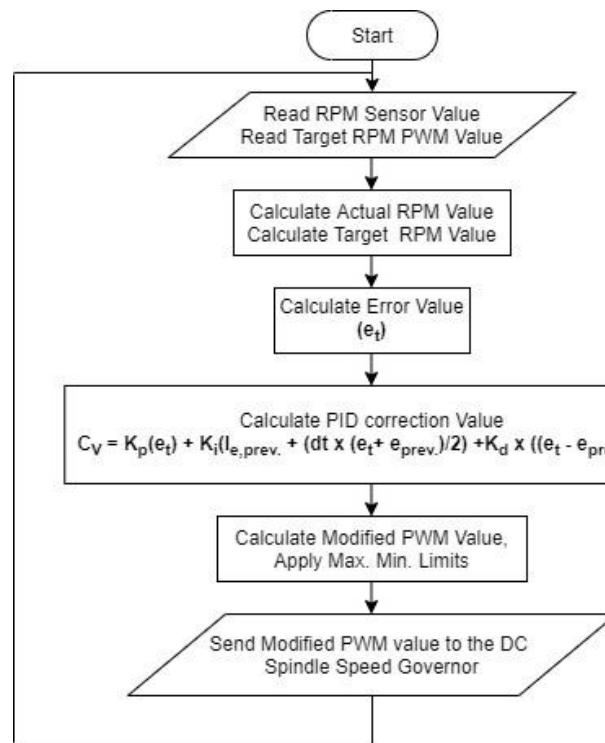


Figure 41: PID speed control flowchart

The open source codes are quite extensive and detailed. We can write our code using the proposed pseudo code. Main digital signal governing the RPM is provided by the Ramps 1.4 board. In the closed loop configuration, the Ramps board would provide this 0-5V PWM signal to the Arduino UNO (Proposed PID controller) instead of sending it to the speed governor directly. The Arduino Uno would take this PWM value and convert it to the target RPM value using mapping function. 0V at Arduino UNO input would correspond to 0 RPM and 5V would correspond to 12,000 RPM. In-between, we would have linear increase in RPM from 0 to 12,000 with the PWM value increasing from 0 to 5V. Arduino UNO would also be receiving signals from the IR RPM sensor based on which it would calculate actual RPM values. After comparing these two RPM values Arduino UNO would compute the error. Using this error and the PID gain values the Arduino UNO would compute the PID correction value that would be used to find the

modified PWM value. This correction value can be used directly as the modified PWM signal, but the minimum and maximum limits must be set so that we would not end up having negative PWM values or values greater than the maximum PWM value.

PID tuning is very crucial for proper closed loop speed control. PID gains must be adjusted accordingly to attain better control over the system and to alter the system response to minimize the effect of the changes occurring due to external intervention which in our case is milling loads on the spindle lowering the RPM. PID tuning must be done according to the recommended procedure and repeated tests must be conducted to ensure better PID closed loop speed control. Following are the findings from our research which, we considered, must be mentioned and documented for better setup of closed loop control for future.

Table 15: Effect of increasing gain independently

Parameter	Rise Time	Overshoot	Settling Time	Steady-State Error	Stability
K_p	Decrease	Increase	Small Change	Decrease	Degrade
K_i	Decrease	Increase	Increase	Eliminate	Degrade
K_d	Minor Change	Decrease	Decrease	No effect in theory	Improve if K_d is small

Proposed Concept Diagram

Following is the detailed circuitry and auxiliary electronics connection diagram that must be followed for proper PID closed loop spindle speed control. Rest of the electronics is same, just an IR RPM sensor and Arduino UNO are added to read the actual RPM values and compare them with the target RPM data from Ramps controller, to compute the error and minimize the error using PID correction algorithm.

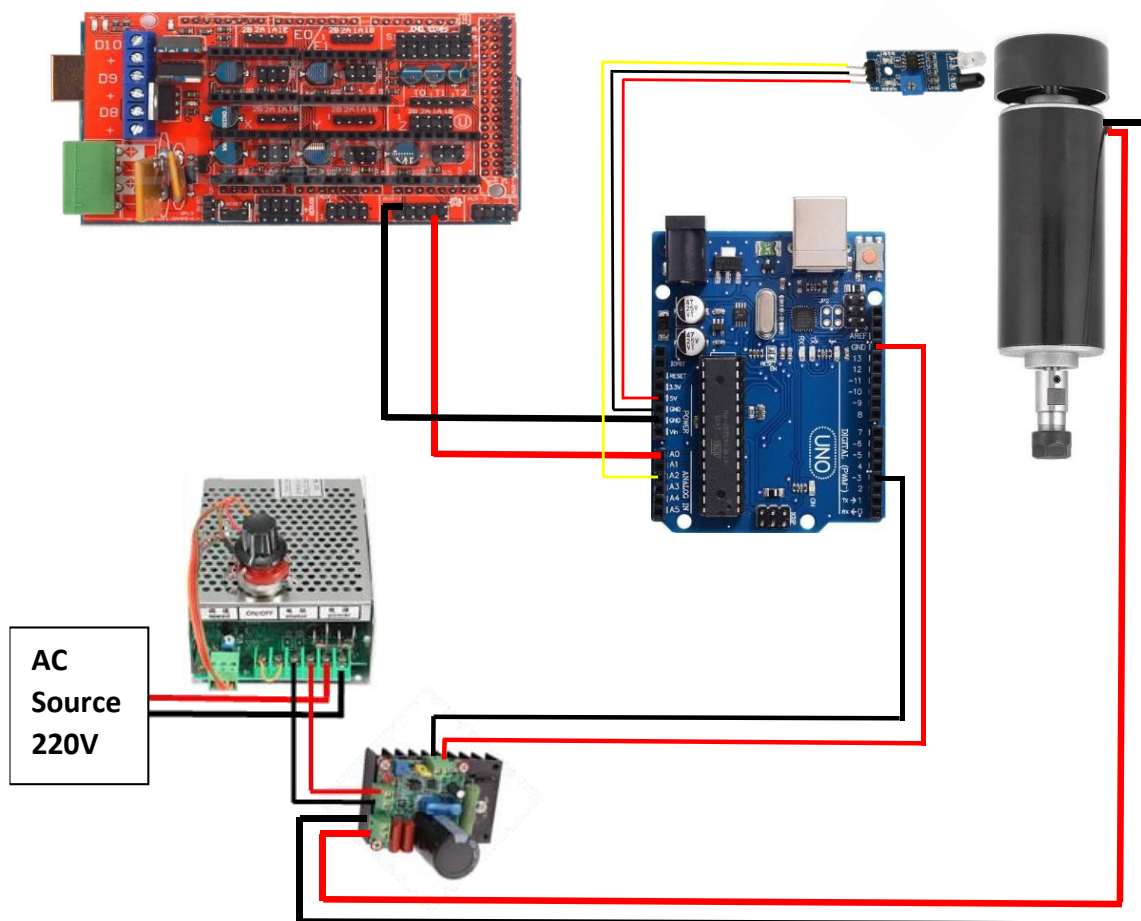


Figure 42: PID control circuit connection

1.5 KW Spindle Attachment

AC spindles overpower the DC spindles because of their high-power ratings and working RPM ranges. Moreover, they have dedicated programmable Variable Frequency Drives that enables them to be used according to the user's requirements and demand. VFDs can monitor the spindle RPM and torque that enables the AC spindles to be quite stable even at low RPMs. With AC spindles we wouldn't need to burn the wood workpiece at high RPMs, we can provide enough torque at low RPM ideal for wood milling due to the VFD's power and RPM monitor and control abilities. VFDs can be programmed to fit any working environment and electronics setup. Most VFDs require just 0-10V analogue signal from the CNC controller to effectively monitor the spindle RPM and power.

AC spindles are usually available in two main variants that are water cooled and air-cooled AC spindles. Water cooled are usually preferred over air cooled spindle as the former have better cooling mechanism and durability. AC spindles usually come in two power ratings, 800W and 1.5KW. Both these variants have same RPM range from 3,000 to 24,000. With such high power, diverse RPM change and closed loop RPM and power control, AC spindles are usually the best choice for small CNC units. They can mill materials ranging from foams to even steel if the gantry has adequate mechanical strength and rigidity. However, this all comes in exchange of high costs. AC spindles are costly as compared to the DC spindles. The complete AC spindle and VFD package costs about 180 dollars, that is almost double the price of the DC spindle.

So far during the design the major focus was on the structural strength and mechanical rigidity of the gantry and machine structure to counter milling stresses and deformations and to handle the inertial loads due to the high-speed motion of heavy parts. The design has enough tolerance and rigidity that it can handle the working loads posed by the attachment of 1.5 KW AC spindle. We purpose the replacement for our 500W DC

spindle with 1.5KW AC spindle for much better, durable and robust milling machine mode.

AC spindle VFDs as discussed earlier require only 0-10V analogue signal from the controller. Unfortunately, our controller that is the Ramps 1.4 board is not capable of providing 0-10V signal. However, we can use a PWM to voltage conversion module to convert the 0-5V PWM signal that is used for DC spindle speed control, to 0-10V analogue signal for VFD control and AC spindle operation. These PWM to analogue conversion modules come in different variants, we recommend the LC-LM358-PWM2. This module has two options for deciding PWM input range using short circuit caps. A PWM input of 0-5V corresponds to 0-10V analogue output which can be fed to the VFD.

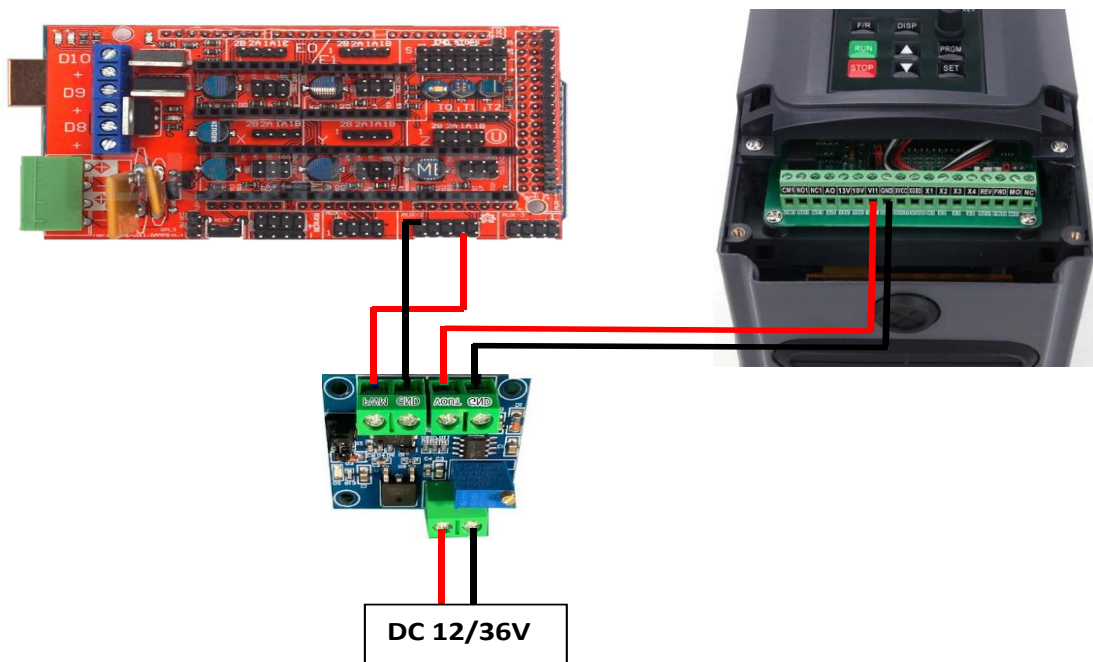


Figure 43: VFD & AC Spindle Integration

Attaching AC spindle is constrained by two obstacles, one is the structural rigidity and sturdiness of the structure and the other factor is the electronics compatibility with the VFD. We have overcome both the issues with proper design considering this future replacement and auxiliary electronics for VFD control. We have just provided the solution to the main issue of connecting the VFD to Ramps board. The rest of configuration and programming of the VFD would help in proper control of the AC spindle speed and power. Connection diagram for VFD and AC spindle integration to the Ramps 1.4 board is shown above. Spindle and AC supply connections are not shown here for simplicity.

Conclusion

The main objective of our final year project was to integrate additive manufacturing and subtractive manufacturing. For this purpose, we integrated the milling, 3D printing and laser engraving features to develop a machine that could address all the manufacturing problems that any manufacturer could face these days. Our focus was on the Rapid prototyping because as we can see at this time manufacturing has gone advanced but the only issue that still needs to be addressed is the time management. How to cut down the time required for the manufacturing operations? This is the real question of the hour. Traditional Manufacturing techniques such as milling, forging, forming etc. are unable to solve this issue when there are lot of customized parts to be manufactured as every single custom part needs to have its own set of dies. This is really a time consuming and costly process. That is why our final year project has a special focus on rapid prototyping techniques to cut down the time required and cut down the costs associated with the manufacturing. This became possible by integrating the additive and subtractive manufacturing. The combination of the features that we introduced on our machine i.e. milling, 3D printing and laser engraving significantly reduced the costs and time required as there is no die using requirement for manufacturing a part on our

machine. For excellent finish and greater accuracy for manufacturing a product and as a guidance to the people who would like to take on this project as their final year project in the future , we have made some recommendations that if applied correctly will make this make this project extra efficient. These recommendations are:

- Auto bed levelling
- PID Speed Spindle Control
- 1.5kW Spindle Integration

These concepts have been explained in the FYP report more accurately. As we look on our objectives that we had set for ourselves before starting this project. We have performed extra ordinarily. We have divided our final year project into the following phases:

- Literature review
- Design
- Market Survey
- Manufacturing

As far as literature review is concerned, we have done an excellent work. Our focus was on to determine is it possible to integrate all the features that we want to integrate. After going through literature review, we reached the conclusion that yes, we can integrate. In the design phase, we have performed the design calculations and design validations. We have used softwares like SolidWorks, Deform 3D, Abaqus for simulation purposes. Besides this, we have also performed all the calculations theoretically as well on the paper because we believe as a mechanical engineer it is very important that we are comfortable with making design calculations on the paper and then validating those results on the modern simulation softwares. We have achieved this objective in its true sense. We also have performed market survey in much detail. As far as manufacturing is

concerned, we were able to assemble the structure of our machine before Covid 19 situation. We learned a lot from this project in the sense what it really means to be a Mechanical Engineer. Thanks to Dr. Mushtaq who provided us the opportunity to work on this wonderful project.

REFERENCES

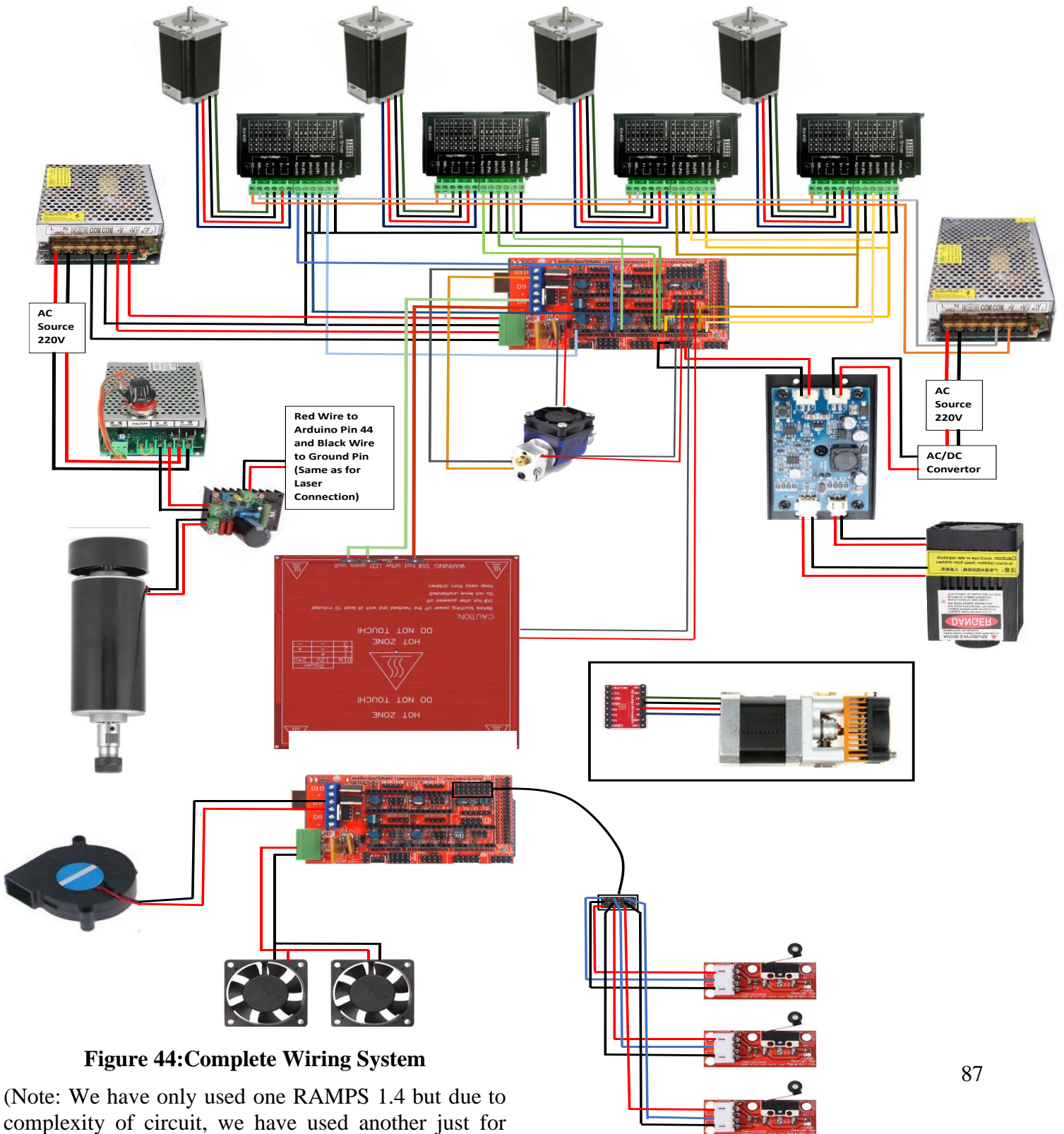
- [1] “Building Your Own CNC Router/milling Machine : 11 Steps (with Pictures) - Instructables.” [Online]. Available: <https://www.instructables.com/id/Building-your-own-CNC-milling-machine/>. [Accessed: 15-Jun-2020].
- [2] “(PDF) Prototype CNC machine design.” [Online]. Available: https://www.researchgate.net/publication/241180827_Prototype_CNC_machine_design. [Accessed: 15-Jun-2020].
- [3] “RepRap - RepRap.” [Online]. Available: <https://reprap.org/wiki/RepRap>. [Accessed: 15-Jun-2020].
- [4] “CNC Design Guide - Geomiq.” [Online]. Available: <https://geomiq.com/cnc-design-guide/>. [Accessed: 15-Jun-2020].
- [5] “Basics of Linear Bearings | Nippon Bearing.” [Online]. Available: <https://www.nbcorporation.com/basics-linear-bearings/>. [Accessed: 15-Jun-2020].
- [6] T. Drive and C. Company, “Linear Motion Technology Handbook.”
- [7] “Linear Bearings: Understanding the 2:1 Ratio and How to Overcome the Stick-Slip Phenomenon | Machine Design.” [Online]. Available: <https://www.machinedesign.com/mechanical-motion-systems/article/21836017/linear-bearings-understanding-the-2-1-ratio-and-how-to-overcome-the-stickslip-phenomenon>. [Accessed: 15-Jun-2020].
- [8] “DC motor vs AC motor for spindle.” [Online]. Available: <https://www.cnczone.com/forums/benchtop-machines/18529-dc-motor-vs-ac-motor-spindle.html>. [Accessed: 15-Jun-2020].
- [9] “A New Milling 101: Milling Forces and Formulas : Modern Machine Shop.” [Online]. Available: <https://www.mmsonline.com/articles/a-new-milling-101-milling-forces-and-formulas>. [Accessed: 15-Jun-2020].
- [10] “RAMPS 1.4 - RepRap.” [Online]. Available: https://reprap.org/wiki/RAMPS_1.4. [Accessed: 15-Jun-2020].
- [11] “Wiring 3D Printer RAMPS 1.4 : 12 Steps (with Pictures) - Instructables.” [Online]. Available: <https://www.instructables.com/id/Wiring-3D-Printer-RAMPS-14/>. [Accessed: 15-Jun-2020].
- [12] “Configuring Marlin | Marlin Firmware.” [Online]. Available: <https://marlinfw.org/docs/configuration/configuration.html>. [Accessed: 15-Jun-2020].
- [13] “Control spindle RPM through RAMPS - Mostly Printed CNC - MPCNC / Advice - V1 Engineering Forum.” [Online]. Available: <https://forum.v1engineering.com/t/control-spindle-rpm-through-ramps/5510>.

- [Accessed: 15-Jun-2020].
- [14] “GRBL vs. Marlin for milling - Mostly Printed CNC - MPCNC / Advice - V1 Engineering Forum.” [Online]. Available: <https://forum.v1engineering.com/t/grbl-vs-marlin-for-milling/6624>. [Accessed: 15-Jun-2020].
 - [15] “Introduction to SOLIDWORKS Simulation - Finite Element Analysis.” [Online]. Available: <https://blog.alignex.com/getting-started-with-solidworks-simulation-introduction-to-finite-element-analysis>. [Accessed: 15-Jun-2020].
 - [16] “Simulation Solutions | SOLIDWORKS.” [Online]. Available: <https://www.solidworks.com/category/simulation-solutions>. [Accessed: 15-Jun-2020].
 - [17] “Topology optimization - Wikipedia.” [Online]. Available: https://en.wikipedia.org/wiki/Topology_optimization. [Accessed: 15-Jun-2020].
 - [18] “Topology Optimization Comes to SOLIDWORKS - Engineers Rule.” [Online]. Available: <https://www.engineersrule.com/topology-optimization-comes-solidworks/>. [Accessed: 15-Jun-2020].
 - [19] “How can I make a cutting chip simulation in ABAQUS without having element distortion?” [Online]. Available: https://www.researchgate.net/post/How_can_I_make_a_cutting_chip_simulation_in_ABAQUS_without_having_element_distortion. [Accessed: 15-Jun-2020].
 - [20] “(18) Abaqus Tutorial 10 : Chip Formation Part1 - YouTube.” [Online]. Available: <https://www.youtube.com/watch?v=tnyWxQYylZc>. [Accessed: 15-Jun-2020].
 - [21] “(18) Abaqus Tutorial 10 : Chip Formation Part2 - YouTube.” [Online]. Available: <https://www.youtube.com/watch?v=9KKQNTwTVzk>. [Accessed: 15-Jun-2020].
 - [22] P. Specifications, “DEFORM -3D DEFORM-3D,” 1980.
 - [23] “(18) (4e+) Upmilling simulation setup using DEFORM 3D - YouTube.” [Online]. Available: https://www.youtube.com/watch?v=_68pKR9-edI&feature=youtu.be. [Accessed: 15-Jun-2020].
 - [24] “(18) DEFORM 2D and 3D Machining Tutorials - YouTube.” [Online]. Available: https://www.youtube.com/watch?v=_73JEsnhhqI. [Accessed: 15-Jun-2020].
 - [25] “Experimental evaluation of cutting force parameters applying mechanistic model in orthogonal milling.” [Online]. Available: https://www.scielo.br/scielo.php?script=sci_arttext&pid=S1678-58782003000300005. [Accessed: 15-Jun-2020].
 - [26] R. T. Coelho, A. Braghini, C. M. O. Valente, and G. C. Medalha, “Experimental evaluation of cutting force parameters applying mechanistic model in orthogonal milling,” *J. Brazilian Soc. Mech. Sci. Eng.*, vol. 25, no. 3, pp. 247–253, 2003.
 - [27] B. Wu, X. Yan, M. Luo, and G. Gao, “Cutting force prediction for circular end

milling process,” *Chinese J. Aeronaut.*, vol. 26, no. 4, pp. 1057–1063, Aug. 2013.

- [28] “Cutting force prediction for circular end milling process - ScienceDirect.” [Online]. Available: <https://www.sciencedirect.com/science/article/pii/S100093611300054X>. [Accessed: 15-Jun-2020].
- [29] “Machining Simulator | FANUC America.” [Online]. Available: <https://www.fanucamerica.com/products/cnc/fanuc-simulators/machining-simulator>. [Accessed: 15-Jun-2020].
- [30] “SINUMERIK 808D Tutorials Milling | Tutorials, Tips, Tricks (Milling) | Siemens Global.” [Online]. Available: <https://new.siemens.com/global/en/markets/machinebuilding/machine-tools/cnc4you/cnc4you-videos/ttt-mill/808d-tutorials-milling.html>. [Accessed: 15-Jun-2020].

APPENDIX I: ELECTRONICS



(Note: We have only used one RAMPS 1.4 but due to complexity of circuit, we have used another just for easiness of the circuit)

APPENDIX II: BOM

Final Year Project Title	Vendor's Name	Part Number	Quantity (numbers)	Dimensions in cm (L x W x H)	Weight (KG)	Specification (if any)	Price (PKR)	
Name of Student 1	Arslan Ali							
Name of Student 2	Fahad Khan							
Name of Student 3	Umer Farooq							
Name of Student 4	Usman Tahir							
Name of Final Year Project Supervisor	Dr. Mushthaq Khan							
Sr. No.	Brief Description of Part	Vendor's Name	Part Number	Quantity (numbers)	Dimensions in cm (L x W x H)	Weight (KG)	Specification (if any)	Price (PKR)
1	Laser Module and TTL Modulation Board	Banggood	LA03-3500	1	16.3x4.0x4.0	1.1	Wave length: 450nm Power: 3.5W	10095.61
2	Spindle and Power Supply Unit	Shenzhen Hanpose 3D Store, Aliexpress	0010-Z-500W	1	124.0x 13.0x 16.0	2	Power: 500W RPM: 3000-12000	9125
3	MK8 3D Printer Extruder	Kingroon Official Store, Aliexpress	80068F2-80	1	1.15x0.12x5x 11.0	0.6	Filament Size: 1.75mm	2534.38
4	E3D V6 Hotend	Super 3D Technology Co., Aliexpress	V6-175-B12V	1	1.10x0.10x0.8.0	0.18	Voltage: 12V Filament Size: 1.75mm	1270.38
5	Nema 23 Stepper Motor	Guangzhou Fude Electronic Technology Co., Alibaba	57SHD4934-348	4	4.5.64x 5.64x 10.0	1.3	Bipolar, Holding Torque: 3Nm	9710.65
6	Aluminium Extrusions	Electronics Panga, Faisalabad	C01-1.02-02/762	2	2.4x0.4x0.762	1.5	Base Extrusion Type C01-1	2250
7	Aluminium Extrusions	Electronics Panga, Faisalabad	C01-1.02-02/457.2	1	1.4x0.4x0.45.72	0.9	Base Extrusion Type C01-1	675
8	Aluminium Extrusions	Electronics Panga, Faisalabad	C01-3.02-02/762	2	2.8x0.4x0.762	2.6	Base Extrusion Type C01-3	3750
9	Mild Steel Plate	Abdul Rehman Traders, Rawalpindi	N/A	1	173.5x 73.5x 1.2	51	N/A	7500
10	Linear Rails	Electronics Panga, Faisalabad	HRC15MN	6	61.5x 1.5x 67.3	0.87	Static Load Capacity: 17.5KN	6000
11	Linear Bearing Blocks	Electronics Panga, Faisalabad	HRC15MN	12	5.9x 3.4 x 2.47	0.2	Dynamic Load Capacity: 9.9KN	7200
12	Ball Screw	Yueqing Ogy Bearing Co., Alibaba	SF-U1610	4	463.7x 1.6(L x D)	0.75	End Machined, Lead: 10mm	4210.77
13	Support Bearing Unit	Yueqing Ogy Bearing Co., Alibaba	BF12	4	46.0x 2.0x 3.9	0.35	Guide Diameter: 12mm	2000
14	Fixed Bearing Unit	Yueqing Ogy Bearing Co., Alibaba	BK12	4	46.0x 3.0x 3.9	0.45	Guide Diameter: 12mm	1550.57
15	XB Couplers	Yueqing Ogy Bearing Co., Alibaba	D30L40	4	4.0x 0.30(L x D)	0.03	Shaft Diameters : 8mm to 10mm	1101.78
16	Ball Screw Nut and Housing	Yueqing Ogy Bearing Co., Alibaba	DSG16H	4	4.5x 2.4x 0.4.0	0.5	SF-U1610, Lead: 10mm	4210.77
17	Aluminium Plate	Ismael Sons	N/A	1	1125.0x 160x 1.9	10	N/A	9500
18	HSS End Mill, 2 Flute	Banggood	N/A	5	5 N/A	0.08	2mm/3mm/4mm/5mm/6mm	812.73
19	PCB Drill Bits	Milling Grandmaster Store, Aliexpress	N/A	10	13.0x 11.0x 1.0	0.056	0.8-3.175mm	869.8
20	HSS End Mill, 2 Flute	Milling Grandmaster Store, Aliexpress	558004	5	57.0x 60x 2.0	0.08	2mm/3mm/4mm/5mm/6mm	585.72
21	Carbide Ball Nose End Mills	High Five Store, Aliexpress	N/A	10	10 N/A	0.04	1mm/1.5mm/2mm/2.5mm/3.175mm	1311.88
22	HSS End Mill, 4 Flute	High Five Store, Aliexpress	N/A	10	10.0x 0.8x 0.3.0	0.145	1.5-6mm	992.69
23	LAVIE Double Flute Straight End Mills	Lavie Store, Aliexpress	MIC06021	7	71.5x 5.0x 5.0	0.21	3-12mm	1278.36
24	ER16 Spring Collet	Banggood	ER16-10	1	12.75 x 1.7(L x D)	0.15	10mm Gripping Range	517.62
25	ER16 Collet Chuck Holder	Banggood	N/A	1	13.8x 2.0(L x D)	0.15	8mm Inner Diameter	1503.95
26	ER11 Spring Collets	Banggood	ER11-A	7	1.8x 1.15(L x D)	0.8	1-7mm Gripping Range	1423.47
27	Carbide End Mill	Waseem Enterprises	N/A	1	18.3x 1.2(L x D)	0.4	N/A	2500
28	HSS Drill Bits	Waseem Enterprises	N/A	8	8 N/A	N/A	3.3mm/5mm/6mm/12mm	1690
29	Socket Head Bolts	Nawaz Hardwares	N/A	80	80 N/A	N/A	M4/M6/M16	1450
30	Nut and Bolts	Noor Hardwares	N/A	6	6.35(L)	N/A	M16	180
31	M4 Tap Set	Manzoor Sons	N/A	1	1 N/A	0.13	N/A	150
32	M6 Tap Set	Nawaz Hardwares	N/A	1	1 N/A	0.2	N/A	650
33	M16 Tap Set	Noor Hardwares	N/A	1	1 N/A	0.35	N/A	350
34	Polishing Disk	Noor Hardwares	N/A	1	1 N/A	N/A	N/A	100
35	T-Slots Nut	Electronics Panga	N/A	12	12 N/A	N/A	M4	525
36	Arduino Mega	The IC Shop, Lahore	Mega 2560 R3	1	110.0x 5.3(L x W)	0.037	Microcontroller: ATmega2560	1200
37	RAMPS 1.4	The IC Shop, Lahore	N/A	1	112.3x 6.2(L x W)	0.07	N/A	500
38	Stepper Motor Driver	Electronics PRO, Lahore	TB6600	4	49.6x 5.7x 2.8	0.12	Rated Current: 3.5A Voltage: 40V	4600
39	Power Supply, 432W	Digitlog Electronics, Lahore	N/A	1	1 N/A	N/A	Voltage: 36V Current: 12A	6000
40	Power Supply, 240W	Digitlog Electronics, Lahore	N/A	1	1 N/A	N/A	Voltage: 12V Current: 20A	2500
41	3D Printer Heat Bed	Silver Lines, Lahore	MK3-4030	1	135.0x 33.0(L x W)	0.6	Voltage: 12V	2500
42	3D Printing Filament	Torwell Technologies Co., Ltd	N/A	1	1 N/A	0.5	PLA, 1.75mm	2900
43	3D Printing Filament	Torwell Technologies Co., Ltd	N/A	1	1 N/A	0.5	ABS, 1.75mm	2000
44	Nylon Rod	M Sardar, Sadar Rawalpindi	N/A	2	15.0x 6.0(L x D)	0.35	N/A	400
45	Spray Paint	Manzoor Sons	N/A	3	3 N/A	N/A	Volume: 300ml Per Bottle	600
46	Socket Head Bolts	Nawaz Hardwares	N/A	130	130 N/A	N/A	M3/M4/M5/M6	2000
47	MS Block	Ismael Sons	N/A	1	2.85x 6.5x 2.5	1	N/A	130
48	Aluminium Block	Ismael Sons	N/A	1	110.0x 90x 40	1	N/A	800
49	MS Block	Ismael Sons	N/A	1	110.0x 80x 20	1.3	N/A	170

Appendix III: Calculations

Motor torque calculations					
$F_A := 400$	N	$\theta := 0$	deg	$u := 0.05$	$m := 2 + 5 = 7$
$P_b := 0.01$	m	$\eta := 0.9$	$U_0 := 0.3$	$g := 9.8$	$\frac{m}{s^2}$
$F_t = F_A + m \cdot g \cdot (\sin(\theta) + u \cdot \cos(\theta)) = 403.43$					
$F_0 := \frac{1}{3} \cdot F_t$					
$T_L = \frac{(F_t \cdot P_b)}{2 \cdot \pi \cdot \eta} + \frac{(U_0 \cdot F_0 \cdot P_b)}{2 \cdot \pi} = 0.778$					
$\frac{N}{m}$					
Velocity for cutting = $V := 0.13333$					
$\frac{m}{s}$					
Acceleration = $a := 2$					
$\frac{m}{s^2}$					
Now time = $t_1 := \frac{V}{a} = 0.067$					
s					
Motor RPM = $N_m := 800$					
rpm					
$J_L = J_{coup} + J_{LS} + J_{nut} + J_{housing} + J_{bed} + J_{workpiece}$					
For calculations of J_{coup}					
$L = 0.025$	m	$D = 0.019$	m	$Den = 2700$	$\frac{kg}{m^3}$
$J_{coup} = \frac{\pi}{32} \cdot Den \cdot L \cdot D^4 = 8.636 \cdot 10^{-7}$					
$\frac{kg}{m^2}$					
For calculation of lead screw moment of inertia					
$L = 0.5$	m	$D = 0.016$	m	$Den = 8050$	$\frac{kg}{m^3}$
$J_{LS} = \frac{\pi}{32} \cdot Den \cdot L \cdot D^4 = 2.59 \cdot 10^{-5}$					
$\frac{kg}{m^3}$					
For calculation of moment of inertia of nut					
$Density := 8050$	$\frac{kg}{m^3}$	$A := 0.01$	$\frac{m}{rev}$		
$L_1 := 0.047$	m	$L_2 := 0.010$	m	$D_1 := 0.028$	m
				$D_2 := 0.016$	m
				$D_3 := 0.048$	m

$$Volume := \frac{\pi}{4} \cdot (D_3^2 - D_2^2) \cdot L_2 + \frac{\pi}{4} \cdot (D_1^2 - D_2^2) \cdot L_1 = 3.558 \cdot 10^{-5} \text{ m}^3$$

$$J_{nut} := Density \cdot Volume \cdot \left(\frac{A}{2 \cdot \pi} \right)^2 = 7.254 \cdot 10^{-7} \frac{kg}{m^2}$$

For calculation of nut housing moment of inertia

$$Volume := 4.80976 \cdot 10^{-5} \text{ m}^3 \quad Density := 2700 \frac{kg}{m^3} \quad Pitch := 0.01 \text{ m}$$

$$J_{housing} := Density \cdot Volume \cdot \left(\frac{Pitch}{2 \cdot \pi} \right)^2 = 3.289 \cdot 10^{-7} \frac{kg}{m^2}$$

For calculation of bed moment of inertia

$$Mass \text{ of bed} = m_{bed} := 5 \text{ kg} \quad Pitch := 0.01 \text{ m}$$

$$J_{bed} := m_{bed} \cdot \left(\frac{Pitch}{2 \cdot \pi} \right)^2 = 1.267 \cdot 10^{-5} \frac{kg}{m^2}$$

For calculation of work piece moment of inertia

$$Mass \text{ of bed} = m_{workpiece} := 2 \text{ kg} \quad Pitch := 0.01 \text{ m}$$

$$J_{workpiece} := m_{workpiece} \cdot \left(\frac{Pitch}{2 \cdot \pi} \right)^2 = 5.066 \cdot 10^{-6} \frac{kg}{m^2}$$

$$J_L := J_{comp} + J_{LS} + J_{nut} + J_{housing} + J_{bed} + J_{workpiece} = 4.555 \cdot 10^{-5} \frac{kg}{m^2}$$

For Nema 23 Model Number:57SHD4934

$$\text{From the documentation} = J_0 := 0.000065 \frac{kg}{m^2}$$

$$\text{Acceleration torque} = T_a := \frac{(J_0 \cdot i^2 + J_L)}{9.55} \cdot N_m = 0.009$$

$$\text{Safety factor of motor} = S_f := 2.5$$

$$\text{Motor torque} = T_M := (T_L + T_a) \cdot S_f = 1.967 \frac{N}{m}$$

Motor torque calculations

$$F_A := 0 \text{ N} \quad \theta := 90 \text{ deg} \quad u := 0.05 \quad m := 15 \text{ kg}$$

$$P_b := 0.01 \text{ m} \quad \eta := 0.9 \quad U_o := 0.3 \quad g := 9.8 \frac{\text{m}}{\text{s}^2}$$

$$F_t = F_A + m \cdot g \cdot \left(\sin \left(\theta \cdot \frac{\pi}{180} \right) + u \cdot \cos \left(\theta \cdot \frac{\pi}{180} \right) \right) = 147 \text{ N}$$

$$F_o := \frac{1}{3} \cdot F_t = 49 \text{ N}$$

$$T_L := \frac{(F_t \cdot P_b)}{2 \cdot \pi \cdot \eta} + \frac{(U_o \cdot F_o \cdot P_b)}{2 \cdot \pi} = 0.283 \frac{\text{N}}{\text{m}}$$

$$\text{Velocity for cutting} = V := 0.13333 \frac{\text{m}}{\text{s}}$$

$$\text{Acceleration} = a := 2 \frac{\text{m}}{\text{s}^2}$$

$$\text{Now time} = t_1 := \frac{V}{a} = 0.067 \text{ s}$$

$$\text{Motor RPM} = N_m := 800 \text{ rpm}$$

$$J_L = J_{\text{coup}} + J_{LS} + J_{\text{nut}} + J_{\text{housing}} + J_{\text{bed}} + J_{\text{totalmax}}$$

For calculations of J_{coup}

$$L = 0.025 \text{ m} \quad D := 0.019 \text{ m} \quad \text{Den} := 2700 \frac{\text{kg}}{\text{m}^3}$$

$$J_{\text{coup}} := \frac{\pi}{32} \cdot \text{Den} \cdot L \cdot D^4 = 8.636 \cdot 10^{-7} \frac{\text{kg}}{\text{m}^2}$$

For calculation of lead screw moment of inertia

$$L = 0.5 \text{ m} \quad D := 0.016 \text{ m} \quad \text{Den} := 8050 \frac{\text{kg}}{\text{m}^3}$$

$$J_{LS} := \frac{\pi}{32} \cdot \text{Den} \cdot L \cdot D^4 = 2.59 \cdot 10^{-5} \frac{\text{kg}}{\text{m}^2}$$

For calculation of moment of inertia of nut

$$\text{Density} := 8050 \frac{\text{kg}}{\text{m}^3} \quad A = 0.01 \text{ m}^2$$

$$L_1 = 0.047 \text{ m} \quad L_2 = 0.010 \text{ m} \quad D_1 = 0.028 \text{ m} \quad D_2 = 0.016 \text{ m} \quad D_3 = 0.048 \text{ m}$$

|| V

$$Volume := \frac{\pi}{4} \cdot (D_3^2 - D_2^2) \cdot L_2 + \frac{\pi}{4} \cdot (D_1^2 - D_2^2) \cdot L_1 = 3.558 \cdot 10^{-5} \text{ m}^3$$

$$J_{nut} := Density \cdot Volume \cdot \left(\frac{A}{2 \cdot \pi} \right)^2 = 7.254 \cdot 10^{-7} \frac{kg}{m^2}$$

For calculation of nut housing moment of inertia

$$Volume := 4.80976 \cdot 10^{-5} \text{ m}^3 \quad Density := 2700 \frac{kg}{m^3} \quad Pitch := 0.01 \text{ m}$$

$$J_{housing} := Density \cdot Volume \cdot \left(\frac{Pitch}{2 \cdot \pi} \right)^2 = 3.289 \cdot 10^{-7} \frac{kg}{m^2}$$

For finding moment of inertia of total mass

$$Total \ mass = \quad m_{totalmass} := 15 \text{ kg} \quad Pitch := 0.01 \text{ m}$$

$$J_{totalmass} := m_{totalmass} \cdot \left(\frac{Pitch}{2 \cdot \pi} \right)^2 = 3.8 \cdot 10^{-5} \frac{kg}{m^2}$$

$$J_L := J_{coup} + J_{LG} + J_{nut} + J_{housing} + J_{totalmass} = 6.581 \cdot 10^{-5} \frac{kg}{m^2}$$

For Nema 23 Model Number:57SHD4934

$$From \ the \ documentation = \quad J_0 := 0.000065 \frac{kg}{m^2} \quad i := 1$$

$$Acceleration \ torque = \quad T_a := \frac{(J_0 \cdot i^2 + J_L)}{9.55} \cdot N_m = 0.011 \frac{N}{m}$$

$$Safety \ factor \ of \ motor = \quad S_f := 2.5$$

$$Motor \ torque = \quad T_M := (T_L + T_a) \cdot S_f = 0.736 \frac{N}{m}$$

Milling forces calculation

Machine tool efficiency= $E := 0.8$

Tool wear factor= $W := 1.25$

Feed Factor= $C := 0.86$

Power constant= $K_p := 0.25$

Width of cut= $WOC := 2.5$

Depth of cut= $DOC := 1.05$

$P_b := 0.005$

Feed per tooth= $Z := 0.55$ (Recommended for wood)

Tool diameter= $d := 5$

Cutting Velocity= $V_C := 183 \frac{m}{min}$

Revolutions per minute= $RPM := V_C \cdot \frac{1000}{\pi \cdot d} = 1.165 \cdot 10^4 \text{ rpm}$

Number of teeth= $n := 2$

Feed rate= $f := RPM \cdot Z \cdot n = 1.282 \cdot 10^4$

Material removal rate= $MRR := f \cdot DOC \cdot WOC = 3.364 \cdot 10^4 \frac{mm^3}{min}$

MRR in inch³/min= $Q = \frac{MRR}{0.0254^3 \cdot 1000^3} = 2.053 \frac{inch^3}{min}$

Cutting Power= $CP := Q \cdot C \cdot K_p \cdot W = 0.552 \text{ hp}$

Spindle power(hp)= $SP := \frac{CP}{E} = 0.69 \text{ hp}$

Spindle power(kw)= $SP_{kw} := SP \cdot 0.7457 = 0.514 \text{ kW}$

Torque(Nm)= $T := SP_{kw} \cdot 30 \cdot \frac{1000}{RPM \cdot \pi} = 0.422 \text{ Nm}$

Tangential Cutting force= $F_t := \frac{SP_{kw} \cdot 1000 \cdot 60}{V_C} = 168.607 \text{ N}$

Radial Cutting force= $F_r := 0.8 \cdot F_t = 134.885 \quad N$

Total cutting force= $C_f := \sqrt{F_r^2 + F_t^2} = 215.922 \quad N$

Ball screw efficiency= $\eta := 0.9$ Lead= $P_B := 0.01$

Stepper motor torque= $T := 3.1 \quad Nm$

$$F := \frac{(2 \cdot \pi \cdot \eta \cdot T)}{P_b} = 3.506 \cdot 10^3 \quad N$$

Worst case scenario force in design $F_w = F + C_f = 3.722 \cdot 10^3 \quad N$

Clamp Design Calculations

1) Translation of forces:

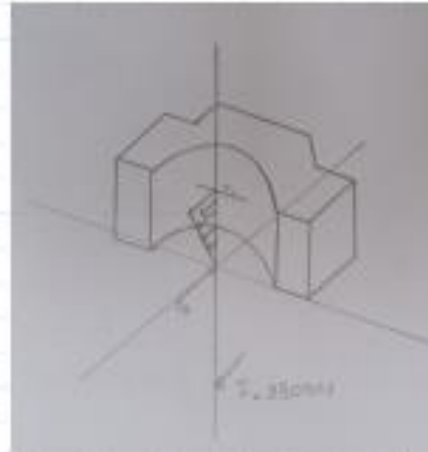
$$r_z := 0.2$$

$$F := 3800$$

$$l_z := 0.026667$$

$$F_a := 2.85 \cdot 10^4$$

$$F_b := F_a + F = 3.23 \cdot 10^4$$



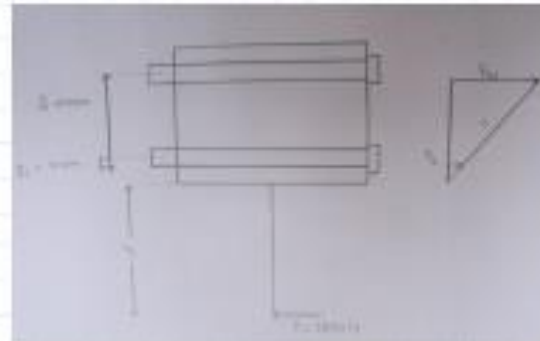
2) Tensile load calculations in clamp bolts:

$$y_1 := 0.010$$

$$y_2 := 0.030$$

$$F_{t1} := \frac{(F \cdot r_z \cdot y_1)}{2 (y_1^2 + y_2^2)} = 3.8 \cdot 10^3$$

$$F_{t2} := \frac{(F \cdot r_z \cdot y_2)}{2 (y_1^2 + y_2^2)} = 1.14 \cdot 10^4$$



3) Bolt design and Bolt load factor calculations:

Effective grip length = $l := 0.057$ m (From table 8.7, case B)

Hence Fastener Length = $L := 0.071$ m

$d = 0.006$ m

Threaded length = $L_T := 2 \cdot d + 0.006 = 0.018$ (From table 8.7 case B)

Length of unthreaded portion and grip grip = $l_d := L - L_T = 0.053$ m

Length of threaded portion in grip = $l_1 := l - l_d = 0.004$ m

Area of unthreaded portion = $A_d := \pi \cdot \frac{d^2}{4} = 2.827 \cdot 10^{-5}$ sq. meter

Area of threaded portion = $A_t := 20.1 \cdot 10^{-6}$ sq. meter From table 8.1

We assume bolts are made of gray cast iron

$$E := 100 \cdot 10^9 \text{ Pa} \quad (\text{From table 8.8})$$

$$K_b := \frac{(A_d \cdot A_t \cdot E)}{A_d \cdot l_t + A_t \cdot l_d} = 4.823 \cdot 10^7 \text{ N/m}$$

Calculating K_m for the clamp material

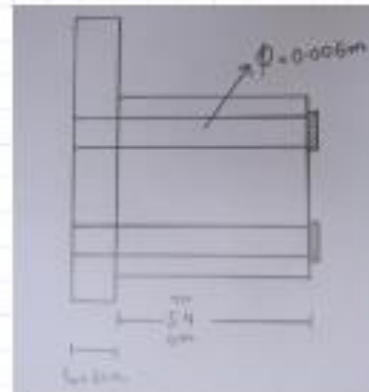
$$A := 0.7967 \quad \text{From table 8.8}$$

$$B := 0.63816$$

$$E_{\text{aluminium}} := 71 \cdot 10^9 \text{ Pa}$$

$$K_m := E_{\text{aluminium}} \cdot d \cdot A^{-1} = 4.195 \cdot 10^8$$

$$C := \frac{K_b}{K_b + K_m} = 0.103$$



Now we want to calculate the number of bolts used if load factor is 2.5

Load factor = $n = 3$

Proof strength = $S_p := 225 \cdot 10^6 \text{ Pa}$ (From table 8.11)

$$F_1 := 0.75 \cdot S_p \cdot A_t = 3.392 \cdot 10^3 \text{ N}$$

$$\text{Number of bolts} = N := n \cdot \frac{(C \cdot F_{t2})}{S_p \cdot A_t - F_1} = 3.119$$

4) Calculation of bearing stress induced by bolt head due to tensile load in bolts

$$\text{Diameter of bolt} = d_{\text{bolt}} := 0.006 \text{ m}$$

$$\text{Diameter of head} = d_{\text{head}} := 0.010 \text{ m}$$

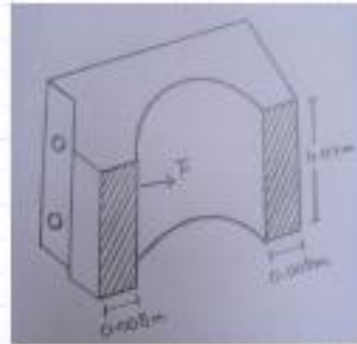
$$\text{Bearing stress} = \sigma := \frac{F_{t2}}{\frac{\pi}{4} \cdot (d_{\text{head}}^2 - d_{\text{bolt}}^2)} = 2.268 \cdot 10^8$$



5) Shear stress in clamp

$$A_1 := 2 \cdot 0.008 \cdot 0.040 = 6.4 \cdot 10^{-4} \text{ sq.meter}$$

$$\text{Shear stress in clamp} = \sigma_{\text{shear}} := \frac{F}{A_1} = 5.938 \cdot 10^6 \text{ Pa}$$



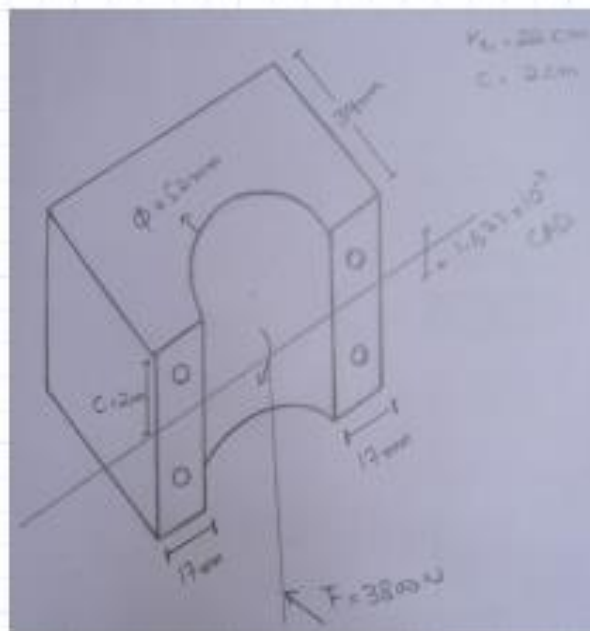
6) Bending stress calculation in clamp

$$r_{st} := 0.220 \text{ m}$$

$$c := 0.020 \text{ m}$$

$$I := 1.677 \cdot 10^{-7} \text{ m}^4$$

$$\text{Bending stress} = \sigma_{\text{bend}} := F \cdot \frac{(r_{st} \cdot c)}{I} = 9.97 \cdot 10^7 \text{ Pa}$$



7) Shear force calculation in clamp bolts

$$\theta := 105.96$$

$$M := F \cdot r_{s1} = 836 \text{ Nm}$$

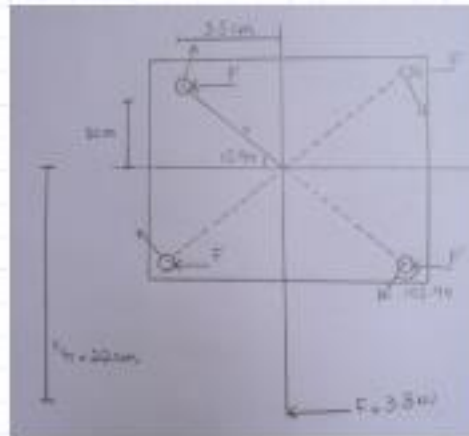
$$F_{\text{primaryShear}} := \frac{F}{4} = 950 \text{ Pa}$$

$$r := \sqrt{0.035^2 + 0.010^2} = 0.036 \text{ m}$$

$$F_{\text{SecondaryShear}} := M \cdot \frac{r}{4 \cdot r^2} = 5.742 \cdot 10^3$$

$$F_{\text{shearmax}} := \sqrt{F_{\text{SecondaryShear}}^2 + F_{\text{primaryShear}}^2 - 2 \cdot F_{\text{SecondaryShear}} \cdot F_{\text{primaryShear}} \cdot \cos\left(\theta \cdot \frac{\pi}{180}\right)}$$

$$F_{\text{shearmax}} = 6.072 \cdot 10^3 \text{ N}$$



8) Shear stress calculation in bolts of clamp

$$A_r := 17.9 \cdot 10^{-6} \text{ sq.metre}$$

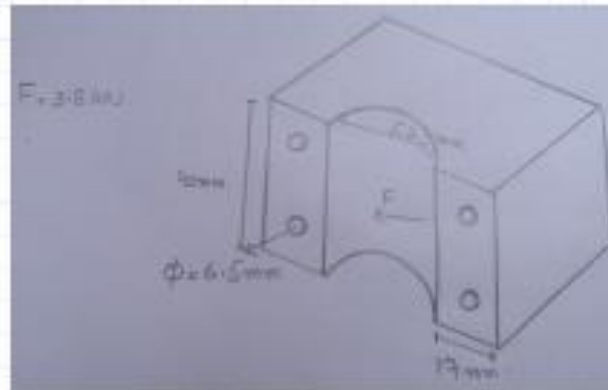
$$\tau := \frac{F_{\text{shearmax}}}{A_r} = 3.392 \cdot 10^8 \text{ Pa}$$



9) Shear Stress in clamp

$$A_2 := 2 \cdot 0.019 \cdot 0.040 - 4 \cdot (\pi \cdot 0.00325^2) = 0.001 \text{ sq meters}$$

$$\sigma_{\text{shear},X} := \frac{F}{A_2} = 2.739 \cdot 10^6 \text{ Pa}$$



10) Bearing stress calculation due to shear force of bolt holes

$$\sigma := \frac{F_{\text{shear,max}}}{0.0065 \cdot 0.054} = 1.73 \cdot 10^7 \text{ Pa}$$

Material Selection:

99.7 Mpa is the maximum Stress magnitude that the spindle clamp has to bear. Now we will compare this value to the Ultimate Tensile Strength of various other materials.

Ultimate Tensile Strength:

1. Aluminum	110 MPa
2. Cast Iron	170 MPa
3. Steel High Strength Alloy ASTM A-514	760 MPa
4. Titanium Alloy	900 MPa
5. Structural Steel ASTM A-36	400 MPa

Here we can see that all of these materials are suitable for use as a clamp. However, we chose to use aluminum due to the following reasons, where it stood better than all of its competitors. These were mainly.

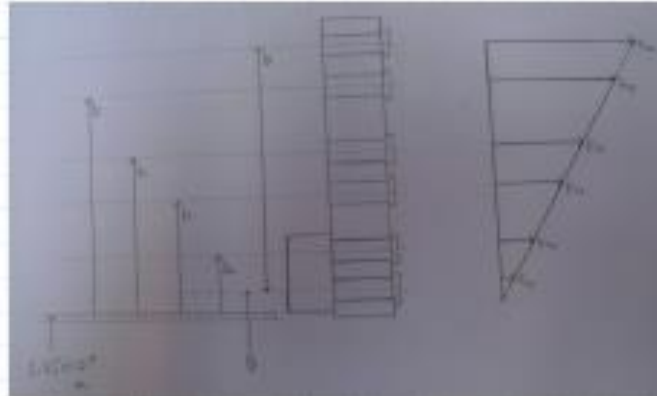
1. Availability of material
2. Cost of procurement
3. Low weight requirement
4. Machinability
5. Adequate Strength

X-axis Plate design calculations

1) Tensile load calculations in X axis plate bolts

$$F := 3800 \text{ N} \quad y_1 := 0.0053 \quad y_2 := 0.0303 \quad y_3 := 0.0528$$

$$y_4 := 0.0928 \quad y_5 := 0.1153 \quad y_6 := 0.1403 \quad r_z := 0.14723$$



$$F_{t1} := \frac{(F \cdot r_z \cdot y_1)}{(4 \cdot y_1^2 + 4 \cdot y_2^2 + 2 \cdot y_3^2 + 2 \cdot y_4^2 + 4 \cdot y_5^2 + 4 \cdot y_6^2)} = 18.708$$

$$F_{t2} := \frac{(F \cdot r_z \cdot y_2)}{(4 \cdot y_1^2 + 4 \cdot y_2^2 + 2 \cdot y_3^2 + 2 \cdot y_4^2 + 4 \cdot y_5^2 + 4 \cdot y_6^2)} = 106.955$$

$$F_{t3} := \frac{(F \cdot r_z \cdot y_3)}{(4 \cdot y_1^2 + 4 \cdot y_2^2 + 2 \cdot y_3^2 + 2 \cdot y_4^2 + 4 \cdot y_5^2 + 4 \cdot y_6^2)} = 186.377$$

$$F_{t4} := \frac{F \cdot r_z \cdot y_4}{(4 \cdot y_1^2 + 4 \cdot y_2^2 + 2 \cdot y_3^2 + 2 \cdot y_4^2 + 4 \cdot y_5^2 + 4 \cdot y_6^2)} = 327.572$$

$$F_{t5} := \frac{(F \cdot r_z \cdot y_5)}{(4 \cdot y_1^2 + 4 \cdot y_2^2 + 2 \cdot y_3^2 + 2 \cdot y_4^2 + 4 \cdot y_5^2 + 4 \cdot y_6^2)} = 406.995$$

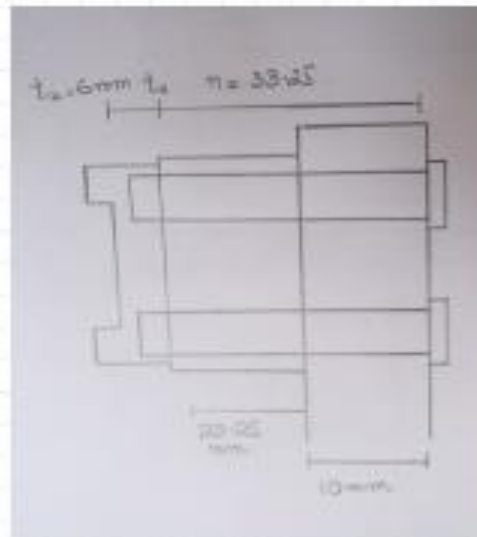
$$F_{t6} := \frac{(F \cdot r_z \cdot y_6)}{(4 \cdot y_1^2 + 4 \cdot y_2^2 + 2 \cdot y_3^2 + 2 \cdot y_4^2 + 4 \cdot y_5^2 + 4 \cdot y_6^2)} = 495.242$$

2) Bolt design and bolt load factor calculations

Effective grip length = $l = 0.012$ (From table 8.7 case B)

Hence Fastener length = $L = 0.016$

$d = 0.004$



Threaded length = $L_T = 2 \cdot d + 0.006 = 0.014$ (From table 8.7 case B)

Length of unthreaded portion and grip = $l_d = L - L_T = 0.002$

Length of threaded portion in grip = $l_t = l - l_d = 0.01$

Area of unthreaded portion = $A_d = \pi \cdot \frac{d^2}{4} = 1.257 \cdot 10^{-5}$

Area of threaded portion = $A_t = 8.78 \cdot 10^{-6}$ From table 8.1

We assume bolts are made of gray cast iron

$E = 100 \cdot 10^9$ From table 8.8

$$K_b = \frac{(A_d \cdot A_t \cdot E)}{A_d \cdot l_t + A_t \cdot l_d} = 7.704 \cdot 10^7$$

Calculating Km for the material

$$A := 0.7967$$

$$B := 0.63816$$

$$E_{\text{aluminium}} := 71 \cdot 10^9$$

$$K_m := E_{\text{aluminium}} \cdot d \cdot A \cdot \frac{(B-d)}{l} = 2.706 \cdot 10^8$$

$$C := \frac{K_b}{K_b + K_m} = 0.222$$

$$F_{t1\text{clamp}} := 3.8 \cdot 10^3$$

$$F_{t2\text{clamp}} := 1.14 \cdot 10^4$$

Now we want to calculate the number of bolts used if load factor is 2.5

$$P := 2 \cdot (F_{t1\text{clamp}} + F_{t2\text{clamp}}) = 3.04 \cdot 10^4$$

$$\text{Number of bolts} = N := 16$$

$$\text{Proof strength} = S_p := 310 \cdot 10^6 \text{ Pa} \quad \text{From table 8.11}$$

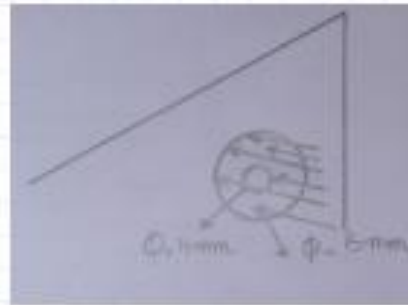
$$F_i := 0.75 \cdot S_p \cdot A_t = 2.041 \cdot 10^3$$

$$\text{Load Safety Factor} = n := N \cdot \frac{(S_p \cdot A_t - F_i)}{C \cdot P} = 1.616$$

3) Calculation of bearing stress induced by bolt head due to tensile load in bolts

$$\text{Diameter of bolt} = d_{\text{bolt}} = 0.004$$

$$\text{Diameter of head} = d_{\text{head}} = 0.006$$



$$\text{Bearing stress} = \sigma := \frac{F_{\text{tens}}}{\frac{\pi}{4} \cdot (d_{\text{head}}^2 - d_{\text{bolt}}^2)} = 3.153 \cdot 10^7$$

4) Shear force calculation in X-axis plate bolts

$$r_{z1} = 0.220$$

$$M_1 := F \cdot r_{z1} = 836$$

$$r_a = \sqrt{0.020^2 + 0.012^2} = 0.023$$

$$r_b = \sqrt{0.0425^2 + 0.05815^2} = 0.072$$

$$r_c = \sqrt{0.0675^2 + 0.02815^2} = 0.073$$

$$r_d = \sqrt{0.0425^2 + 0.02815^2} = 0.051$$

$$r_e = \sqrt{0.0675^2 + 0.05815^2} = 0.089$$

$$F' := \frac{F}{20} = 190$$

$$F''_a := M_1 \cdot \frac{r_a}{4 \cdot (r_a^2 + r_b^2 + r_c^2 + r_d^2 + r_e^2)} = 225.505$$

$$F''_b := M_1 \cdot \frac{r_b}{4 \cdot (r_a^2 + r_b^2 + r_c^2 + r_d^2 + r_e^2)} = 696.375$$

$$F''_c := M_1 \cdot \frac{r_c}{4 \cdot (r_a^2 + r_b^2 + r_c^2 + r_d^2 + r_e^2)} = 707.099$$

$$F''_d := M_1 \cdot \frac{r_d}{4 \cdot (r_a^2 + r_b^2 + r_c^2 + r_d^2 + r_e^2)} = 492.871$$

$$F''_e := M_1 \cdot \frac{r_e}{4 \cdot (r_a^2 + r_b^2 + r_c^2 + r_d^2 + r_e^2)} = 861.398$$

$$Theta_A := 153.4 \quad Theta_B := 126.2 \quad Theta_C := 157.4$$

$$Theta_D := 146.5 \quad Theta_E := 139.3$$

$$F_{shearmaxA} := \sqrt{F''_a^2 + F''^2 - 2 \cdot F' \cdot F''_a \cdot \cos\left(Theta_A \cdot \frac{\pi}{180}\right)} = 404.443$$

$$F_{shearmaxB} := \sqrt{F''_b^2 + F''^2 - 2 \cdot F' \cdot F''_b \cdot \cos\left(Theta_B \cdot \frac{\pi}{180}\right)} = 822.998$$

$$F_{shearmaxC} := \sqrt{F''_c^2 + F''^2 - 2 \cdot F' \cdot F''_c \cdot \cos\left(Theta_C \cdot \frac{\pi}{180}\right)} = 885.524$$

$$F_{shearmaxD} := \sqrt{F''_d^2 + F''^2 - 2 \cdot F' \cdot F''_d \cdot \cos\left(Theta_D \cdot \frac{\pi}{180}\right)} = 659.697$$

$$F_{shearmaxE} := \sqrt{F''_e^2 + F''^2 - 2 \cdot F' \cdot F''_e \cdot \cos\left(Theta_E \cdot \frac{\pi}{180}\right)} = 1.013 \cdot 10^3$$

5) Shear stress calculation in bolts of clamp

$$A_r := 7.75 \cdot 10^{-6} \quad \text{From table 8.1}$$

$$\tau := \frac{F_{shearmaxE}}{A_r} = 1.307 \cdot 10^8 \quad \text{Pa}$$

6) Calculation of thickness of plate using allowable bearing stress on bolt holes

$$FS = 3$$

Yield Strength of aluminium = $\sigma_y = 241 \cdot 10^6 \text{ Pa}$

$$\sigma_{\text{allowable}} := \frac{\sigma_y}{FS} = 8.033 \cdot 10^7 \text{ Pa}$$

$$\sigma_{\text{bearing}} = \frac{F_{\text{shearmax}}}{0.004 \cdot t}$$

To find minimum thickness of the plate, $t \sigma_{\text{bearing}} = \sigma_{\text{allowable}}$

This implies that

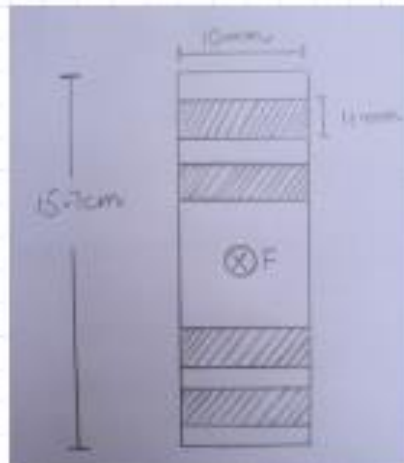
$$t := \frac{F_{\text{shearmax}}}{0.004 \cdot \sigma_{\text{bearing}}} = 0.003 \text{ m}$$

To increase the rigidity and compactness of the structure and keeping in mind the clearances for bolts we decided to use 10 mm thickness plate

7) Normal stress calculations in X axis plate

$$A_3 := 0.157 \cdot 0.01 - 4 \cdot 0.004 \cdot 0.01 = 0.001 \text{ m}^2$$

$$\sigma_{\text{normal}} := \frac{F}{A_3} = 2.695 \cdot 10^8 \text{ Pa}$$



Material Selection:

31.5 Mpa is the maximum Stress magnitude that the X-axis plate has to bear. Now we will compare this value to the Ultimate Tensile Strength of various other materials.

Ultimate Tensile Strength:

1. Aluminum	110 MPa
2. Cast Iron	170 MPa
3. Steel High Strength Alloy ASTM A-514	760 MPa
4. Titanium Alloy	900 MPa
5. Structural Steel ASTM A-36	400 MPa

Here we can see that all of these materials are suitable for use as a clamp. However, we chose to use aluminum due to the following reasons, where it stood better than all of its competitors. These were mainly.

1. Availability of material
2. Cost of procurement
3. Low weight requirement
4. Machinability
5. Adequate Strength

Z-axis Plate design calculations

1) Tensile load calculations in Z axis plate bolts

$$F = 3800 \text{ N} \quad y_1 := 0.01565 \quad y_2 := 0.04565 \quad y_3 := 0.0618$$

$$y_4 := 0.0858 \quad y_5 := 0.16195 \quad y_6 := 0.13195 \quad r_z := 0.14623$$

$$F_{t1} = \frac{(F \cdot r_z \cdot y_1)}{(4 \cdot y_1^2 + 4 \cdot y_2^2 + 4 \cdot y_3^2 + 4 \cdot y_4^2 + 4 \cdot y_5^2 + 4 \cdot y_6^2)} = 38.043$$

$$F_{t2} = \frac{(F \cdot r_z \cdot y_2)}{(4 \cdot y_1^2 + 4 \cdot y_2^2 + 4 \cdot y_3^2 + 4 \cdot y_4^2 + 4 \cdot y_5^2 + 4 \cdot y_6^2)} = 110.968$$

$$F_{t3} = \frac{(F \cdot r_z \cdot y_3)}{(4 \cdot y_1^2 + 4 \cdot y_2^2 + 4 \cdot y_3^2 + 4 \cdot y_4^2 + 4 \cdot y_5^2 + 4 \cdot y_6^2)} = 150.226$$

$$F_{t4} = \frac{F \cdot r_z \cdot y_4}{(4 \cdot y_1^2 + 4 \cdot y_2^2 + 4 \cdot y_3^2 + 4 \cdot y_4^2 + 4 \cdot y_5^2 + 4 \cdot y_6^2)} = 208.566$$

$$F_{t5} = \frac{(F \cdot r_z \cdot y_5)}{(4 \cdot y_1^2 + 4 \cdot y_2^2 + 4 \cdot y_3^2 + 4 \cdot y_4^2 + 4 \cdot y_5^2 + 4 \cdot y_6^2)} = 393.675$$

$$F_{t6} = \frac{(F \cdot r_z \cdot y_6)}{(4 \cdot y_1^2 + 4 \cdot y_2^2 + 4 \cdot y_3^2 + 4 \cdot y_4^2 + 4 \cdot y_5^2 + 4 \cdot y_6^2)} = 320.749$$

2) Bolt design and bolt load factor calculations

Effective grip length = $l := 0.04025 \text{ m}$ (From table 8.7 case B)

Hence Fastener length = $L := 0.045 \text{ m}$

$$d = 0.004$$

Threaded length = $L_T := 2 \cdot d + 0.006 = 0.014$ (From table 8.7 case B)

Length of unthreaded portion and grip = $l_d := L - L_T = 0.031$

Length of threaded portion in grip = $l_t := l - l_d = 0.009$

Area of unthreaded portion = $A_d := \pi \cdot \frac{d^2}{4} = 1.257 \cdot 10^{-5}$

Area of threaded portion = $A_t := 8.78 \cdot 10^{-6}$ From table 8.1

We assume bolts are made of gray cast iron

$E := 100 \cdot 10^9$ From table 8.8

$$K_b := \frac{(A_d \cdot A_t \cdot E)}{A_d \cdot l_t + A_t \cdot l_d} = 2.841 \cdot 10^7$$

Calculating K_m for the material

$$A := 0.7967$$

$$B := 0.63816$$

$$E_{\text{aluminium}} := 71 \cdot 10^9$$

$$K_m := E_{\text{aluminium}} \cdot d \cdot A^{\frac{(B-d)}{t}} = 2.799 \cdot 10^8$$

$$C := \frac{K_b}{K_b + K_m} = 0.092$$

$$F_{t1\text{clamp}} := 3.8 \cdot 10^3$$

$$F_{t2\text{clamp}} := 1.14 \cdot 10^4$$

Now we want to calculate the number of bolts used if load factor is 2.5

$$P := 2 \cdot (F_{t1\text{clamp}} + F_{t2\text{clamp}}) = 3.04 \cdot 10^4$$

Number of bolts = $N := 16$

Proof strength = $S_p := 310 \cdot 10^6 \text{ Pa}$ From table 8.11

$$F_t := 0.75 \cdot S_p \cdot A_t = 2.041 \cdot 10^3$$

$$\text{Load Safety Factor} = n := N \cdot \frac{(S_p \cdot A_t - F_t)}{C \cdot P} = 3.888$$

3) Calculation of bearing stress induced by bolt head due to tensile load in bolts

$$\text{Diameter of bolt} = d_{\text{bolt}} := 0.004$$

$$\text{Diameter of head} = d_{\text{head}} := 0.006$$

$$\text{Bearing stress} = \sigma := \frac{F_t}{\frac{\pi}{4} \cdot (d_{\text{head}}^2 - d_{\text{bolt}}^2)} = 2.042 \cdot 10^7$$

4) Shear force calculation in X-axis plate bolts

$$r_{z1} := 0.220$$

$$M_1 := F \cdot r_{z1} = 836$$

$$r_a := \sqrt{0.1875^2 + 0.05815^2} = 0.196$$

$$r_b := \sqrt{0.05815^2 + 0.2125^2} = 0.22$$

$$r_c := \sqrt{0.1875^2 + 0.02815^2} = 0.19$$

$$r_d := \sqrt{0.2125^2 + 0.02815^2} = 0.214$$

$$r_e := \sqrt{0.22675^2 + 0.012^2} = 0.227$$

$$r_f := \sqrt{0.26675^2 + 0.012^2} = 0.267$$

$$F' := \frac{F}{24} = 158.333 \text{ N}$$

$$F''_a := M_1 \cdot \frac{r_a}{4 \cdot (r_a^2 + r_b^2 + r_c^2 + r_d^2 + r_e^2 + r_f^2)} = 140.591$$

$$F''_b := M_1 \cdot \frac{r_b}{4 \cdot (r_a^2 + r_b^2 + r_c^2 + r_d^2 + r_e^2 + r_f^2)} = 157.78$$

$$F''_c := M_1 \cdot \frac{r_c}{4 \cdot (r_a^2 + r_b^2 + r_c^2 + r_d^2 + r_e^2 + r_f^2)} = 135.786$$

$$F''_d := M_1 \cdot \frac{r_d}{4 \cdot (r_a^2 + r_b^2 + r_c^2 + r_d^2 + r_e^2 + r_f^2)} = 153.515$$

$$F''_e := M_1 \cdot \frac{r_e}{4 \cdot (r_a^2 + r_b^2 + r_c^2 + r_d^2 + r_e^2 + r_f^2)} = 162.618$$

$$F''_f := M_1 \cdot \frac{r_f}{4 \cdot (r_a^2 + r_b^2 + r_c^2 + r_d^2 + r_e^2 + r_f^2)} = 191.23$$

$$Theta_A := 107.23 \quad Theta_B := 105.3 \quad Theta_C := 98.54$$

$$Theta_D := 97.55 \quad Theta_E := 93.03 \quad Theta_F := 92.78$$

$$F_{shearmaxA} := \sqrt{F''_a^2 + F''^2 - 2 \cdot F'' \cdot F''_a \cdot \cos\left(Theta_A \cdot \frac{\pi}{180}\right)} = 240.879$$

$$F_{shearmaxB} := \sqrt{F''_b^2 + F''^2 - 2 \cdot F'' \cdot F''_b \cdot \cos\left(Theta_B \cdot \frac{\pi}{180}\right)} = 251.293$$

$$F_{shearmaxC} := \sqrt{F''_c^2 + F''^2 - 2 \cdot F'' \cdot F''_c \cdot \cos\left(Theta_C \cdot \frac{\pi}{180}\right)} = 223.367$$

$$F_{shearmaxD} := \sqrt{F''_d^2 + F''^2 - 2 \cdot F'' \cdot F''_d \cdot \cos\left(Theta_D \cdot \frac{\pi}{180}\right)} = 234.571$$

$$F_{shearmaxE} := \sqrt{F''_e^2 + F''^2 - 2 \cdot F'' \cdot F''_e \cdot \cos\left(Theta_E \cdot \frac{\pi}{180}\right)} = 232.886$$

$$F_{shearmaxF} := \sqrt{F''_f^2 + F''^2 - 2 \cdot F'' \cdot F''_f \cdot \cos\left(Theta_F \cdot \frac{\pi}{180}\right)} = 254.117$$

5) Shear stress calculation in bolts of clamp

$$A_r = 7.75 \cdot 10^{-6} \quad \text{From table 8.1}$$

$$\tau := \frac{F_{shearmax}}{A_r} = 3.279 \cdot 10^7 \text{ Pa}$$

6) Calculation of thickness of plate using allowable bearing stress on bolt holes

$$FS := 5$$

Yield Strength of aluminium = $\sigma_y := 241 \cdot 10^6 \text{ Pa}$

$$\sigma_{allowable} := \frac{\sigma_y}{FS} = 4.82 \cdot 10^7 \text{ Pa}$$

$$\sigma_{bearing} = \frac{F_{shearmax}}{0.004 \cdot t}$$

To find minimum thickness of the plate, $t \sigma_{bearing} := \sigma_{allowable}$

This implies that

$$t := \frac{F_{shearmax}}{0.004 \cdot \sigma_{bearing}} = 0.001 \text{ m}$$

To increase the rigidity and compactness of the structure and keeping in mind the clearances for bolts we decided to use 10 mm thickness plate

7) Normal stress calculations in X axis plate

$$A_3 := 0.150 \cdot 0.01 - 4 \cdot 0.004 \cdot 0.01 = 0.001 \text{ m}^2$$

$$\sigma_{normal} := \frac{F}{A_3} = 2.836 \cdot 10^6 \text{ Pa}$$

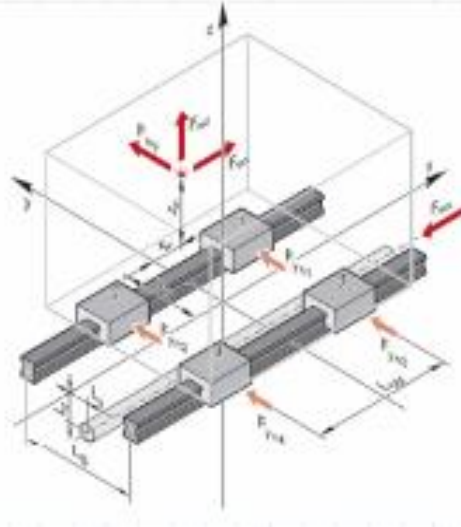
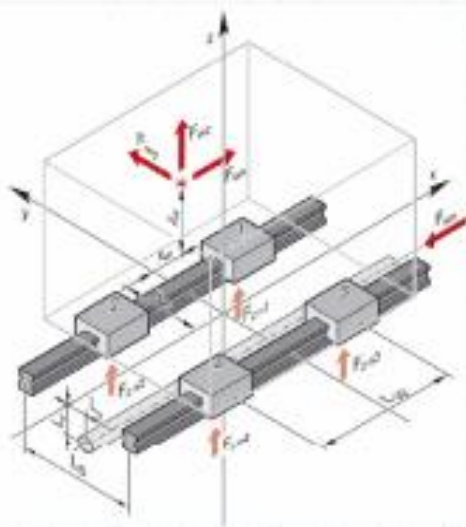
Y-axis linear bearing selection

Case 1: (Force in Y axis)

$$L_x = 0.175 \quad L_y = 0 \quad L_w = 0.0863 \quad L_z = 0.010 \quad F_{WX} = 3800$$

$$y_W = 0.150 \quad x_W = 0.220 \quad Z_W = 0.150 \quad F_{WZ} = 7 \cdot 9.8 = 68.6$$

$$F_{WY} = 0$$



$$F_{Z1} = \frac{F_{WZ}}{4} + \frac{\langle F_{WZ} \cdot y_W \rangle}{2 \cdot L_x} - \frac{\langle F_{WY} \cdot Z_W \rangle}{2 \cdot L_x} + \frac{\langle F_{WZ} \cdot x_W \rangle}{2 \cdot L_w} - \frac{\langle F_{WX} \cdot (Z_W - L_z) \rangle}{2 \cdot L_w} = -2.948 \cdot 10^3$$

$$F_{Z2} = \frac{F_{WZ}}{4} + \frac{\langle F_{WZ} \cdot y_W \rangle}{2 \cdot L_x} - \frac{\langle F_{WY} \cdot Z_W \rangle}{2 \cdot L_x} + \frac{\langle F_{WX} \cdot (Z_W - L_z) \rangle}{2 \cdot L_w} - \frac{\langle F_{WZ} \cdot x_W \rangle}{2 \cdot L_w} = 3.041 \cdot 10^3$$

$$F_{Z3} = \frac{F_{WZ}}{4} + \frac{\langle F_{WY} \cdot Z_W \rangle}{2 \cdot L_x} - \frac{\langle F_{WY} \cdot y_W \rangle}{2 \cdot L_x} + \frac{\langle F_{WZ} \cdot x_W \rangle}{2 \cdot L_w} - \frac{\langle F_{WX} \cdot (Z_W - L_z) \rangle}{2 \cdot L_w} = -2.978 \cdot 10^3$$

$$F_{Z4} = \frac{F_{WZ}}{4} + \frac{\langle F_{WY} \cdot Z_W \rangle}{2 \cdot L_x} - \frac{\langle F_{WZ} \cdot y_W \rangle}{2 \cdot L_x} + \frac{\langle F_{WX} \cdot (Z_W - L_z) \rangle}{2 \cdot L_w} - \frac{\langle F_{WZ} \cdot x_W \rangle}{2 \cdot L_w} = 2.983 \cdot 10^3$$

$$F_{Y1} := \frac{F_{WY}}{4} + \frac{\langle F_{WY} \cdot x_W \rangle}{2 \cdot L_w} - \frac{\langle F_{WX} \cdot (y_W - L_y) \rangle}{2 \cdot L_w} = -3.302 \cdot 10^3 \quad F_{Y3} := F_{Y1}$$

$$F_{Y2} := \frac{F_{WY}}{4} - \frac{\langle F_{WY} \cdot x_W \rangle}{2 \cdot L_w} + \frac{\langle F_{WX} \cdot (y_W - L_y) \rangle}{2 \cdot L_w} = 3.302 \cdot 10^3 \quad F_{Y4} := F_{Y2}$$

$$F_1 := |F_{Z1}| + |F_{Y1}| = 6.251 \cdot 10^3 \quad F_2 := |F_{Z2}| + |F_{Y2}| = 6.344 \cdot 10^3$$

$$F_3 := |F_{Z3}| + |F_{Y3}| = 6.28 \cdot 10^3 \quad F_4 := |F_{Z4}| + |F_{Y4}| = 6.285 \cdot 10^3$$

Case 2:(Force in X axis)

$$L_x := 0.175 \quad L_y := 0 \quad L_w := 0.0863 \quad L_z := 0.010 \quad F_{WX} := 0$$

$$y_W := 0.150 \quad x_W := 0.220 \quad Z_W := 0.150 \quad F_{WZ} := -7 \cdot 9.8 = -68.6$$

$$F_{WY} = 3800$$

$$F_{Z1} := \frac{F_{WZ}}{4} + \frac{\langle F_{WZ} \cdot y_W \rangle}{2 \cdot L_x} - \frac{\langle F_{WY} \cdot Z_W \rangle}{2 \cdot L_x} + \frac{\langle F_{WZ} \cdot x_W \rangle}{2 \cdot L_w} - \frac{\langle F_{WX} \cdot (Z_W - L_z) \rangle}{2 \cdot L_w} = -1.763 \cdot 10^3$$

$$F_{Z2} := \frac{F_{WZ}}{4} + \frac{\langle F_{WZ} \cdot y_W \rangle}{2 \cdot L_x} - \frac{\langle F_{WY} \cdot Z_W \rangle}{2 \cdot L_x} + \frac{\langle F_{WX} \cdot (Z_W - L_z) \rangle}{2 \cdot L_w} - \frac{\langle F_{WZ} \cdot x_W \rangle}{2 \cdot L_w} = -1.588 \cdot 10^3$$

$$F_{Z3} := \frac{F_{WZ}}{4} + \frac{\langle F_{WY} \cdot Z_W \rangle}{2 \cdot L_x} - \frac{\langle F_{WZ} \cdot y_W \rangle}{2 \cdot L_x} + \frac{\langle F_{WZ} \cdot x_W \rangle}{2 \cdot L_w} - \frac{\langle F_{WX} \cdot (Z_W - L_z) \rangle}{2 \cdot L_w} = 1.553 \cdot 10^3$$

$$F_{Z4} := \frac{F_{WZ}}{4} + \frac{\langle F_{WY} \cdot Z_W \rangle}{2 \cdot L_x} - \frac{\langle F_{WZ} \cdot y_W \rangle}{2 \cdot L_x} + \frac{\langle F_{WX} \cdot (Z_W - L_z) \rangle}{2 \cdot L_w} - \frac{\langle F_{WZ} \cdot x_W \rangle}{2 \cdot L_w} = 1.728 \cdot 10^3$$

$$F_{Y1} := \frac{F_{WY}}{4} + \frac{\langle F_{WY} \cdot x_W \rangle}{2 \cdot L_w} - \frac{\langle F_{WX} \cdot (y_W - L_y) \rangle}{2 \cdot L_w} = 5.794 \cdot 10^3 \quad F_{Y3} := F_{Y1}$$

$$F_{Y2} := \frac{F_{WY}}{4} - \frac{(F_{WY} \cdot x_W)}{2 \cdot L_w} + \frac{(F_{WX} \cdot (y_W - L_y))}{2 \cdot L_w} = -3.894 \cdot 10^3 \quad F_{Y4} := F_{Y2}$$

$$F_1 := |F_{Z1}| + |F_{Y1}| = 7.556 \cdot 10^3 \quad F_2 := |F_{Z2}| + |F_{Y2}| = 5.481 \cdot 10^3$$

$$F_3 := |F_{Z3}| + |F_{Y3}| = 7.347 \cdot 10^3 \quad F_4 := |F_{Z4}| + |F_{Y4}| = 5.622 \cdot 10^3$$

Case 3:(Force in X and Y both axis)

$$L_x := 0.175 \quad L_y := 0 \quad L_w := 0.0863 \quad L_z := 0.010 \quad F_{WX} := -2687$$

$$y_W := 0.150 \quad x_W := 0.220 \quad z_W := 0.150 \quad F_{WZ} := -7 \cdot 9.8 = -68.6$$

$$F_{WY} = 2687$$

$$F_{Z1} := \frac{F_{WZ}}{4} + \frac{(F_{WZ} \cdot y_W)}{2 \cdot L_x} - \frac{(F_{WY} \cdot z_W)}{2 \cdot L_x} + \frac{(F_{WZ} \cdot x_W)}{2 \cdot L_w} - \frac{(F_{WX} \cdot (z_W - L_z))}{2 \cdot L_w} = 893.93$$

$$F_{Z2} := \frac{F_{WZ}}{4} + \frac{(F_{WZ} \cdot y_W)}{2 \cdot L_x} - \frac{(F_{WY} \cdot z_W)}{2 \cdot L_x} + \frac{(F_{WX} \cdot (z_W - L_z))}{2 \cdot L_w} - \frac{(F_{WZ} \cdot x_W)}{2 \cdot L_w} = -3.29 \cdot 10^3$$

$$F_{Z3} := \frac{F_{WZ}}{4} + \frac{(F_{WY} \cdot z_W)}{2 \cdot L_x} - \frac{(F_{WZ} \cdot y_W)}{2 \cdot L_x} + \frac{(F_{WZ} \cdot x_W)}{2 \cdot L_w} - \frac{(F_{WX} \cdot (z_W - L_z))}{2 \cdot L_w} = 3.256 \cdot 10^3$$

$$F_{Z4} := \frac{F_{WZ}}{4} + \frac{(F_{WY} \cdot z_W)}{2 \cdot L_x} - \frac{(F_{WZ} \cdot y_W)}{2 \cdot L_x} + \frac{(F_{WX} \cdot (z_W - L_z))}{2 \cdot L_w} - \frac{(F_{WZ} \cdot x_W)}{2 \cdot L_w} = -928.23$$

$$F_{Y1} := \frac{F_{WY}}{4} + \frac{(F_{WY} \cdot x_W)}{2 \cdot L_w} - \frac{(F_{WX} \cdot (y_W - L_y))}{2 \cdot L_w} = 6.432 \cdot 10^3 \quad F_{Y3} := F_{Y1}$$

$$F_{Y2} := \frac{F_{WY}}{4} - \frac{(F_{WY} \cdot x_W)}{2 \cdot L_w} + \frac{(F_{WX} \cdot (y_W - L_y))}{2 \cdot L_w} = -5.088 \cdot 10^3 \quad F_{Y4} := F_{Y2}$$

$$F_1 := |F_{Z1}| + |F_{Y1}| = 7.326 \cdot 10^3$$

$$F_2 := |F_{Z2}| + |F_{Y2}| = 8.379 \cdot 10^3$$

$$F_3 := |F_{Z3}| + |F_{Y3}| = 9.688 \cdot 10^3$$

$$F_4 := |F_{Z4}| + |F_{Y4}| = 6.017 \cdot 10^3$$

For the selection of bearing we take the maximum force that acts in both XY axis i.e $F=9.688$ KN

Static safety factor = $f := 2.3$

$$\text{Static load Rating} = C_0 := f \cdot F_3 = 2.228 \cdot 10^4 \text{ N}$$

Keeping in view the above static load rating , from tables of Linear bearing we select HGR 15 linear guide rail and static load rating of HGR 15 is 23.47 KN which is greater than our required static load rating so we can select it

From table of linear guide rails bearing basic dynamic loading of HGR 15 is $C=14.7$ kN

$$C := 14.7 \cdot 10^3$$

$$\text{Life of bearing} = L := \left(\frac{C}{F_3} \right)^3 \cdot 50 = 174.687 \text{ km}$$

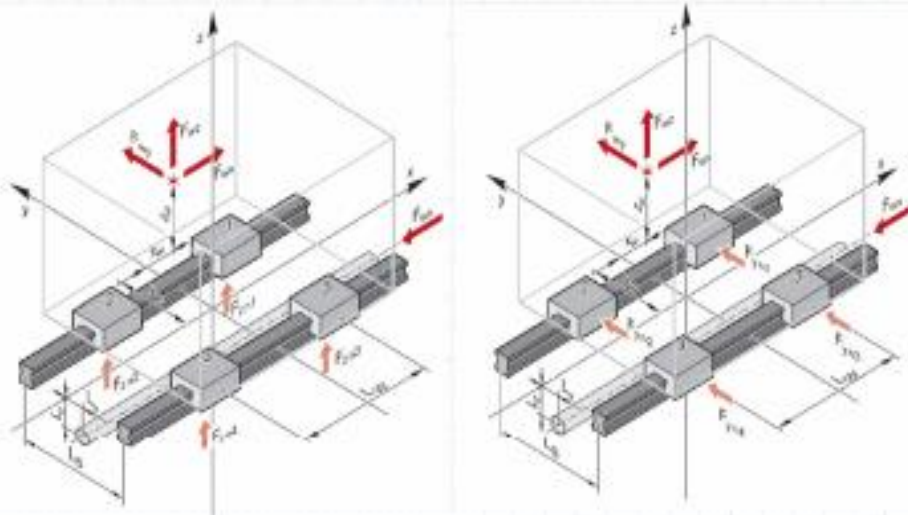
X-axis linear bearing selection

Case 1: (Force in Y axis)

$$L_x := 0.11 \quad L_y := 0 \quad L_w := 0.0863 \quad L_z := -0.0175 \quad F_{WX} := 0$$

$$y_W := -0.22 \quad x_W := 0 \quad Z_W := 0.050 \quad F_{WZ} := -3800$$

$$F_{WY} := -2.5 \cdot 9.81 = -24.525$$



$$F_{Z1} := \frac{F_{WZ}}{4} + \frac{\langle F_{WZ} \cdot y_W \rangle}{2 \cdot L_x} - \frac{\langle F_{WY} \cdot Z_W \rangle}{2 \cdot L_x} + \frac{\langle F_{WZ} \cdot x_W \rangle}{2 \cdot L_w} - \frac{\langle F_{WX} \cdot (Z_W - L_z) \rangle}{2 \cdot L_w} = 2.856 \cdot 10^3$$

$$F_{Z2} := \frac{F_{WZ}}{4} + \frac{\langle F_{WZ} \cdot y_W \rangle}{2 \cdot L_x} - \frac{\langle F_{WY} \cdot Z_W \rangle}{2 \cdot L_x} + \frac{\langle F_{WX} \cdot (Z_W - L_z) \rangle}{2 \cdot L_w} - \frac{\langle F_{WZ} \cdot x_W \rangle}{2 \cdot L_w} = 2.856 \cdot 10^3$$

$$F_{Z3} := \frac{F_{WZ}}{4} + \frac{\langle F_{WY} \cdot Z_W \rangle}{2 \cdot L_x} - \frac{\langle F_{WY} \cdot y_W \rangle}{2 \cdot L_x} + \frac{\langle F_{WZ} \cdot x_W \rangle}{2 \cdot L_w} - \frac{\langle F_{WX} \cdot (Z_W - L_z) \rangle}{2 \cdot L_w} = -980.099$$

$$F_{Z4} := \frac{F_{WZ}}{4} + \frac{\langle F_{WY} \cdot Z_W \rangle}{2 \cdot L_x} - \frac{\langle F_{WZ} \cdot y_W \rangle}{2 \cdot L_x} + \frac{\langle F_{WX} \cdot (Z_W - L_z) \rangle}{2 \cdot L_w} - \frac{\langle F_{WZ} \cdot x_W \rangle}{2 \cdot L_w} = -4.756 \cdot 10^3$$

$$F_{Y1} := \frac{F_{WY}}{4} + \frac{(F_{WY} \cdot x_W)}{2 \cdot L_w} - \frac{(F_{WX} \cdot (y_W - L_y))}{2 \cdot L_w} = -6.131 \quad F_{Y3} := F_{Y1}$$

$$F_{Y2} := \frac{F_{WY}}{4} - \frac{(F_{WY} \cdot x_W)}{2 \cdot L_w} + \frac{(F_{WX} \cdot (y_W - L_y))}{2 \cdot L_w} = -6.131 \quad F_{Y4} := F_{Y2}$$

$$F_1 := |F_{Z1}| + |F_{Y1}| = 2.862 \cdot 10^3 \quad F_2 := |F_{Z2}| + |F_{Y2}| = 2.862 \cdot 10^3$$

$$F_3 := |F_{Z3}| + |F_{Y3}| = 986.23 \quad F_4 := |F_{Z4}| + |F_{Y4}| = 4.762 \cdot 10^3$$

Case 2:(Force in X axis)

$$L_x := 0.11 \quad L_y := 0 \quad L_w := 0.0863 \quad L_z := -0.0175 \quad F_{WX} := 3800$$

$$y_W := -0.22 \quad x_W := 0 \quad Z_W := 0.050 \quad F_{WZ} := 0$$

$$F_{WY} := -2.5 \cdot 9.81 = -24.525$$

$$F_{Z1} := \frac{F_{WZ}}{4} + \frac{(F_{WZ} \cdot y_W)}{2 \cdot L_x} - \frac{(F_{WY} \cdot Z_W)}{2 \cdot L_x} + \frac{(F_{WZ} \cdot x_W)}{2 \cdot L_w} - \frac{(F_{WX} \cdot (Z_W - L_z))}{2 \cdot L_w} = -1.481 \cdot 10^3$$

$$F_{Z2} := \frac{F_{WZ}}{4} + \frac{(F_{WZ} \cdot y_W)}{2 \cdot L_x} - \frac{(F_{WY} \cdot Z_W)}{2 \cdot L_x} + \frac{(F_{WX} \cdot (Z_W - L_z))}{2 \cdot L_w} - \frac{(F_{WZ} \cdot x_W)}{2 \cdot L_w} = 1.492 \cdot 10^3$$

$$F_{Z3} := \frac{F_{WZ}}{4} + \frac{(F_{WY} \cdot Z_W)}{2 \cdot L_x} - \frac{(F_{WZ} \cdot y_W)}{2 \cdot L_x} + \frac{(F_{WZ} \cdot x_W)}{2 \cdot L_w} - \frac{(F_{WX} \cdot (Z_W - L_z))}{2 \cdot L_w} = -1.492 \cdot 10^3$$

$$F_{Z4} := \frac{F_{WZ}}{4} + \frac{(F_{WY} \cdot Z_W)}{2 \cdot L_x} - \frac{(F_{WZ} \cdot y_W)}{2 \cdot L_x} + \frac{(F_{WX} \cdot (Z_W - L_z))}{2 \cdot L_w} - \frac{(F_{WZ} \cdot x_W)}{2 \cdot L_w} = 1.481 \cdot 10^3$$

$$F_{Y1} := \frac{F_{WY}}{4} + \frac{(F_{WY} \cdot x_W)}{2 \cdot L_w} - \frac{(F_{WX} \cdot (y_W - L_y))}{2 \cdot L_w} = 4.837 \cdot 10^3 \quad F_{Y3} := F_{Y1}$$

$$F_{Y2} := \frac{F_{WY}}{4} - \frac{(F_{WY} \cdot x_W)}{2 \cdot L_w} + \frac{(F_{WX} \cdot (y_W - L_y))}{2 \cdot L_w} = -4.85 \cdot 10^3 \quad F_{Y4} = F_{Y2}$$

$$F_1 := |F_{Z1}| + |F_{Y1}| = 6.318 \cdot 10^3 \quad F_2 := |F_{Z2}| + |F_{Y2}| = 6.341 \cdot 10^3$$

$$F_3 := |F_{Z3}| + |F_{Y3}| = 6.329 \cdot 10^3 \quad F_4 := |F_{Z4}| + |F_{Y4}| = 6.33 \cdot 10^3$$

Case 3:(Force in X and Y both axis)

$$L_x := 0.11 \quad L_y := 0 \quad L_w := 0.0863 \quad L_z := -0.0175 \quad F_{WX} := -2687$$

$$y_W := -0.22 \quad x_W := 0 \quad z_W := 0.050 \quad F_{WZ} := 2687$$

$$F_{WY} := -2.5 \cdot 9.81 = -24.525$$

$$F_{Z1} := \frac{F_{WZ}}{4} + \frac{(F_{WZ} \cdot y_W)}{2 \cdot L_x} - \frac{(F_{WY} \cdot z_W)}{2 \cdot L_x} + \frac{(F_{WZ} \cdot x_W)}{2 \cdot L_w} - \frac{(F_{WX} \cdot (z_W - L_z))}{2 \cdot L_w} = -958.851$$

$$F_{Z2} := \frac{F_{WZ}}{4} + \frac{(F_{WZ} \cdot y_W)}{2 \cdot L_x} - \frac{(F_{WY} \cdot z_W)}{2 \cdot L_x} + \frac{(F_{WX} \cdot (z_W - L_z))}{2 \cdot L_w} - \frac{(F_{WZ} \cdot x_W)}{2 \cdot L_w} = -3.061 \cdot 10^3$$

$$F_{Z3} := \frac{F_{WZ}}{4} + \frac{(F_{WY} \cdot z_W)}{2 \cdot L_x} - \frac{(F_{WZ} \cdot y_W)}{2 \cdot L_x} + \frac{(F_{WZ} \cdot x_W)}{2 \cdot L_w} - \frac{(F_{WX} \cdot (z_W - L_z))}{2 \cdot L_w} = 4.404 \cdot 10^3$$

$$F_{Z4} := \frac{F_{WZ}}{4} + \frac{(F_{WY} \cdot z_W)}{2 \cdot L_x} - \frac{(F_{WZ} \cdot y_W)}{2 \cdot L_x} + \frac{(F_{WX} \cdot (z_W - L_z))}{2 \cdot L_w} - \frac{(F_{WZ} \cdot x_W)}{2 \cdot L_w} = 2.302 \cdot 10^3$$

$$F_{Y1} := \frac{F_{WY}}{4} + \frac{(F_{WY} \cdot x_W)}{2 \cdot L_w} - \frac{(F_{WX} \cdot (y_W - L_y))}{2 \cdot L_w} = -3.431 \cdot 10^3 \quad F_{Y3} = F_{Y1}$$

$$F_{Y2} := \frac{F_{WY}}{4} - \frac{(F_{WY} \cdot x_W)}{2 \cdot L_w} + \frac{(F_{WX} \cdot (y_W - L_y))}{2 \cdot L_w} = 3.419 \cdot 10^3 \quad F_{Y4} = F_{Y2}$$

$$F_1 := |F_{Z1}| + |F_{Y1}| = 4.39 \cdot 10^3$$

$$F_2 := |F_{Z2}| + |F_{Y2}| = 6.479 \cdot 10^3$$

$$F_3 := |F_{Z3}| + |F_{Y3}| = 7.835 \cdot 10^3$$

$$F_4 := |F_{Z4}| + |F_{Y4}| = 5.721 \cdot 10^3$$

For the selection of bearing we take the maximum force that acts in both XY axis i.e $F=7.835$ KN

Static safety factor = $f := 3$

$$\text{Static load Rating} = C_0 := f \cdot F_3 = 2.351 \cdot 10^4 \text{ N}$$

Keeping in view the above static load rating , from tables of Linear bearing we select HGR 15 linear guide rail and static load rating of HGR 15 is 23.47 KN which is greater than our required static load rating so we can select it

From table of linear guide rails bearing basic dynamic loading of HGR 15 is $C=14.7$ kN

$$C = 14.7 \cdot 10^3$$

$$\text{Life of bearing} = L := \left(\frac{C}{F_3} \right)^3 \cdot 50 = 330.215 \text{ km}$$